

# **Study of chaotic circuits, their design, and applications**

A Thesis

Submitted in partial fulfilment of the requirements  
for the award of the degree of  
Doctor of Philosophy

in  
**Department of Electronics & Communication Engineering**  
by

**Kriti Suneja**  
**2K18/PhDEC/09**  
Under the Supervision of

**Prof. Rajeshwari Pandey**  
Department of Electronics &  
Communication Engineering,  
Delhi Technological University,  
Delhi –110 042

**Prof. Neeta Pandey**  
Department of Electronics &  
Communication Engineering,  
Delhi Technological University  
Delhi –110 042



**Delhi Technological University**  
**Shahbad Daultpur, Main Bawana Road**  
**Delhi-110042**

**Department of Electronics and Communication Engineering**  
Delhi Technological University  
(Formerly Delhi College of Engineering) Bawana Road, Delhi-110042

**CERTIFICATE**

This is to certify that the thesis titled “*Study of chaotic circuits, their design and applications*” being submitted by **Ms. Kriti Suneja** in partial fulfilment of the requirements for the award of the degree of Doctor of Philosophy in Department of Electronics and Communication Engineering, Delhi Technological University, Delhi is a record of candidate’s own work carried out by her under our supervision and guidance. In our opinion, the thesis has reached the standards fulfilling the requirements of the regulations relating to the degree. The results contained in this thesis have not been submitted to any other university or institute for the award of any degree or diploma.

**Prof. Rajeshwari Pandey**  
Department of Electronics &  
Communication Engineering,  
Delhi Technological University,  
Delhi –110 042

**Prof. Neeta Pandey**  
Department of Electronics &  
Communication Engineering,  
Delhi Technological University  
Delhi –110 042

**Prof. O.P. Verma**  
HoD, Department of Electronics &  
Communication Engineering,  
Delhi Technological University  
Delhi-110042

**Department of Electronics and Communication Engineering**  
Delhi Technological University  
(Formerly Delhi College of Engineering) Bawana Road, Delhi-110042

**CANDIDATE'S DECLARATION**

I hereby declare that the work presented in this thesis titled “**Study of chaotic circuits, their design and applications**” has been carried out by me under the guidance of **Dr. Neeta Pandey**, Professor of ECE Department, Delhi Technological University, Delhi and **Dr. Rajeshwari Pandey**, Professor of ECE Department, Delhi Technological University, Delhi and is hereby submitted for the partial fulfilment of the requirement for the award of the degree of Doctor of Philosophy in Department of Electronics and Communication Engineering, Delhi Technological University, Delhi.

I further undertake that the work embodied in this thesis has not been submitted for the award of any other degree elsewhere.

**Kriti Suneja**  
**2K18/PhDEC/09**

**Department of Electronics and Communication Engineering**  
Delhi Technological University  
(Formerly Delhi College of Engineering) Bawana Road, Delhi-110042

## **Acknowledgement**

I would like to express my sincere gratitude to my supervisor **Prof. Neeta Pandey** and co-supervisor **Prof. Rajeshwari Pandey**, for their invaluable guidance, support, and encouragement throughout my doctoral studies. Their expertise in the field and dedication to teaching have been instrumental in shaping my research and fostering my growth as a scholar. I am deeply grateful for their insightful feedback and contributions to my research. Their thoughtful critiques and suggestions have challenged me to think more deeply and critically about my work.

I would also like to express my sincere thanks to **Prof. O. P. Verma**, HoD, Electronics and Communication Engineering. It is indeed my privilege to submit this thesis during his headship.

I would like to thank my colleagues with whom I have had the pleasure of working with throughout my time at DTU. Their support, encouragement, and camaraderie have made my experience in the doctoral program truly memorable.

I am indebted to my family and friends for their unwavering love and support, even during the most challenging times. I find myself at loss of words to acknowledge support from my parents and parents-in law for graceful acceptance of my lack of attention towards them. My father has always been an inspiration for me and it is his constant support that has helped me to reach this stage in life. My mother, who raised me and taught me everything about being a good human being and shaped me in who I am. Special credit to my husband for his most valuable consent to spend long hours on work. I wish if I could know how to thank my brother, who has always been a cheerful companion and true friend. Without the collective support and guidance of these individuals, this research would not have been possible.

Finally, I thank the Almighty in giving me the strength to carry out the present research work.

Kriti Suneja

## Abstract

Chaos is an exceptional phenomenon occurring in non-linear dynamic systems. Our lives are full of non-linear dynamic systems, such as the Solar System, the weather, the stock market, the human body, plant and animal populations, cancer growth, spread of pandemics, chemical reactions, the electrical power grid, the Internet, etc. the behaviour of which can be best modelled as chaotic system.

More and more chaotic systems are being invented in an effort to simplify their algebraic representation but with high degree of complexity in output. With the development of non-linear dynamics and chaos theory, the hardware realization of chaotic systems has become a useful way to use them in real world applications for reliable and portable communication devices. In this direction, this thesis is primarily concerned with the hardware optimized design of chaotic systems. The idea is to design a circuit with minimum possible number of active and passive components which obeys the governing equations of a chaotic system.

In chaotic systems, a single or more non-linear terms are always present in the governing equations which is responsible for output's complexity. Quadratic, exponential, hyperbolic are some of the representative nonlinearities present in chaotic systems. Generally, implementation of the governing equations of a chaotic system requires the addition, subtraction, scaling operations besides the non-linearity. The Operational Amplifier (OpAmp) is commonly used active block in hardware implementation of chaotic systems. Current mode active block, such as Current Feedback Operational Amplifier (CFOA), has capabilities of handling both current and voltage signals which culminates in compact realizations in comparison to the existing OpAmp counterparts. In addition to CFOAs, suitable active and passive components are used to realize the non-linearity(ies) present in the governing equations and any scaling required therein.

The design of Rössler chaotic system having single quadratic non-linear term, is addressed first by presenting CFOA based realization. It also uses an analog multiplier (AM) namely AD633. The presented design is a compact realization in comparison to existing OpAmp based counterparts. A complete circuitry for adaptive control synchronization between two Rössler chaotic systems is also put forward.

A chaotic system based on two quadratic non-linearities namely Pehlivan–Uyaröglu Chaotic System (PUCS), is focused next. Four variants of PUCS are introduced which appear

to be distinct in the sense that there is no obvious transformation of one into another. Non-linear dynamic properties of these variants are investigated and expatiated through bifurcation diagrams, Lyapunov exponents, Kaplan Yorke Dimension, nature of fixed points through eigenvalues and chaotic phase space diagrams. A CFOA based realization is put forward that can realize the existing PUCS and its proposed variants, by simply adjusting component values.

In AD633, there is a possibility of realizing algebraic functions including single multiplication, subtraction of two multiplication terms, and accumulation. The versatility of AD633 is gainfully exploited in presenting generalized circuit topology to implement chaotic systems with quadratic type non-linearities.

The use of AM is inevitable in hardware realization of chaotic systems with quadratic nonlinearity, leading to increased active block count. A new chaotic system with exponential non-linearity has been put forward. It is realized using CFOAs and diodes, thus reducing the count of active building blocks. This new chaotic system has been verified for different properties, including Lyapunov Exponents, Kaplan Yorke Dimension and dissipativity.

With the increase in demand of higher complexity for security, the dimension of the chaotic system can be extended beyond three. Such higher dimensional systems, also known as hyperchaotic systems, can be useful in those applications. One such four dimensional hyperchaotic system with two quadratic type non-linearities has been proposed and tested for different properties, including Lyapunov Exponents, Kaplan Yorke Dimension and dissipativity. The circuit implementation using CFOAs and AMs is also presented.

All the above designs are verified either through LTspice simulations or combination of LTspice simulations and experimental evaluations.

An attempt has also been made to realize chaotic systems on digital platform namely Field Programmable Gate Arrays (FPGAs). Ten different chaotic systems have been compared based on hardware utilization and delay on the target FPGA device Artix 7. Besides numerical simulations in python for confirmation of the correctness of the implemented systems via observations, the functional verification of the synthesized designs has been done using inbuilt simulator of Xilinx Vivado design suite.

## CONTENTS

Certificate	i
Candidate's Declaration	ii
Acknowledgement	iii
Abstract	iv
Contents	vi
List of Figures	x
List of Tables	xiv
List of Abbreviations	xv

### CHAPTER 1      INTRODUCTION

1.1	Background.....	1
1.2	Available Literature.....	1
	1.2.1 Chaotic Systems.....	2
	1.2.2 Analog Circuit Realization of Chaotic Systems.....	3
	1.2.3 Synchronization in Chaotic Systems.....	4
	1.2.4 Digital Design of Chaotic Systems.....	4
1.3	Research Gaps.....	5
1.4	Research Objectives.....	6
1.5	Organization of Thesis.....	6

### CHAPTER 2      BASIC TERMINOLOGY

2.1	Introduction.....	9
2.2	Estimation of Parameters and Properties of a Chaotic System.....	9
	2.2.1 Bifurcation Diagrams.....	10
	2.2.2 Lyapunov Exponents.....	10
	2.2.3 Kaplan Yorke Dimension.....	11
	2.2.4 Dissipativity.....	11
2.3	Analysis of Fixed Points.....	12
2.4	Analog Building Blocks.....	15
	2.4.1 Current Feedback Operational Amplifier (CFOA).....	15
	2.4.1.1 CFOA Characterization.....	16
	2.4.1.2 Basic Circuit Applications.....	17

	2.4.1.2.1 Subtractor/ Summer.....	17
	2.4.1.2.2 Integrator.....	18
	2.4.2 Analog Multiplier (AM).....	19
	2.4.2.1 AD633 Characterization.....	20
2.5	Concluding Remarks.....	21
<b>CHAPTER 3</b>	<b>CHAOTIC SYSTEMS WITH SINGLE QUADRATIC NON-LINEARITY</b>	
3.1	Introduction.....	22
3.2	Mathematical Model of Rössler Chaotic System.....	22
3.3	Circuit Realization.....	23
	3.3.1 Simulation Results.....	24
3.4	Synchronization between Rössler Chaotic Systems.....	29
	3.4.1 Master and Slave Representation.....	29
	3.4.2 Error Dynamics.....	30
	3.4.3 Adaptive Controller.....	31
	3.4.4 Error in Parameters' Estimation.....	31
	3.4.5 Lyapunov Stability.....	31
	3.4.6 Adaptive Laws.....	32
3.5	Concluding Remarks.....	35
<b>CHAPTER 4</b>	<b>CHAOTIC SYSTEMS WITH TWO QUADRATIC NON-LINEARITIES</b>	
4.1	Introduction.....	36
4.2	The Pehlivan Uyaröglu Chaotic System (PUCS).....	36
	4.2.1 Proposed Variants of PUCS.....	37
	4.2.1.1 First Proposed Variant of PUCS (PUCS I).....	37
	4.2.1.2 Second Proposed Variant of PUCS (PUCS II).....	37
	4.2.1.3 Third Proposed Variant of PUCS (PUCS III).....	37
	4.2.1.4 Fourth Proposed Variant of PUCS (PUCS IV).....	38
4.3	Estimation of parameters and properties of the PUCS and its Proposed Variants.....	38



4.4	Analysis of Fixed Points.....	42
4.5	The Circuit Realization.....	44
4.6	Simulation Results.....	47
4.7	Experimental Verification.....	51
4.8	Concluding Remarks.....	53
<b>CHAPTER 5</b>	<b>GENERALIZED HARDWARE EFFICIENT TOPOLOGY OF CHAOTIC SYSTEMS WITH QUADRATIC NON-LINEARITY</b>	
5.1	Introduction.....	54
5.2	The Generic Circuit Topology.....	54
5.3	Customization of Proposed Generic Topology for Rabinovich Chaotic System (RCS).....	55
5.4	Simulation Results.....	58
	5.4.1 Rabinovich Chaotic System (RCS).....	59
	5.4.2 Lorenz Chaotic System (LCS).....	59
	5.4.3 Yang Chen Chaotic System (YCCS).....	59
5.5	Concluding Remarks.....	61
<b>CHAPTER 6</b>	<b>NEW CHAOTIC SYSTEM WITH EXPONENTIAL NON-LINEARITY</b>	
6.1	Introduction.....	62
6.2	Proposed Chaotic System and its Numerical Analysis.....	62
6.3	Properties and Behaviors of the Novel Chaotic System.....	63
6.4	Analysis of Fixed Points.....	65
6.5	Circuit Design of the Proposed Chaotic System.....	66
6.6	Adaptive Control Synchronization of the Proposed Chaotic System...68	
	6.6.1 Master and Slave Representation.....	68
	6.6.2 Error Dynamics.....	69
	6.6.3 Adaptive Controller.....	69
	6.6.4 Error in Parameters' Estimation.....	69
	6.6.5 Lyapunov Stability.....	70
	6.6.6 Adaptive Laws.....	70

6.7	Concluding Remarks.....	74
<b>CHAPTER 7</b>	<b>NOVEL HYPERCHAOTIC SYSTEM WITH TWO QUADRATIC NON-LINEARITIES</b>	
7.1	Introduction.....	76
7.2	Proposed Hyperchaotic System (HCS).....	76
7.3	Properties of the proposed HCS.....	77
7.4	Analysis of Fixed Points.....	77
7.5	Circuit Design of the Proposed HCS.....	78
7.6	Adaptive Control Synchronization Scheme.....	82
	7.6.1 Master and Slave Representation.....	82
	7.6.2 Error Dynamics.....	83
	7.6.3 Adaptive Controller.....	83
	7.6.4 Error in Parameters' Estimation.....	83
	7.6.5 Lyapunov Stability.....	84
	7.6.6 Adaptive Laws.....	85
7.7	Concluding Remarks.....	89
<b>CHAPTER 8</b>	<b>DIGITAL DESIGN OF CHAOTIC SYSTEMS</b>	
8.1	Introduction.....	91
8.2	Design Methodology.....	91
8.3	Results.....	94
	8.3.1 Synthesis Results.....	95
	8.3.2 Simulation Results.....	97
8.4	Concluding Remarks.....	105
<b>CHAPTER 9</b>	<b>CONCLUSION AND FUTURE SCOPE</b>	
9.1	Summary of Work Presented in this Thesis.....	106
9.2	Author's Ending Note.....	108
9.3	Future Scope.....	109
	References.....	110
	List of Publications.....	118

## LIST OF FIGURES

- Fig. 2.1 Bifurcation plot of PUCS with respect to parameter  $a$
- Fig. 2.2 The block diagram of CFOA
- Fig. 2.3 Pin diagram of AD 844
- Fig. 2.4 DC characteristics of AD844 between (a) Voltages at X and Y terminal; (b) Current in Z and X terminal; (c) Voltages at W and Z terminal
- Fig. 2.5 CFOA based summer
- Fig. 2.6 CFOA based integrator
- Fig. 2.7 Pin diagram and internal schematic of Analog Multiplier
- Fig. 2.8 Output voltage of AD633 with respect to variations in input voltages
- Fig. 3.1 Proposed CFOA based Rössler system
- Fig. 3.2 Simulated chaotic outputs at (a)  $V_x$  (b)  $V_y$  (c)  $V_z$
- Fig. 3.3 Frequency spectrum of (a)  $V_x$  (b)  $V_y$  (c)  $V_z$
- Fig. 3.4 Simulated phase trajectories in (a)  $V_x - V_y$ , (b)  $V_y - V_z$  and (c)  $V_x - V_z$  planes
- Fig. 3.5 Simulated phase trajectories in (a)  $V_x - V_y$ , (b)  $V_y - V_z$  and (c)  $V_x - V_z$  planes with MC analysis
- Fig. 3.6 (a) Experimental setup; (b) Breadboard circuit for implementation of Rössler chaotic system
- Fig. 3.7 Experimental time domain outputs for state variables (c)  $V_x, V_y$  (d)  $V_y, V_z$  (e)  $V_x, V_z$  and phase trajectories in (f)  $V_x - V_y$ , (g)  $V_y - V_z$  and (h)  $V_x - V_z$  plane
- Fig. 3.8 Error functions of adaptive control synchronization
- Fig. 3.9 Estimated parameters  $a$  and  $c$
- Fig. 3.10 Proposed CFOA based slave circuit
- Fig. 3.11 Simulated plots between chaotic signals of master and slave in adaptive synchronization: (a)  $V_{x1}$  versus  $V_{x2}$ , (b)  $V_{y1}$  versus  $V_{y2}$ , (c)  $V_{z1}$  versus  $V_{z2}$
- Fig. 4.1 Bifurcation diagrams for (a) PUCS (b) PUCS I (c) PUCS II (d) PUCS III (e) PUCS IV
- Fig. 4.2 Dynamics of Lyapunov exponents for (a) PUCS, (b) PUCS I, (c) PUCS II, (d) PUCS III, (e) PUCS IV
- Fig. 4.3 Design for state variable  $x$
- Fig. 4.4 Design for state variable  $y$

- Fig. 4.5 Design for state variable  $z$
- Fig. 4.6 Time domain response of state variables (a) PUCS, (b) PUCS I, (c) PUCS II, (d) PUCS III, (e) PUCS IV
- Fig. 4.7 Simulated phase space trajectory  $yx$ ,  $yz$  and  $xz$  for (a) PUCS, (b) PUCS I, (c) PUCS II, (d) PUCS III, (e) PUCS IV
- Fig. 4.8 Frequency spectrum plots of state variables (a)  $V_x$ , (b)  $V_y$ , (c)  $V_z$
- Fig. 4.9 Monte Carlo Analysis of phase trajectories of state variables: (a)  $x$ - $y$ , (b)  $z$ - $y$ , (c)  $z$ - $x$
- Fig. 4.10 Experimental setup to implement PUCS I
- Fig. 4.11 Experimental setup to implement PUCS IV
- Fig. 4.12 Experimentally obtained phase space trajectories of PUCS I (a)  $yx$ , (b)  $yz$ , (c)  $xz$  and PUCS IV (d)  $yx$ , (e)  $yz$ , (f)  $xz$
- Fig. 5.1 (a) AD633 in current mode; (b) Proposed generalized topology to implement chaotic systems; (c) Complete schematic
- Fig. 5.2 AD633 based complete circuit design of Rabinovich chaotic system
- Fig. 5.3 Phase space plots of (a) RCS and (b) LCS and (c) YCCS in  $x$ - $y$ ,  $x$ - $z$  and  $y$ - $z$  planes
- Fig. 6.1 Bifurcation diagrams with change in parameter (a) 'a,' (b) 'b'
- Fig. 6.2 Dynamics of Lyapunov exponents with respect to time
- Fig. 6.3 Schematic of CFOA based novel chaotic system
- Fig. 6.4 Phase space plots of the designed circuit in (a)  $y$ - $x$  plane, (b)  $y$ - $z$  plane, (c)  $x$ - $z$  plane
- Fig. 6.5 Time variation of state variables  $x$ ,  $y$  and  $z$  with different initial states for master and slave
- Fig. 6.6 Trace of slave's parameter in synchronization with master system
- Fig. 6.7 Trajectories of error functions of state variables with time
- Fig. 6.8 Circuit design of adaptive synchronization of the proposed system: (a) Master circuit, (b) Error functions, (c) Updation law of slave's parameter, (d) Complete slave circuit
- Fig. 6.9 LTspice plot between respective variables of master and slave circuit: (a)  $x_1x_2$ , (b)  $y_1y_2$ , (c)  $z_1z_2$

- Fig.7.1 Circuit representation of the proposed HCS
- Fig.7.2 Simulated time series waveforms for (a)  $V_x$ , (b)  $V_y$ , (c)  $V_z$  and (d)  $V_w$
- Fig. 7.3 Frequency spectrum plots of state variables (a)  $V_x$ , (b)  $V_y$ , (c)  $V_z$  and (d)  $V_w$
- Fig. 7.4 Circuit simulations for the proposed HCS
- Fig. 7.5 Adaptively synchronized state variables  $x$ ,  $y$ ,  $z$  and  $w$  with different initial conditions for the proposed system
- Fig. 7.6 Study of parameter variation in adaptively controlled master-slave system for the proposed system
- Fig. 7.7 Error analysis of the adaptively controlled master-slave for the proposed system
- Fig. 7.8 Circuit design of adaptive control synchronization of the proposed hyperchaotic system: (a) Master circuit, (b) Error functions, (c) Updation law of slave's parameter, (d) Complete slave circuit
- Fig. 7.9 Simulated plots between hyperchaotic signals of master and slave in adaptive control synchronization
- Fig. 8.1 ASM chart of the control path of chaotic system
- Fig. 8.2 Top module of RK4 method in Verilog
- Fig. 8.3 Numerical simulation and Xilinx Vivado simulation results of Chen chaotic system
- Fig. 8.4 Numerical simulation and Xilinx Vivado simulation results of Lorenz chaotic system
- Fig. 8.5 Numerical simulation and Xilinx Vivado simulation results of Rössler chaotic system
- Fig. 8.6 Numerical simulation and Xilinx Vivado simulation results of Pehlivan chaotic system
- Fig. 8.7 Numerical simulation and Xilinx Vivado simulation results of Li chaotic system
- Fig. 8.8 Numerical simulation and Xilinx Vivado simulation results of Lü chaotic system
- Fig. 8.9 Numerical simulation and Xilinx Vivado simulation results of MACM chaotic system
- Fig. 8.10 Numerical simulation and Xilinx Vivado simulation results of chaotic system

Fig. 8.11 Numerical simulation and Xilinx Vivado simulation results of Rabinovich chaotic system

Fig. 8.12 Numerical simulation and Xilinx Vivado simulation results of chaotic system

## LIST OF TABLES

- Table 3.1: Table 3.1 Comparison of the proposed design with the existing circuit designs of Rössler chaotic system
- Table 3.2: Percentage error in adaptive synchronization with respect to parameter 'c'
- Table 4.1: Summary of range of parameters 'a' and 'b' for PUCS and its proposed variants
- Table 4.2: Summary of Lyapunov Exponents and Kaplan York Dimensions for PUCS
- Table 4.3: Parameters of PUCS and its chaotic variants
- Table 4.4: Features of the proposed variants
- Table 4.5: Normalized element values of the proposed PUCS circuit
- Table 5.1: Chaotic systems mapped on proposed topology
- Table 6.1: Components' values for the CFOA based design of the proposed system
- Table 6.2: Components' values for the CFOA based design of the proposed adaptive synchronization scheme
- Table 7.1: Component Values of the circuit realization of the proposed systems
- Table 7.2: Comparison table of the existing designs with the proposed design
- Table 8.1: Summary of the hardware and delay requirements for FPGA based implementation of chaotic systems

## LIST OF ABBREVIATIONS

LCS	Lorenz Chaotic System
PUCS	Pehlivan Uyaröglu Chaotic System
MACM	Méndez-Arellano-Cruz-Martínez
HCS	Hyper Chaotic System
OpAmp	Operational Amplifier
CFOA	Current Feedback Operational Amplifier
OTRA	Operational Transresistance Amplifier
VDBA	Voltage Differencing Buffered Amplifier
CC	Current Conveyor
VDTA	Voltage Differencing Transconductance Amplifier
DVCCTA	Differential Voltage Current Conveyor Transconductance Amplifier
AM	Analog Multiplier
IC	Integrated Circuit
ASIC	Application Specific Integrated Circuit
FPGA	Field Programmable Gate Array
RK	Runge Kutta
HDL	Hardware Description Language
KCL	Kirchoff's Current Law
MC	Monte Carlo
RCS	Rabinovich Chaotic System
KVL	Kirchoff's Voltage Law
YCCS	Yang Chen Chaotic System



# **Chapter 1**

## **Introduction**

---

## **1.1 Background**

Chaos is an inherently unpredictable phenomenon of non-linear deterministic dynamic systems, but with an underlying structure in three-dimensional space. The chaotic systems have been a hot spot in research since Lorenz Chaotic System (LCS) was discovered in 1963 [1], which was followed by Rössler chaotic system proposed in 1976 [2], the Chua's circuit realized in 1983 [3], and a series of other chaotic systems thereafter. These chaotic systems were developed while the scientists were trying to model a natural phenomenon. For instance, Lorenz developed the chaotic system while trying to make weather predictions.

Chaotic systems find wide range of applications in secure communication [4-7], speech encryption [8], image encryption [9,10], text encryption [11,12], weather prediction [13] and solar irradiance forecasting [14] due to their high sensitivity on initial conditions, nonlinearity, and non-repeatability of trajectory. For a system to behave chaotically, it should have minimum three number of state variables. However, with the increase in the demand of high security of data, the systems with more than three number of state variables, with an increased degree of complexity have also been developed. Hyperchaotic systems belong to this class of chaotic systems with more than three state variables. The analog circuits using off the shelf components which can mimic the behaviour of chaotic systems can be very useful, especially in the field of communication. Besides, digital design of chaotic systems has their own advantages in terms of reconfigurability, parallelism, etc.

Also, the applications of chaotic systems in describing the different phenomena, the synchronization between two chaotic systems is equally important. A complete hardware circuitry of a synchronized system can be very beneficial in the portable devices.

This work revolves around the development of new chaotic and hyperchaotic systems, their hardware efficient realizations in analog and digital domains, and their synchronization.

## **1.2 Available literature**

This section reviews the major developments in the field of design and analysis of chaotic systems and circuits. The analog and digital implementation of chaotic systems, development of new chaotic and hyperchaotic systems, synchronization between chaotic systems, etc. are some of the key points that are covered in this section based on the survey done.

### 1.2.1 Chaotic systems

A chaotic system is mathematically represented by set of governing equations. It requires minimum three state variables for supporting sustained aperiodic oscillations. Also, there must be at least one non-linear term in the set of governing equations for the system to behave chaotically. Further, any three- dimensional set of non-linear differential equations can be said to have chaos if it has a positive largest Lyapunov exponent, a fractional Kaplan Yorke dimension and a period-doubling route to chaos. The phase space trajectories of a system are visual evidence of its chaoticity, and are known as strange attractors.

The available chaotic systems can be classified based on type of non-linearity used. Quadratic non-linearity [1,2,15-38] cubic non-linearity [39,40], quartic non-linearity [41], absolute non-linearity [42], sine hyperbolic non-linearity [43], exponential non-linearity [42,44], quadratic exponential non-linearity [45-47] etc. are some of the representatives of the respective class. The chaotic systems with quadratic non-linearity can further be grouped in terms of the number of non-linear terms. Rössler chaotic system [2], chaotic system in [22] and Sprott case F-S (out of the sixteen different chaotic systems ‘A-S’ proposed by J.C. Sprott) [16] use single nonlinear term, while Lorenz [1], Pehlivan Uyaröglu chaotic system (PUCS) [15], Sprott case A-E [16], and many other chaotic systems [17-36] employ two nonlinear terms, and [37,38] has three non-linear terms. The chaotic systems with similar nonlinearity may use different number of terms to describe the system’s dynamics. For instance, Sprott case A-E use five terms [16], Sprott case F-S [16], Lu chaotic system [33], T chaotic system [35] and PUCS [15] with six terms, seven terms in Lorenz [1], Li [32], Chen [34] and Méndez-Arellano-Cruz-Martínez (MACM) chaotic system [36]; and eight in Rabinovich chaotic system [37,38].

Another view of the chaotic systems can be from the point of type of fixed point. A fixed point, sometimes called an equilibrium point or singular point, is the state variables’ values where the corresponding time derivative has zero values. The existing chaotic systems can be categorized as those having single hyperbolic type fixed point, such as Sprott case I,J,L,N,R [16] and others in [48-50], finite number of hyperbolic fixed points [1,2,15,26], infinite number of fixed points[28], no fixed point [22, 28], non-hyperbolic type fixed point [29], etc.

Also, the type of attractors being generated by these systems can be single scroll, as in Rössler [2], double scroll in Lorenz [2], PUCS [15], Chen [34], and 4-scroll in [51].

In order to increase the degree of complexity, the dimensions of the chaotic systems can be extended beyond three and such systems are referred as Hyperchaotic Systems (HCSs). The

available HCSs are either expansion of existing chaotic systems [52-61] by adopting feedback laws, or altogether new systems are developed [62-70]. For instance, HCSs have been derived from Lü chaotic system [52], T chaotic system [53], Chen chaotic system [54,55], Lorenz chaotic system [56,57], Rabinovich chaotic system [58], MACM chaotic system [59], Liu chaotic system [60,61] and many more. The new HCSs use different types of non-linearities such as quadratic [62-67], sine hyperbolic [68], hyperbolic tangent [69], etc. These systems can also be categorized as ones with one hyperbolic type fixed point [62,69], finite number of hyperbolic fixed points [63-65], infinite number of hyperbolic fixed points [68], no fixed point [67], non-hyperbolic type fixed points [66], etc. Also, the type of attractors being produced by these HCSs can be two scroll [62, 65, 68], four scroll [70], irregular [64,67,69] in shape.

### **1.2.2 Analog circuit realization of chaotic systems**

The development of chaotic systems was confined to mathematical abstraction and computer simulations till 1983. The actual physical implementation of a chaotic system started with the design of Chua's circuit [3] in 1983. It uses two capacitors, one inductor, one passive resistor and one non-linear negative resistor, also known by name Chua's diode. Thereafter, a variety of both voltage and current mode active blocks have been used to implement Chua's diode over the years, including Operational Amplifiers (OpAmps) [71,72], Current Feedback Operational Amplifier (CFOA) [73], Operational Transresistance Amplifier (OTRA) [74], Voltage Differencing Buffered Amplifier (VDBA) [75], Current Conveyor- II (CC-II) [76], Voltage Differencing Transconductance Amplifier (VDTA) [77], and Differential Voltage Current Conveyor Transconductance Amplifier (DVCCTA) [78].

The hardware realization of other chaotic systems is obtained by implementing constituent governing equations. In general, the hardware realization of a chaotic system requires three energy storing elements that correspond to three state variables. Here, analog blocks, such as OpAmps [15,32,36,79,80] and CFOAs [81], are used for performing addition/ subtraction and scaling. Further, an Analog Multiplier (AM) is used to realize quadratic non-linearity. It is pertinent to mention that CFOAs and AMs are available commercially in the form of Integrated Circuit (IC) AD844 and AD633 respectively. The versatility of AD633 in performing operations, such as, addition, subtraction, scaling and generating quadratic nonlinear terms has been exploited in [82]. Here, for implementation of VB2 chaotic system, a methodology has been proposed wherein minor modifications are suggested in governing equations for their simplification and OpAmp is used if AD633 is overloaded.

It may be noted that chaotic systems with quadratic non-linearity use analog multiplier in addition to other active blocks. In order to reduce overall footprint and power consumption, chaotic system with exponential non-linearity is presented in [44-47] which use diodes for realizing non-linear terms.

### **1.2.3 Synchronization in chaotic systems**

The dynamical nature of the chaotic systems has an extreme dependence on the initial conditions and system parameters. This dependency does not allow even the identical chaotic systems to have similar trajectories at a given point of time. Synchronizing two chaotic systems is a process by which they proceed to behave in unison with time, even for different initial conditions and parameters.

In order to utilize chaotic signals in private communications, the receiver's chaotic signals must match with that of transmitter. Chaos synchronization, thus refers to development of control laws using the known information so that the controlled receiver (slave) is synchronized with transmitter (master) and their dynamic behaviors are identical with respect to time. Carroll and Pecora were the first ones to introduce synchronization among chaotic systems by linking them through a common signal [83]. Different synchronization schemes have been developed since then to synchronize receiver with the transmitter. If the system parameters are precisely known, non-adaptive controls such as unidirectional, bidirectional, sliding mode control [84] methods can be used. In the presence of uncertainties in parameter values, adaptive control methods can achieve the synchronization. Adaptive control synchronization is popularly used for synchronizing two identical chaotic/ hyperchaotic systems even with an uncertainty in their parameter values [17,85-95]. However, the circuit implementation of synchronization schemes has not been explored.

### **1.2.4 Digital design of chaotic systems**

An alternative practical platform for chaotic systems to become real time applications friendly is the digital platform. Digital design of chaotic systems can be done based on Application Specific Integrated Circuits (ASICs), and Field Programmable Gate Arrays (FPGAs). ASICs are capable of providing better performance than its counterparts, however, the prototype productions of ASIC based applications are time and cost intensive than the alternate solutions. Also, in order to bring down the cost, ASIC based applications stand in need of mass production which is intolerant to even minute errors. FPGAs provide enough resources at low cost and

desired flexibility for the implementation of chaotic systems. Thus, in early design phases, FPGAs are best fit for rapid prototyping and low-cost design.

Moreover, due to the high potential in parallel computing, faster speed, extensive available resources and reconfigurability, FPGAs have been popularly used for the implementation of chaotic systems in literature [96-103].

The governing equations of chaotic system are converted in discrete form for implementation in digital platform using numerical methods, such as Heun [96,97], Euler [103] and fourth order Runge Kutta (RK4) method [97]. These discrete equations are coded in Hardware Description Languages (HDLs) for further implementation in FPGAs. In HDLs, while Verilog has been chosen in [98, 101, 102], VHDL is used in [96, 97, 99, 100,103].

An extensive literature survey suggests that different combinations of numerical methods, HDLs and FPGA families have been used to design chaotic systems. For instance, in [96-98,103], Virtex FPGA family has been used to map chaotic systems while Artix, Zynq, Kintex and Altera Cyclone are employed in [99], [100], [101] and [102] respectively. Though Artix has lesser resources than Kintex and Virtex in 7 series, but all of these have sufficient resources to implement a chaotic system. Thus, the choice of family does not affect the performance unless the resources are depleted here.

### **1.3 Research Gaps**

Based on the comprehensive literature survey, the research gaps have been identified as follows:

- Most of the existing designs of chaotic systems use voltage mode active block namely OpAmps. On the other hand, the current mode active blocks have capabilities of providing compact realizations. There is a lean presence of realization of chaotic circuits using current mode active blocks.
- A generalized circuit topology to implement chaotic systems has not been widely explored in literature.
- There is limited literature available on hyperchaotic systems, their circuit design, and applications.
- There is lean presence of hardware realization of adaptive control synchronization scheme in chaotic and hyperchaotic systems.
- The digital design of chaotic systems based on FPGAs has not been widely explored in the literature. Also, the comparison of implementation of different chaotic systems on

same FPGA platform has not been reported yet.

## 1.4 Research objectives

The identified research gaps have promoted to set up the following research objectives:

1. To implement chaotic circuits with reduced active block/ component count.
2. To develop new designs for chaotic systems with more than three number of variables.
3. To design complete circuit topologies of synchronization schemes for chaotic systems.
4. To explore the digital design of chaotic circuits.

## 1.5 Organization of thesis

In this study, some investigations on the design of chaotic systems with reduced hardware, development of new chaotic systems, formulation and analog circuit design of their applications in synchronization and digital design of chaotic systems, have been carried out. The work has been described in nine chapters.

**Chapter 1** is devoted to the study of chaotic systems with an aim to bring most of the published information related to chaotic systems' implementations. A review of existing work on adaptive control synchronization of chaotic systems and digital design as well has been presented thereafter. This is followed by identification of research gaps and setting up of the research objectives.

**Chapter 2** presents the basic terminology related to the thesis, which includes the definitions of the dynamic properties of chaotic systems. The port relationships and characterization of the active blocks, namely CFOA and AM, used in the circuit designing are briefly described. The numerical methods for digitization of differential equations and the summary of the available resources on target FPGA device have also been highlighted in this chapter.

**Chapter 3** presents realization of a chaotic system with one quadratic non-linearity, namely Rössler chaotic system, using CFOA and AM and the functionality of the circuit is tested through LTspice simulations and experimentation. It includes simulation results for time domain, frequency domain and phase space trajectories in various planes. The robustness of the circuit is inspected against variation in component values through Monte Carlo analysis.

The adaptive control synchronization scheme between two Rössler chaotic systems is formulated first followed by the complete circuit realization of the scheme using CFOAs and Analog Multipliers (AMs).

In **Chapter 4**, four variants of PUCS with two non-linear terms have been proposed, and the properties are studied through numerical simulations. The stability of the fixed points of PUCS and its proposed variants is examined using Jacobi stability analysis. The properties of the proposed PUCSs are examined through numerical simulations and the parameter values are obtained by observing bifurcation diagrams for state variables. Further, the convergence/divergence of nearby orbits is investigated by noticing the evolution of Lyapunov exponents with time. A CFOA based circuit is put forward that can realize the existing PUCS and its proposed variants, by simply adjusting component values. The behaviour of the proposed variants in time domain, frequency domain and phase space have been examined through simulations in LTspice design environment. Furthermore, the feasibility of the proposed variants is also discussed through presenting the electronic circuit implementation of two of the variants on breadboard and the results are found to be well aligned with the LTspice simulations. Monte Carlo (MC) simulations are also included to show the robustness of the proposed circuit against parameter variations.

**Chapter 5** presents a generic structure to realize chaotic systems, with quadratic type non-linearities, employing only one type of active block, namely AD633, which is a commercially available IC of analog multiplier and few off the shelf passive components, namely resistors and capacitors. The simulations have been performed in LTspice design environment, and the results in the form of phase space diagrams have been presented, the shape of which confirms the feasibility of the presented approach.

In **Chapter 6**, a new three-dimensional chaotic system with two exponential non-linearities is presented. The parameter values are obtained by observing the bifurcation diagrams. The properties of the proposed chaotic system, including Lyapunov exponents, Kaplan Yorke dimension and dissipativity are investigated using numerical simulations. The hardware feasibility of the proposed system is illustrated through CFOA based circuit implementation. To confirm the chaotic nature of the proposed circuit, LTspice simulations are done to obtain phase portraits which are found to be strange attractors and are topologically different from the shape of the existing attractors. Further, the synchronization of the proposed chaotic system is



formulated mathematically using adaptive control synchronization scheme and proposed CFOA based complete circuit for adaptively synchronized system is also designed using CFOAs, diodes, resistors and capacitors.

**Chapter 7** is a record of a new four-dimensional hyperchaotic system with quadratic type nonlinearities. The chaotic dynamical behaviors of the proposed system and its dynamic properties have been examined through numerical simulations. To explore the proposed systems' applications in communication world, adaptive control synchronization scheme for proposed HCS is also examined. The electronic realizability of the proposed system and the complete adaptive control synchronization scheme is examined through CFOA and AM based circuit designs and simulations in LTspice design environment.

**Chapter 8** puts forward a systematic approach to implement chaotic systems with quadratic non-linearities on digital platform using Runge Kutta 4 (RK4) numerical method. FPGAs have been used for the implementation using Verilog Hardware Description Language (HDL) and the state machine control. The synthesis results based on Xilinx Artix device 7a200tffv1156-1, and simulation results using inbuilt simulator of Vivado design suite have been presented. The implemented chaotic systems have been evaluated on the basis of hardware utilization and time delay. The simulations results have been validated by python based numerical simulations as well.

The work is concluded on the roadmap outlined above in **Chapter 9**.

# **Chapter 2**

## **Basic Terminology**

---

## 2.1 Introduction

There has been continuous development of chaotic systems due to the ease with which these explain complex nature of dynamical systems. A chaotic system is characterized by three state variables, whose dynamics follow certain rules, which are represented by non-linear differential equations showing the relation between state variables and certain tunable constant parameters. The properties of the chaotic systems are examined through numerical simulations and the parameter values are obtained by observing bifurcation diagrams. The convergence/divergence of nearby orbits is investigated by noticing the evolution of Lyapunov exponents with time. The complexity of chaotic systems is numerically defined by Kaplan Yorke dimension. The stability of chaotic systems is examined using Jacobi stability analysis. This chapter presents the terminology and parameters pertaining to chaotic systems for easy readability.

Besides, CFOA and AM, the analog building blocks which have been utilized to design chaotic circuits have been described briefly in this chapter.

## 2.2 Estimation of parameters and properties of a chaotic system

For a three-dimensional set of non-linear differential equations to behave chaotically, their mathematical representation should have at least three phase space variables and minimum five terms including one non-linearity. They are then analyzed for other dynamic properties and parameter values to qualify for being chaotic. Consider a three-dimensional chaotic system with two quadratic non-linearities, two parameters, and total six terms, popularly known as Pehlivan Uyaröglu Chaotic System (PUCS). In order to estimate these parameters for which PUCS will behave chaotically, bifurcation plots are required, which depict the variation in the values of state variables with respect to a given parameter. So, this section presents the bifurcation plots and properties of chaotic systems explained taking the example of PUCS.

The representative governing equations of this chaotic system are given in (2.1).

$$\dot{x} = y - x \quad (2.1a)$$

$$\dot{y} = ay - xz \quad (2.1b)$$

$$\dot{z} = xy - b \quad (2.1c)$$

Here, the dots above the state variables  $x$ ,  $y$  and  $z$  represent their time derivatives.

### 2.2.1 Bifurcation diagrams

The effect of parameter variation on the behaviour of a non-linear dynamic system can be studied using bifurcation diagrams, which are plotted between the values of any one state variable and a parameter while keeping other parameters fixed. Out of the two parameters in (2.1), let us plot the bifurcation diagram, keeping parameter 'b' fixed to value 0.5 and varying parameter 'a.' The bifurcation plot is presented in Fig. 2.1, where the maximum value of state variable  $x$  is plotted against the variation in parameter 'a.' The similar procedure can be repeated for  $y$  and  $z$  phase space variables as well. It is evident from the Fig. 2.1 that in the system of equations in (2.1), the route to chaos with period doubling is from right to left, i.e. with the decreasing values of parameter 'a.' It behaves chaotically for  $a \in [0, 0.665]$ .

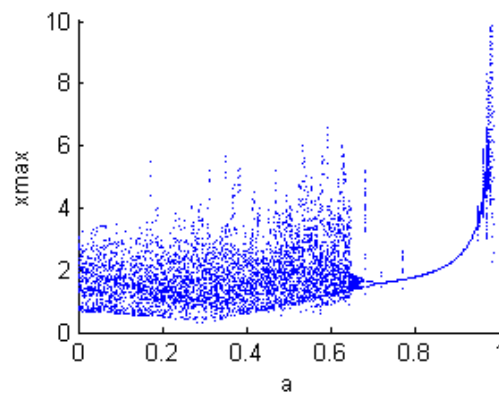


Fig. 2.1 Bifurcation plot of PUCS with respect to parameter  $a$

Once the valid ranges of parameters are determined for the system to behave chaotically, the evolution of Lyapunov exponents with time is observed for a particular value of parameters in order to demonstrate the system dynamics in more detail.

### 2.2.2 Lyapunov Exponents

The property of chaotic systems having a heavy dependence on initial conditions is quantified as Lyapunov exponents. It gives a quantitative measure of the exponential rate of convergence or divergence of nearby trajectories of phase space diagrams plotted among the state variables. Mathematically, the Lyapunov exponent is computed as the average logarithmic rate of separation between two closely spaced trajectories. MATLAB simulations may be used to determine the Lyapunov exponents for a chaotic system. For instance, the Lyapunov exponents for PUCS in (2.1) are 0.3, 0, -0.8. At least one positive Lyapunov exponent indicates chaos.

### 2.2.3 Kaplan Yorke Dimension ( $D_{KY}$ )

The Kaplan Yorke dimension ( $D_{KY}$ ), is an additional parameter that may be used to compare the complexity of the attractors [104]. It is defined in terms of fractional geometrical dimension where a collection of initial conditions will neither contract nor expand as it advances in time.

It is calculated as:

$$D_{KY} = j + \frac{1}{|L_{j+1}|} \sum_{i=1}^j L_i \quad (2.2)$$

Where  $L_i$  is the  $i^{\text{th}}$  Lyapunov exponent and  $j$  is the number of Lyapunov exponents whose summation is positive. Chaotic flows always have  $D_{KY} > 2$ .

For example, calculating  $D_{KY}$  of PUCS,

$$D_{KY} = 2 + \frac{1}{|-0.8|} (0.3 + 0)$$

$$D_{KY} = 2.38$$

### 2.2.4 Dissipativity

The dynamic systems can be dissipative, conservative, and explosive depending on the sign of the gradient of the phase space volume being negative, zero and positive respectively. The chaotic systems can be dissipative with shrinking phase-space volume or conservative with constant phase space volume but not explosive with expanding phase-space volume because of the unbounded dynamics.

The divergence of a system  $f(x, y, z) = \begin{cases} f_1(x, y, z) \\ f_2(x, y, z) \\ f_3(x, y, z) \end{cases}$  is given by

$$\nabla \cdot f = \frac{\partial f_1}{\partial x} + \frac{\partial f_2}{\partial y} + \frac{\partial f_3}{\partial z} \quad (2.3)$$

where

$f_1, f_2$  and  $f_3$  are the functions representing the dynamics of state variables  $x, y$  and  $z$  respectively.

Dissipative dynamical systems [22] satisfy the property (2.4).

$$\nabla \cdot f < 0 \quad (2.4)$$

Where,  $\nabla \cdot f$  is the gradient of the phase space volume.

The divergence of PUCS is

$$\nabla \cdot f = \frac{\partial(y-x)}{\partial x} + \frac{\partial(ay-xz)}{\partial y} + \frac{\partial(xy-b)}{\partial z} \quad (2.5)$$

$$\nabla \cdot f = -1 + a \quad (2.6)$$

From the bifurcation plot in Fig. 2.1, it is evident that the system is chaotic for  $a < 0.665$ . So, the function in (2.6) will always be a negative value, thus PUCS is dissipative.

### 2.3 Analysis of Fixed Points

In mathematics, points at which the dynamics of a function is zero are referred as fixed points, i.e. the given function is neither increasing nor decreasing with time.

The stability of the fixed points is examined using Jacobi stability analysis method outlined in [105]. The description of the step-by-step process is given below:

- Step 1 : Equate the governing equations of a chaotic system to zero for calculating fixed (equilibrium) points, i.e. the time differentiation of state variable may be equated to zero to determine fixed points.
- Step 2 : Form Jacobian matrix J corresponding to fixed points obtained in step (1) for determining the stability. The three rows of this Jacobian matrix are obtained by differentiating corresponding governing equations with respect to x in row 1, y in row 2 and z in row 3.
- Step 3 : Find out eigenvalues corresponding to fixed points by solving the characteristic equations  $|J - \lambda I| = 0$ , where I being the identity matrix,  $\lambda$ s are the eigenvalues and  $| |$  represents the determinant of matrix  $[J - \lambda I]$ . These values will give an indication of the deviation of the neighboring trajectories from the fixed points.

The above procedure is illustrated below for PUCS:

In step 1, the fixed points of PUCS are found by setting  $\dot{x} = 0$ ,  $\dot{y} = 0$  and  $\dot{z} = 0$  in (2.1).

$$\begin{cases} y - x = 0 \\ ay - xz = 0 \\ xy - b = 0 \end{cases} \quad (2.7)$$

It may be noted that for  $y = 0$ , fixed points do not exist because it will not satisfy equation  $xy - b = 0$ , where b is a positive constant. Considering  $y \neq 0$  and solving (2.7) gives the following fixed points:

$$p_1 = (\sqrt{b}, \sqrt{b}, a) \text{ and } p_2 = (-\sqrt{b}, -\sqrt{b}, a).$$

The Jacobian matrix for PUCS consists of three rows. The values in 1<sup>st</sup>, 2<sup>nd</sup> and 3<sup>rd</sup> rows are found by differentiating the three governing equations with respect to x, y and z respectively.

$$J = \begin{bmatrix} -1 & 1 & 0 \\ -z & a & -x \\ y & x & 0 \end{bmatrix} \quad (2.8)$$

The Jacobian matrices  $J_{p1}$  and  $J_{p2}$  corresponding to fixed points  $p_1$  and  $p_2$  are given by (2.9) and (2.10) respectively.

$$J_{p1} = \begin{bmatrix} -1 & 1 & 0 \\ -a & a & -\sqrt{b} \\ \sqrt{b} & \sqrt{b} & 0 \end{bmatrix} \quad (2.9)$$

and

$$J_{p2} = \begin{bmatrix} -1 & 1 & 0 \\ -a & a & \sqrt{b} \\ -\sqrt{b} & -\sqrt{b} & 0 \end{bmatrix} \quad (2.10)$$

respectively.

In step 3, the eigenvalues are computed by equating  $|J_{pi} - \lambda I|$  with 0. This results in characteristic equation of (2.11) for both  $p_1$  and  $p_2$ .

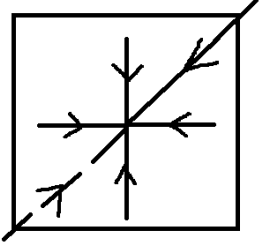
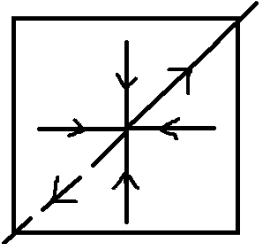
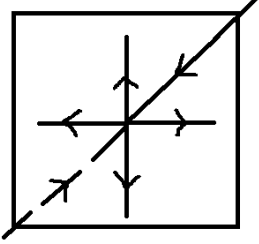
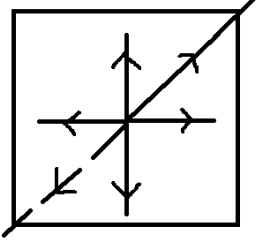
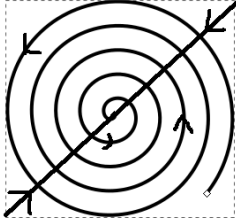
$$\lambda^3 + (1 - a)\lambda^2 + (b - a)\lambda + 2b = 0 \quad (2.11)$$

Considering  $a = b = 0.5$  in (2.11) the eigenvalues are computed as

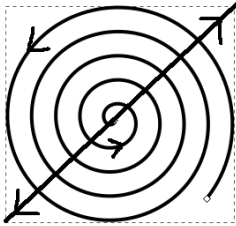
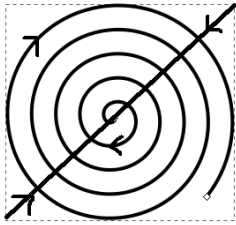
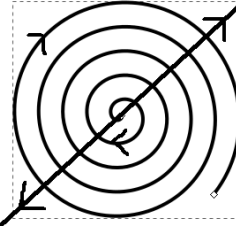
$$\lambda_1 = -1; \lambda_2 = 0.25 + 0.9682i \text{ and } \lambda_3 = 0.25 - 0.9682i.$$

The fixed points can be hyperbolic or non-hyperbolic in nature [106]. The hyperbolic fixed points have all the eigenvalues with non-zero real part, while non-hyperbolic fixed points have one or more eigenvalues with zero real part. The hyperbolic fixed points can further be classified in eight different categories depending on the sign of the real part of their eigenvalues, where index refers to the dimension of unstable manifold i.e. the number of eigenvalues with positive real part. The eight categories have been summarized in Table 2.1 below:

Table 2.1 Types of hyperbolic fixed points in three dimensional chaotic systems

Category	Nature of eigenvalues	Three-dimensional representation
index-0	All the eigenvalues are real negative. The fixed point is a stable node. The trajectories move inward linearly in all three directions , i.e. x, y and z.	
index-1 saddle	The dimension of unstable manifold is 1 and all the eigenvalues are real. The trajectories move inward linearly along two directions and outward linearly in third direction.	
index-2 saddle	Two of the three real eigenvalues are positive. The trajectories move outward linearly along two directions and inward linearly along third direction.	
index-3	All the three real eigenvalues are positive. The fixed point is an unstable node. All the trajectories are moving outwards linearly.	
index-0 spiral	One real negative eigenvalue and two complex conjugates with negative real part. This indicates an inward spiral and a stable linear manifold.	



index-1 spiral saddle	One eigenvalue is real positive and two are complex conjugates with negative real part. This indicates an inward spiral and an unstable linear manifold.	
index-2 spiral saddle	One eigenvalue is real negative and two are complex conjugates with positive real part. This indicates an outward moving spiral and a stable linear manifold.	
index-3 spiral	One eigenvalue is real positive and two are complex conjugates with positive real part. This indicates an outward moving spiral and an unstable linear manifold.	

The shape of the attractors stems from the stretching and folding operations corresponding to the unstable and stable manifolds. So, the eigenvalues obtained from (2.11) indicates that the fixed points are index-2 saddle type.  $\lambda_1 = -1$  indicates a linear stable manifold, while  $\lambda_2$  and  $\lambda_3$  are an indication of unstable spiral manifold because of the positive real part. Here, the unstable spiral manifold stretches the attractor outwards while the stable linear manifold folds it back inside.

## 2.4 Analog Building Blocks

In this work, CFOA and AM active building blocks are used to implement chaotic systems. This section provides a brief overview of these two analog building blocks.

### 2.4.1 Current Feedback Operational Amplifier (CFOA)

The block diagram of CFOA is depicted in Fig. 2.2. An input voltage applied to the 'Y' terminal is buffered by voltage buffer VF, which in turn, produces a current  $I_x$  returning through 'X' terminal. The input port 'Y' has high input impedance, while input port 'X' has low input impedance. The input current is mirrored at 'Z' terminal. The output of the transimpedance source is connected to unity gain buffer VF, which leads to the output port  $V_o$ .

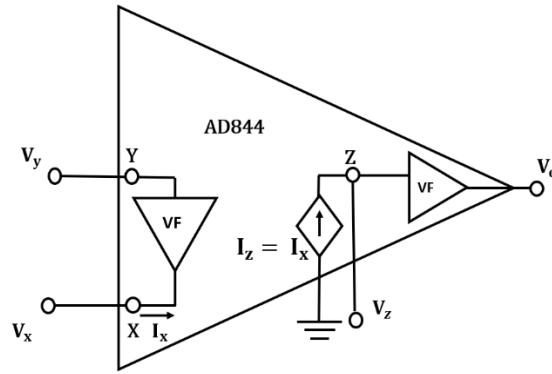


Fig. 2.2 The block diagram of CFOA [107]

The constituent port relations of CFOA are given as:

$$V_x = V_y; I_y = 0; I_z = I_x; V_o = V_z.$$

The CFOA is available commercially in the form of Integrated Circuit (IC) AD844. It is an eight pin IC, whose pin diagram is presented in Fig. 2.3.

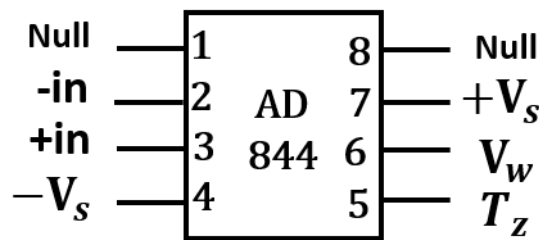


Fig. 2.3 Pin diagram of AD 844

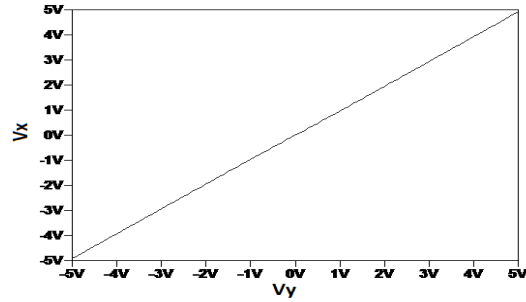
The pins -in, +in,  $T_z$  and  $V_w$  pins refer to ‘X’, ‘Y’, ‘Z’ and ‘O’ ports in Fig. 2.2 respectively. The operation range of voltage supply for AD844 is  $\pm 4.5V$  to  $\pm 18V$ .

### 2.4.1.1 CFOA Characterization

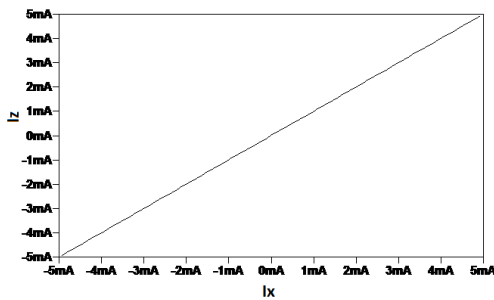
The port relation between  $V_y$  and  $V_x$  is verified through dc simulations. The input voltage at Y port ( $V_y$ ) is varied from  $-5V$  to  $+5V$  and the voltage is observed at port X ( $V_x$ ). The simulation results are depicted in Fig. 2.4(a) which verifies the relation  $V_x = V_y$ .

To verify the current relation between X and Z ports, a dc current is applied at X terminal and is varied from  $-5mA$  to  $+5mA$ . The current through Z terminal ( $I_z$ ) is observed and is plotted in Fig. 2.4(b). It may be observed that  $I_z$  follows  $I_x$  closely and thus verified relation  $I_z = I_x$ .

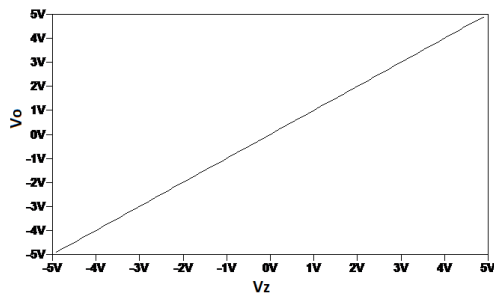
To verify the port relationship between ports W and Z, the voltage  $V_w$  is plotted against variation  $V_z$ . The relationship  $V_w = V_z$  is verified by observation in Fig. 2.4(c).



(a)



(b)



(c)

Fig. 2.4 DC characteristics of AD844 between (a) Voltages at X and Y terminal; (b) Current in Z and X terminal; (c) Voltages at W and Z terminal

### 2.4.1.2 Basic Circuit Applications

This sub-section describes the basic circuit applications of CFOA which have been used in this thesis.

#### 2.4.1.2.1 Subtractor / Summer

A CFOA based summer is shown in Fig. 2.5 (a). The circuit makes use of a single CFOA. The current flowing out of X terminal is

$$I_x = \frac{V_y - V_{in}}{R_1} \quad (2.12)$$

The current through 'Z' terminal is same as  $I_x$ , and the voltage  $V_w$  is same as the voltage at 'Z' terminal. Thus,

$$V_w = \frac{V_y - V_{in}}{R_1} \cdot R_2 \quad (2.13)$$

If the values of resistors  $R_1$  and  $R_2$  are equal, the voltage  $V_w$  is given by

$$V_w = V_y - V_{in} \quad (2.14 a)$$

Thus, it behaves as a subtractor.

Using voltage inverter circuitry as shown in Fig. 2.5(b), the voltage  $V_w$  is given by

$$V_w = V_y + V_{in} \quad (2.14b)$$

Thus, it behaves as a summer.

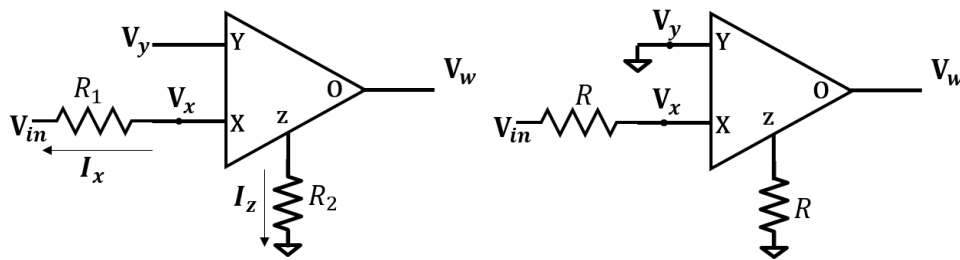


Fig. 2.5 (a) CFOA based summer; (b) CFOA based inverter

#### 2.4.1.2.2 Integrator

The circuit in Fig. 2.6 represents an integrator implemented using a single CFOA.

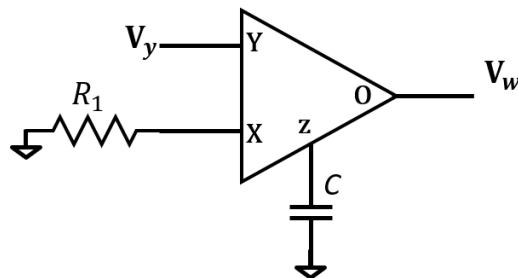


Fig. 2.6 CFOA based integrator

The current through z terminal  $I_z$  is given by (2.15).

$$I_z = C \cdot \frac{dV_z}{dt} \quad (2.15)$$

where,

$V_z$  is the voltage at 'Z' terminal.

Equating (2.15) with the current through 'X' terminal,

$$\frac{V_y}{R_1} = C \cdot \frac{dV_z}{dt} \quad (2.16)$$

(2.16) can be rewritten as

$$V_z = V_w = \frac{1}{R_1 C} \int V_y \quad (2.17)$$

### 2.4.2 Analog Multiplier (AM)

Analog Multiplier (AM), the main building block to implement quadratic non-linearity in chaotic circuits, is available in the form of IC AD633 commercially. For the purpose of the simulations in LTspice, the SPICE model from Analog Devices is used. The pin diagram and internal details of AD633 are given in Fig. 2.7.

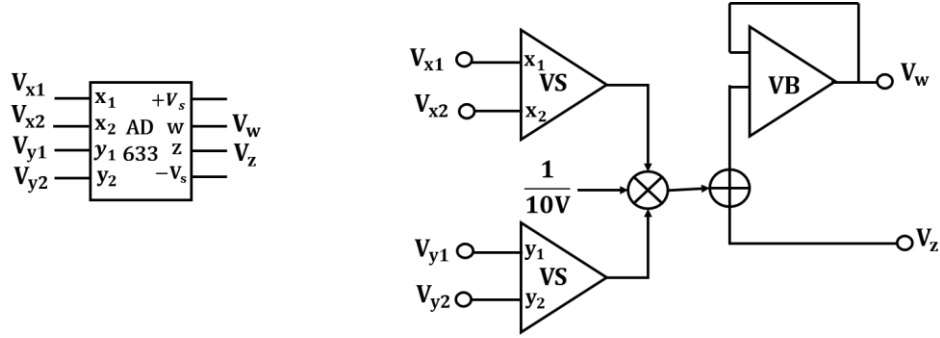


Fig. 2.7 Pin diagram and internal schematic of AD633 [108]

It uses two voltage subtractors for calculating difference between two inputs ( $V_{x1}-V_{x2}$ ,  $V_{y1}-V_{y2}$ ). The multiplier provides the relation  $\left(\frac{(V_{x1}-V_{x2})(V_{y1}-V_{y2})}{10}\right)$ , where the numerator is divided by 10V. One adder is also a part of AD633 to give  $((V_{x1} - V_{x2})(V_{y1} - V_{y2})/10) + V_z$  and one voltage buffer that provides multiplier output at low impedance. The port relation of AD633 is described by (2.18).

$$V_w = \frac{(V_{x1}-V_{x2})(V_{y1}-V_{y2})}{10} + V_z \quad (2.18)$$

By appropriate selection of  $V_{x1}$ ,  $V_{x2}$ ,  $V_{y1}$ ,  $V_{y2}$  and  $V_z$ , AD633 may provide the following outputs:

- (a) Single multiplication (or quadratic) term if  $V_{x2}$ ,  $V_{y2}$  and  $V_z$  are grounded.

$$V_w = \frac{V_{x1}V_{y1}}{10} \quad (2.19)$$

- (b) Single linear term if  $V_{x2}$ ,  $V_{y2}$  and  $V_z$  are grounded and  $V_{y1}$  is set to 1.

$$V_w = \frac{V_{x1}}{10} \quad (2.20)$$

(c) Subtraction of two multiplicative terms if  $V_{x2}$  and  $V_z$  are grounded.

$$V_w = \frac{(V_{x1} \cdot V_{y1} - V_{x1} \cdot V_{y2})}{10} \quad (2.21)$$

(d) Multiplication and accumulation (MAC) term if  $V_{x2}$  and  $V_{y2}$  are grounded.

$$V_w = \frac{V_{x1} \cdot V_{y1}}{10} + V_z \quad (2.22)$$

### 2.4.2.1 AD633 Characterization

The AD633 is characterized through LTspice simulations. The supply voltage is taken as  $\pm 12V$ . The voltage at Z port is taken as a fixed value of  $+1V$ .  $V_{y1}$ ,  $V_{x2}$  and  $V_{y2}$  are set to  $1V$ ,  $0V$  and  $0V$  respectively. The voltage at port X1 is varied from  $1V$  to  $12V$ . The DC voltage characteristics of AD633 in Fig. 2.8 verifies the relation  $V_w = \frac{(V_{x1} - V_{x2})(V_{y1} - V_{y2})}{10} + V_z$ .

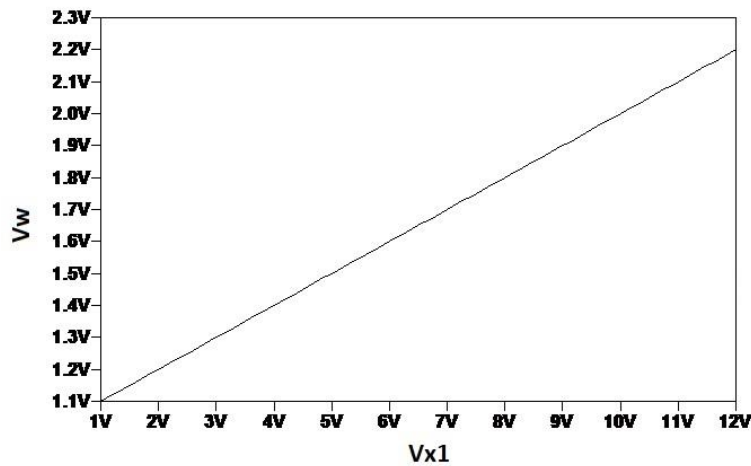


Fig. 2.8 Output voltage of AD633 with respect to variations in input voltages

## 2.5 Concluding Remarks

The terminologies which are being repetitively used in this thesis have been described in this chapter. These include the properties of chaotic systems, such as Lyapunov exponents, Kaplan Yorke dimension and dissipativity. These properties have been elaborated with the help of an example of PUCS. Besides, the study on the nature of fixed points using Jacobi stability

analysis has been done and all possible cases for hyperbolic fixed point have been highlighted in this chapter.

Furthermore, the analog building blocks, CFOA and AM, which have been used in the subsequent chapters for the analog circuit design of chaotic systems, are described in this chapter along with their characteristics.

# Chapter 3

## Chaotic systems with single quadratic non-linearity

---

The content and results of the following paper have been reported in this chapter.

K. Suneja, N. Pandey and R. Pandey, “ **Systematic Realization of CFOA Based Rössler Chaotic System and Its Applications,**” Arabian Journal for Science and Engineering, 10.1007/s13369-021-06379-9.



### **3.1 Introduction**

The mathematical representation of a chaotic system consists of three governing equations corresponding to three state variables. The presence of the non-linear term in the governing equations of a chaotic system is responsible for unpredictability in the output, and the complexity in hardware. Chaotic systems find wide range of applications in secure communication. Synchronization of two chaotic systems may be required in such applications for encoding and decoding of information. Synchronization means that one chaotic system, known as slave, follows the other, known by name master, with time.

This chapter deals with the systematic realization of a chaotic system with one quadratic non-linearity, namely Rössler chaotic system. It has been implemented using popular voltage mode building block namely OpAmp [80, 109]. The circuit reported in [80] uses four OpAmps, one Analog Multiplier (AM), ten resistors and three capacitors while [109] employs six OpAmps, two Analog Multipliers (AMs), thirteen resistors and three capacitors. A variant of Rössler chaotic system is presented in [44, 110] wherein the governing equations are modified while keeping the nature of attractors intact. Both realizations employ five OpAmps, one diode, ten resistors and three capacitors. Current mode building block based realization of Rössler chaotic system is not available in open literature to the best of candidates' exposure in the field. To fill this gap, a CFOA based Rössler chaotic system is presented in this chapter.

The governing equations of Rössler chaotic system are realized with CFOA, considering its advantages in processing both voltage and current signals which results in design flexibility leading to component saving and an Analog Multiplier (AM). The functionality of the design is examined through LTspice simulations and observing the chaotic outputs, their frequency spectrum and phase space trajectories in different planes. The robustness of the proposed circuit is examined against component variation through Monte Carlo analysis. The usability of the chaotic system is illustrated through adaptive control synchronization between two Rössler chaotic systems.

### **3.2 Mathematical model of Rössler chaotic system**

The Rössler chaotic system [2], described by governing equations in (3.1) is a chaotic system with single quadratic non-linearity.

$$\dot{x} = -(y + z) \quad (3.1a)$$

$$\dot{y} = x + ay \quad (3.1b)$$

$$\dot{z} = b + z(x - c) \quad (3.1c)$$

The a, b and c are positive constants whose values for the system to behave chaotically, as studied by Rössler for the first time, are 0.2, 0.2 and 5.7 respectively.

### 3.3 Circuit Realization

In this section, a hardware realization of Rössler chaotic system is presented using CFOAs and Analog Multiplier (AM). The proposed implementation is shown in Fig. 3.1 and corresponding Kirchoff's Current Law (KCL) equations derived through nodal analysis are presented as (3.2).

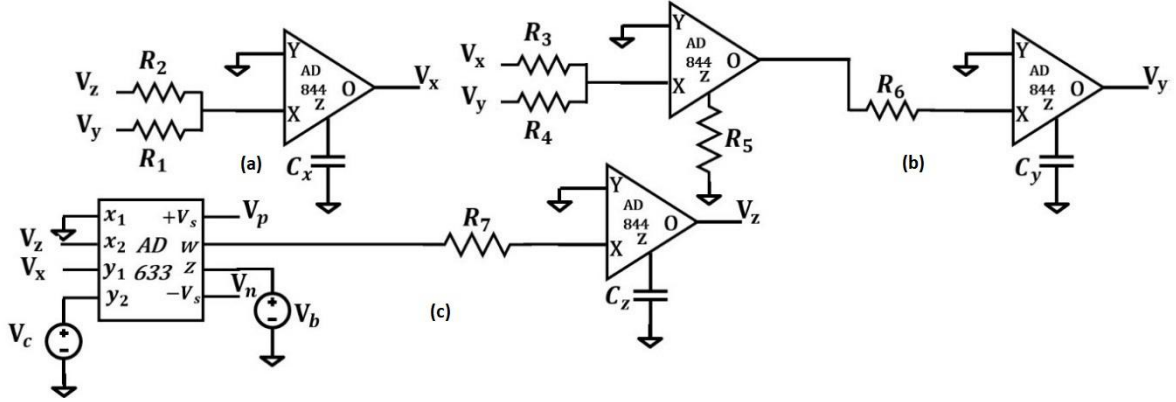


Fig. 3.1 Proposed CFOA based Rössler system

$$\frac{dV_x}{dt} = \frac{-V_y}{R_1 C_x} - \frac{V_z}{R_2 C_x} \quad (3.2a)$$

$$\frac{dV_y}{dt} = \frac{V_y}{R_4 C_y} + \frac{V_x}{R_3 C_y} \quad (3.2b)$$

$$\frac{dV_z}{dt} = \frac{V_x V_z}{10 R_5 C_z} - \frac{V_z V_c}{10 R_5 C_z} - \frac{V_b}{R_7 C_z} \quad (3.2c)$$

Comparing (3.1) and (3.2), the set of equations obtained are put in (3.3).

$$\frac{1}{R_1 C_x} = 1, \frac{1}{R_2 C_x} = 1, \frac{1}{R_3 C_y} = 1, \frac{1}{R_4 C_y} = 0.2, \frac{V_b}{R_7 C_z} = -0.2, \frac{1}{10 R_5 C_z} = 1 \text{ and } V_c = 5.7 \quad (3.3)$$

Comparing the proposed implementation with the existing implementations, it is observed that the proposed realization utilizes four CFOAs, one Analog multiplier (AM), seven resistors, and

three grounded capacitors. Thus, overall component count is minimum in comparison to its OpAmp based counterparts [44, 80, 109, 110].

### 3.3.1 Simulation Results

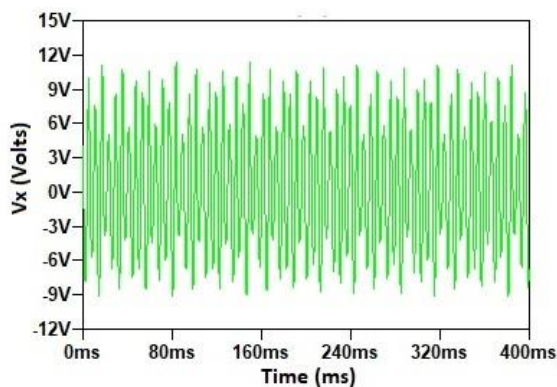
The following simulation steps are used to verify the proposition:

Step 1: Using scaling factor of 1000 in (3.3), component values are found as  $R_1 = R_2 = R_3 = R_5 = R_6 = 10 \text{ k}\Omega$ ,  $R_4 = 50 \text{ k}\Omega$ ,  $R_7 = 1 \text{ k}\Omega$  and  $C_x = C_y = C_z = 100 \text{ nF}$ .

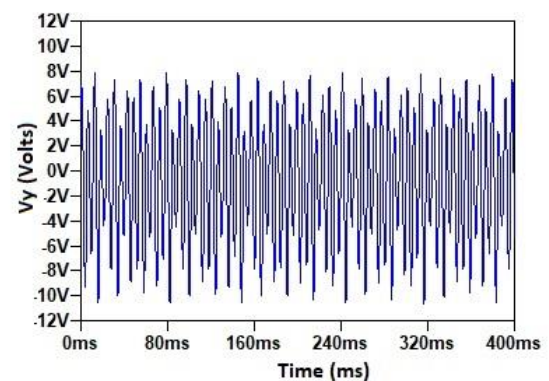
Step 2: The complete circuit was simulated in LTspice design environment using macro models of AD844 and AD633 from Analog Devices [107, 108]. The power supplies are chosen as  $\pm 15 \text{ V}$ .

Step 3: The simulation results are obtained in the form of time series, phase space trajectories and frequency spectrums.

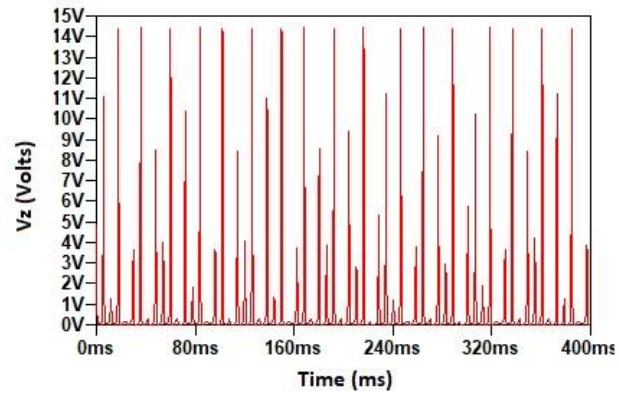
The simulated chaotic outputs in time domain for  $V_x$ ,  $V_y$  and  $V_z$  are shown in Fig. 3.2 and corresponding fourier transforms are depicted in Fig. 3.3. It may be noticed that all the time series waveforms are aperiodic with different shapes. Further, the observed spectrums for state variables  $x$ ,  $y$  and  $z$  are noise like in frequency ranges of (50Hz to 10kHz), (50Hz to 10kHz) and (50Hz to 80kHz) respectively. Thus, the proposed circuit can be used for audio applications. The phase space trajectories, also known as strange attractors, in  $V_x - V_y$ ,  $V_y - V_z$  and  $V_x - V_z$  planes are depicted in Fig. 3.4. The nature of all the phase space trajectories is single scroll.



(a)

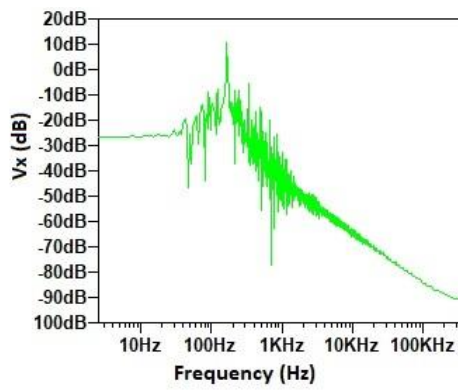


(b)

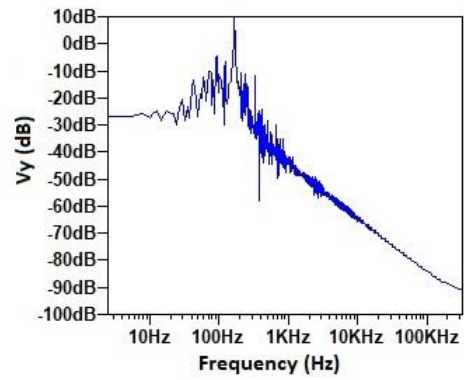


(c)

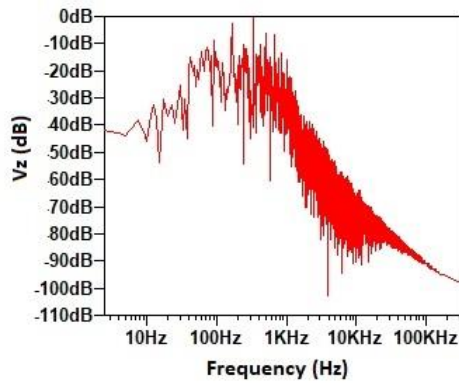
Fig. 3.2 Simulated chaotic outputs at (a)  $V_x$  (b)  $V_y$  (c)  $V_z$



(a)

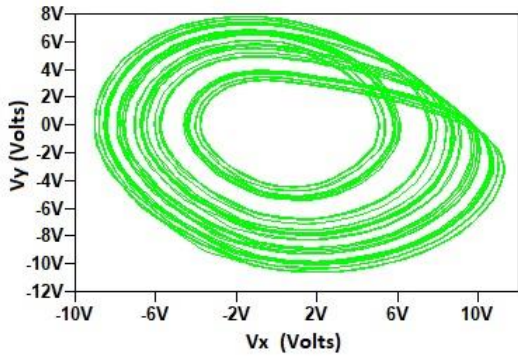


(b)

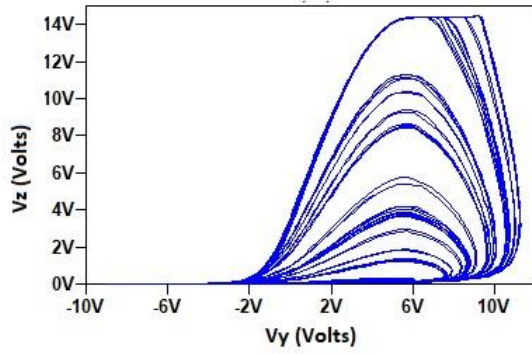


(c)

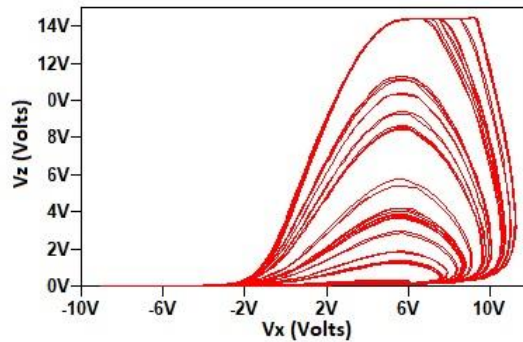
Fig. 3.3 Frequency spectrum of (a)  $V_x$  (b)  $V_y$  (c)  $V_z$



(a)



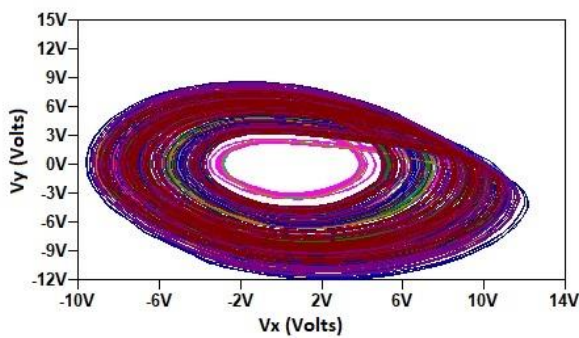
(b)



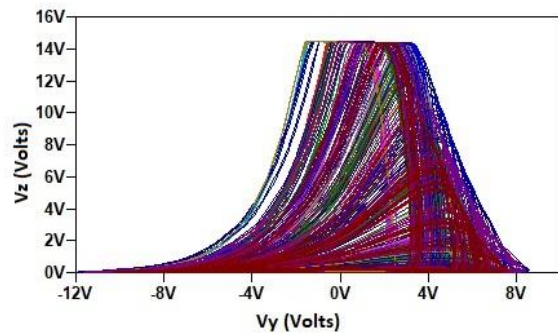
(c)

Fig. 3.4 Simulated phase trajectories in (a)  $V_x - V_y$ , (b)  $V_y - V_z$  and (c)  $V_x - V_z$  planes

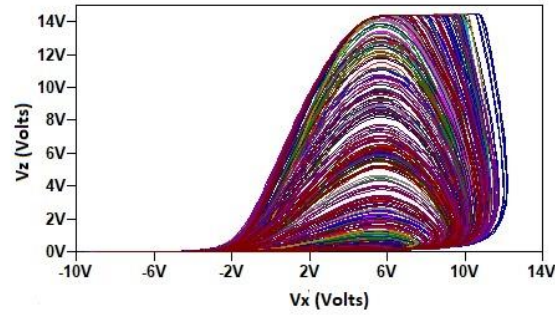
Further, Monte Carlo (MC) analysis is performed by considering 10% tolerance in the passive component values. The simulated phase trajectories in  $V_x - V_y$ ,  $V_y - V_z$  and  $V_x - V_z$  plane are shown in Fig. 3.5, which confirms the robustness of circuit against 10% tolerance in component values.



(a)



(b)



(c)

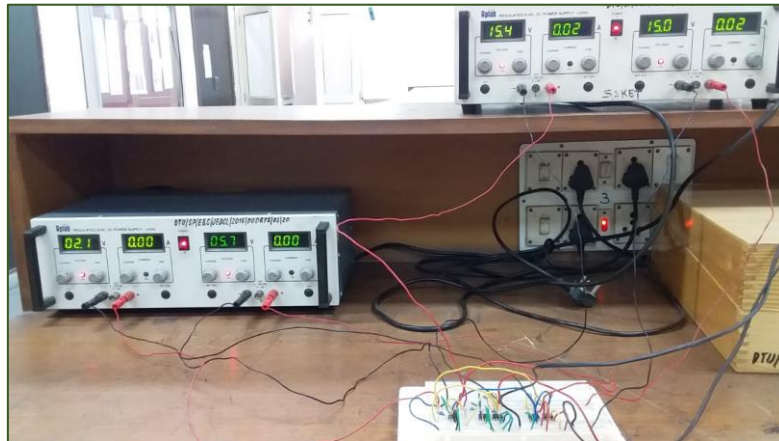
Fig. 3.5 Simulated phase trajectories in (a)  $V_x - V_y$ , (b)  $V_y - V_z$  and (c)  $V_x - V_z$  planes with MC analysis

The proposed realization is compared with the existing ones [44, 80, 109, 110] through simulations. The component values for existing circuits [44, 80, 109, 110] are taken from the respective references and the power supplies are kept same as used in the proposed circuit ( $\pm 15V$ ) for fair comparison. The comparison in terms of hardware and simulated power consumption has been placed in Table 3.1. It is evident from the comparison table that the proposed circuit consumes the least number of passive components and power under same supply voltage conditions.

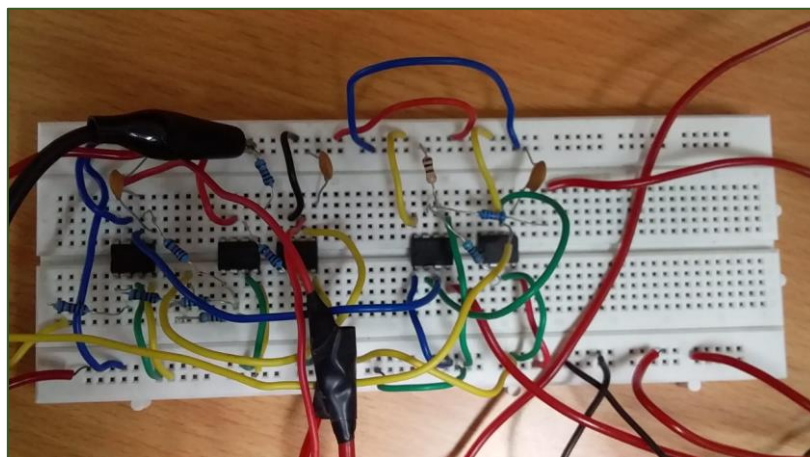
Table 3.1 Comparison of the proposed design with the existing circuit designs of Rössler chaotic system

Reference	Type of active building block	Number of active building blocks	Number of passive elements	Power consumption (in Watts)
[44]	OpAmps	5	14	2.13
[80]	OpAmps and Analog Multiplier	5	13	1.87
[109]	OpAmps and Analog Multiplier	8	16	2.78
[110]	OpAmps	5	14	2.13
Proposed circuit	CFOA and Analog Multiplier	5	10	1.1

Experimental verification of the proposed circuit is also done by bread boarding it using commercially available ICs AD844 and AD633, as shown in Fig. 3.6. The supply voltages and component values are kept same as those used in simulative investigations. The experimental time domain outputs for state variables  $(V_x, V_y)$ ,  $(V_y, V_z)$  and  $(V_x, V_z)$  are shown in Figs. (3.7a) – (3.7c) respectively and corresponding phase trajectories are shown in Figs. (3.7d) – (3.7f). It may be noted that the experimental results are in compliance with the LTspice simulations.



(a)



(b)

Fig. 3.6 (a) Experimental setup; (b) Breadboard circuit for implementation of Rössler chaotic system

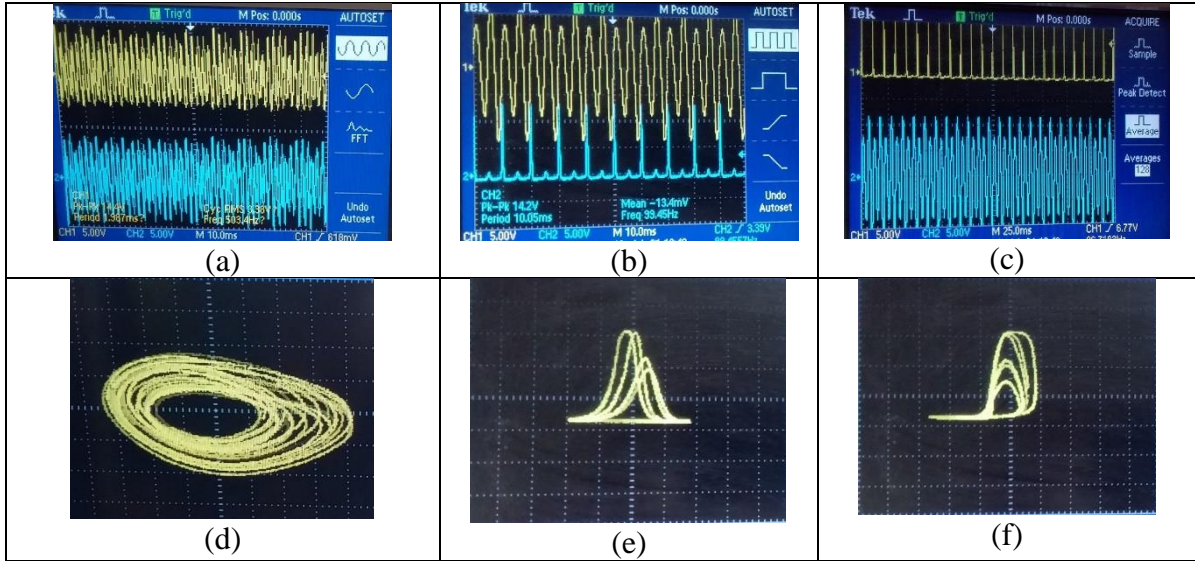


Fig. 3.7 Experimental time domain outputs for state variables (c)  $V_x, V_y$  (d)  $V_y, V_z$  (e)  $V_x, V_z$  and phase trajectories in (f)  $V_x - V_y$ , (g)  $V_y - V_z$  and (h)  $V_x - V_z$  plane

### 3.4 Synchronization between Rössler chaotic systems

In order to utilize chaotic signals in private communications, the receiver's chaotic signals must match with that of transmitter's. In other words, synchronization is required between transmitter and receiver. Adaptive control synchronization is a method to produce adaptive control laws which help one chaotic system (slave) to follow the other chaotic system (master) even in the presence of uncertainties in the value of their parameters. In this method, adaptive control functions are added to the slave system. In order to maintain the error between the respective state variables of master and slave zero, these functions are determined with the help of Lyapunov stability theory. The Lyapunov stability theory states that if a continuously differentiable function  $V$  satisfies the conditions:  $V(0) = 0$ ;  $V(X) > 0$  and  $\dot{V}(X) < 0$ , then the autonomous system  $\dot{X} = f(x)$  is stable. Thus, in this section, step by step process of adaptive control synchronization of two Rössler systems is presented using the methodology suggested in [86].

#### 3.4.1 Master and slave representations

Let master and slave Rössler systems are characterized by state variables  $(x_1, y_1, z_1)$  and  $(x_2, y_2, z_2)$  respectively, and their corresponding governing equations are given by (3.4) and (3.5).



$$\dot{x}_1 = -(y_1 + z_1) \quad (3.4a)$$

$$\dot{y}_1 = x_1 + ay_1 \quad (3.4b)$$

$$\dot{z}_1 = b + z_1(x_1 - c) \quad (3.4c)$$

$$\dot{x}_2 = -(y_2 + z_2) + u_1 \quad (3.5a)$$

$$\dot{y}_2 = x_2 + ay_2 + u_2 \quad (3.5b)$$

$$\dot{z}_2 = b + z_2(x_2 - c) + u_3 \quad (3.5c)$$

where,

$u_1, u_2$  and  $u_3$  are adaptive functions controlling the synchronization between master and slave. The slave system is designed based on these adaptive functions so that it can follow the master.

### 3.4.2 Error dynamics

The errors in synchronization between master and slave are given in (3.6), and the corresponding CFOA based circuit is shown in Fig. 3.8.

$$\begin{aligned} e_x &= x_2 - x_1 \\ e_y &= y_2 - y_1 \\ e_z &= z_2 - z_1 \end{aligned} \quad (3.6)$$

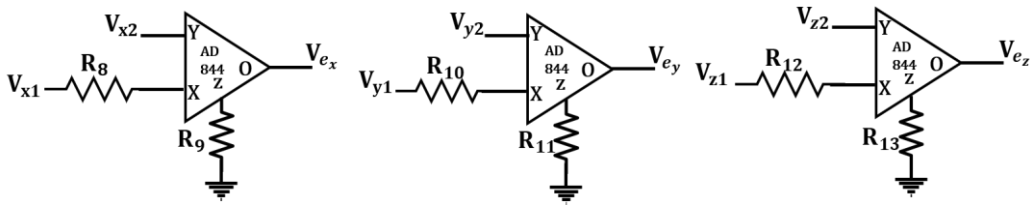


Fig. 3.8 Error functions of adaptive control synchronization

Differentiating (3.6) with respect to time and putting the values of time differentiated state variables from (3.4) and (3.5), the error dynamics is obtained as:

$$\begin{aligned} \dot{e}_x &= -e_y - e_z + u_1 \\ \dot{e}_y &= e_x + ae_y + u_2 \\ \dot{e}_z &= ce_z + x_2z_2 - x_1z_1 + u_3 \end{aligned} \quad (3.7)$$

### 3.4.3 Adaptive Controller

From (3.7), the adaptive functions controlling the synchronization between master and slave are computed as:

$$\begin{aligned} u_1 &= -k_1 e_x + e_y + e_z \\ u_2 &= -k_2 e_y - e_x - \hat{a} e_y \\ u_3 &= -k_3 e_z + \hat{c} e_z - x_2 z_2 + x_1 z_1 \end{aligned} \quad (3.8)$$

where,

$\hat{a}$  and  $\hat{c}$  are the estimates of parameter  $a$  and  $c$  respectively; and  $k_1$ ,  $k_2$  and  $k_3$  are positive constants.

### 3.4.4 Error in parameters' estimation

The parameter estimation error,  $e_a$  and  $e_c$  are defined by

$$e_a = a - \hat{a}, \quad (3.9a)$$

$$e_c = c - \hat{c}, \quad (3.9b)$$

and their dynamics is given as

$$\dot{e}_a = -\dot{\hat{a}} \quad (3.10a)$$

$$\dot{e}_c = -\dot{\hat{c}} \quad (3.10b)$$

Putting  $u_1$ ,  $u_2$  and  $u_3$  from (3.8) in (3.7), we obtain:

$$\begin{aligned} \dot{e}_x &= -k_1 e_x \\ \dot{e}_y &= (a - \hat{a}) e_y - k_2 e_y \\ \dot{e}_z &= (c - \hat{c}) e_z - k_3 e_z \end{aligned} \quad (3.11)$$

### 3.4.5 Lyapunov stability

In order to maintain the stability of the synchronized system, the parameters are updated using Lyapunov function (also known as quadratic scalar function) of (3.12), whose derivative is negative for the system to be stable according to Lyapunov stability theorem [111].

$$V(e_x, e_y, e_z, e_a, e_b, e_c) = \frac{1}{2}(e_x^2 + e_y^2 + e_z^2 + e_a^2 + e_b^2 + e_c^2) \quad (3.12)$$

where,

Differentiating (3.12) with respect to time to determine the stability of the system, we obtain:

$$\dot{V} = -k_1 e_x^2 - k_2 e_y^2 - k_3 e_z^2 + e_a (e_y^2 - \dot{\hat{a}}) - e_b (\dot{\hat{b}}) - e_c (e_z^2 + \dot{\hat{c}}) \quad (3.13)$$

### 3.4.6 Adaptive Laws

For the system to be stable,  $\dot{V}$  has to be negative. The first three terms of (3.13) are negative. If the last three terms are equated to zero, the estimated parameters are updated by the following law:

$$\begin{aligned}\dot{\hat{a}} &= e_y^2 \\ \dot{\hat{b}} &= 0 \\ \dot{\hat{c}} &= -e_z^2\end{aligned}\tag{3.14}$$

The circuit design of (3.14) using CFOAs and AD633 is shown in Fig. 3.9.

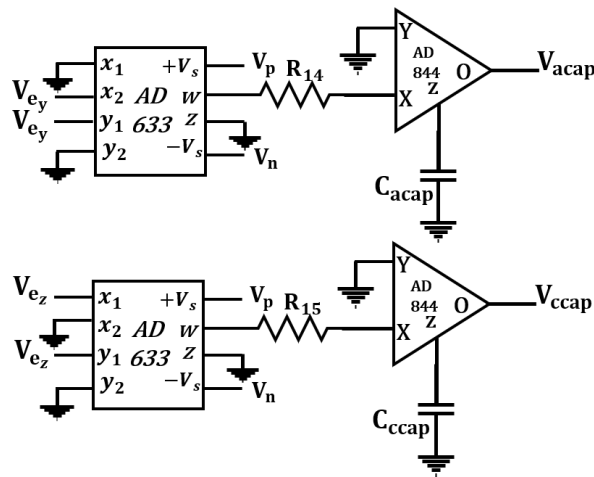


Fig. 3.9 Estimated parameters a and c

The complete set of equations for adaptively synchronized slave system is given by (3.15).

$$\begin{aligned}\dot{x}_2 &= -(y_2 + z_2) - k_1 e_x + e_y + e_z \\ \dot{y}_2 &= x_2 + ay_2 - k_2 e_y - e_x - \hat{a} e_y \\ \dot{z}_2 &= b + z_2(x_2 - c) - k_3 e_z + \hat{c} e_z - x_2 z_2 + x_1 z_1\end{aligned}\tag{3.15}$$

and its complete hardware realization is given in Fig. 3.10. The  $e_i$ 's ( $i = x, y$  and  $z$ ),  $\hat{a}$  and  $\hat{c}$  are obtained from circuit of Figs. 3.8 and 3.9.

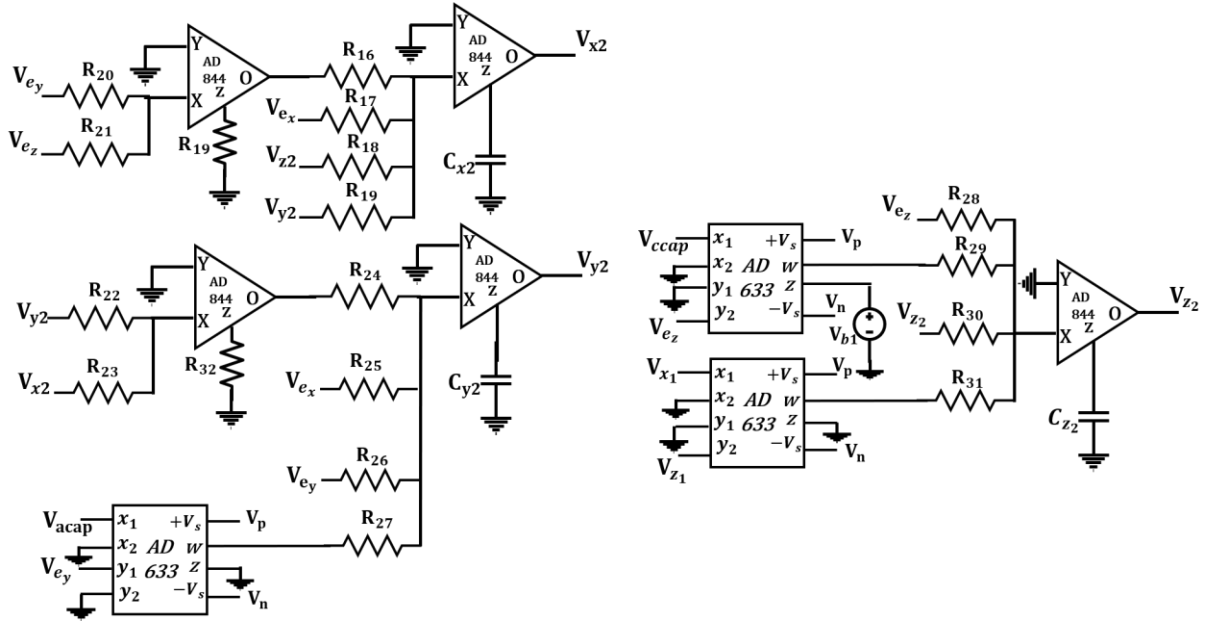


Fig. 3.10 Proposed CFOA based slave circuit

The component values for slave are computed so that the governing equations are satisfied. A scale of 1000 provides the following values of components  $R_{16} - R_{26} = R_{32} = R_{28} = 10 \text{ k}\Omega$ ;  $R_{27} = R_{29} = R_{31} = 1 \text{ k}\Omega$ ,  $R_{30} = 1.695 \text{ k}\Omega$ ,  $R_8 - R_{13} = 10 \text{ k}\Omega$ ,  $R_{14} = R_{15} = 1 \text{ k}\Omega$  and  $C_i (i=4,5,\dots,8) = 100 \text{ nF}$ .

The functionality of complete synchronized design is verified using LTspice software. The time domain response for state variables  $(x_1, x_2)$ ,  $(y_1, y_2)$  and  $(z_1, z_2)$  are plotted and the graphs for corresponding master and slave state variables are extracted to measure the degree of closeness between the respective state variables, as shown in Fig. 3.11. It is observed that  $x$  and  $y$  waveforms of master and slave have linear relationship supporting their synchronization. The  $z$  waveforms also have linear relationship but with 2.18% error in amplitude which may be attributed to the mismatch in the value of parameter ‘ $c$ ’ in master (5.7) and slave (5.9) circuit.

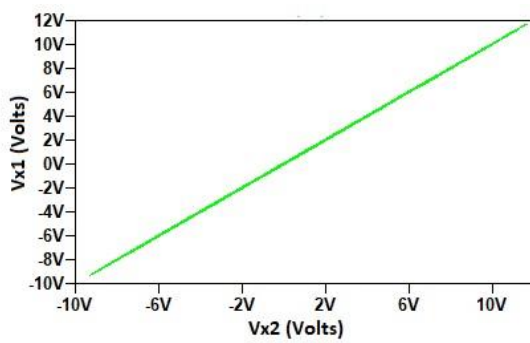
To confirm the assertion that the error is due to mismatch in value of parameter ‘ $c$ ,’ the adaptively controlled synchronized system, extensive simulations have been carried out to obtain synchronization error between the master and slave system for ‘ $a$ ’ = ‘ $b$ ’ = 0.2 and ‘ $c$ ’ = 5, 5.7 5.9 and 6 as Rössler system behaves chaotically for these values [112]. The percentage error with respect to parameter ‘ $c$ ’ is listed in Table 3.2. It may be noted from Table 3.2 that the percentage error when both master and slave are designed with same value of parameter ‘ $c$ ’ is within 1% which is negligibly small to make difference in synchronization. An increasing

trend in percentage error is observed for larger deviations in the values of parameter ‘c’ of master and slave.

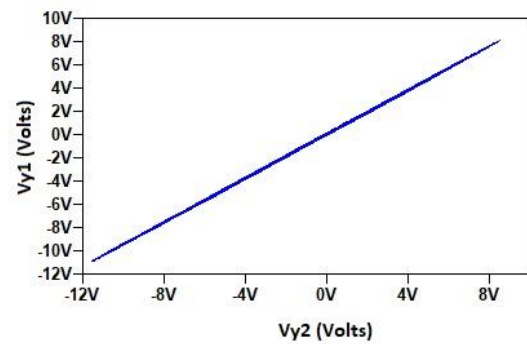
Table 3.2 Percentage error in adaptive synchronization with respect to parameter ‘c’

Receiver (‘c’)→ Transmitter (‘c’) ↓	Error (%)			
	5	5.7	5.9	6
5	0.96	6.19	6.39	6.67
5.7	6.27	0.98	2.18	3.59
5.9	6.84	2.72	0.96	2.17
6	7.48	3.51	1.65	0.93

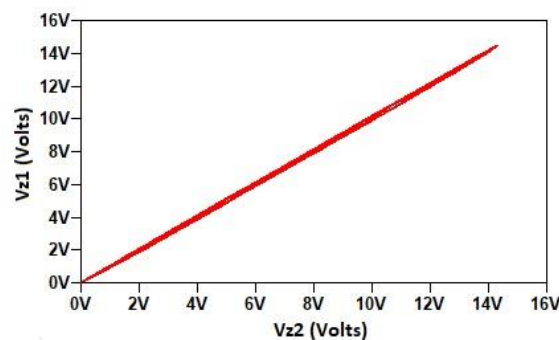
The simulation results of the designed circuit show a minor synchronization error in state variable z at receiver end. This may be due to the dependence of  $z_2$  on more number of variables in (3.15).



(a)



(b)



(c)

Fig. 3.11 Simulated plots between chaotic signals of master and slave in adaptive synchronization: (a)  $V_{x1}$  versus  $V_{x2}$ , (b)  $V_{y1}$  versus  $V_{y2}$ , (c)  $V_{z1}$  versus  $V_z$

### **3.5 Concluding Remarks**

Rössler chaotic system has been systematically designed in this chapter using CFOAs and Analog Multiplier (AM). The proposed design uses four CFOAs, one Analog Multiplier (AM), seven resistors, and three capacitors. The passive component count in proposed circuit is considerably low as compared to existing Rössler chaotic system. The feasibility of the proposed circuit design is examined through LTspice simulations and experimentally using AD844 and AD633 ICs. The observed outputs for state variables are aperiodic and having strange attractors for phase trajectories in different planes, thereby confirming the correctness of the proposed design. The power consumption of the proposed circuit is 1.1 W, at power supplies of  $\pm 15$  V. An application, namely adaptive control synchronization between two Rössler chaotic systems is also put forward to illustrate the usability of the proposed circuit.

# Chapter 4

## Chaotic systems with two quadratic non-linearities

---

The content and results of the following paper have been reported in this chapter.

K. Suneja, N. Pandey and R. Pandey, “**Novel Pehlivan–Uyaröglu Chaotic System Variants and their CFOA Based Realization,**” *Journal of Circuits, Systems and Computers*.  
10.1142/S0218126622501717.

## 4.1 Introduction

Having presented study of chaotic system with single quadratic non-linearity and its systematic hardware implementation in chapter 3, in this chapter we deal with chaotic system with two quadratic non-linearities namely Pehlivan Uyaröglu Chaotic System (PUCS) [15]. In this chapter, four variants of PUCS are proposed, characterised and implemented.

The parameter values are obtained by observing bifurcation diagrams for state variables and properties of the proposed PUCS variants, including Lyapunov exponents, Kaplan Yorke dimension and dissipativity, are examined through numerical simulations. The stability of PUCS and its proposed variants is examined using Jacobi stability analysis. Further, a CFOA based circuit is presented that can realize PUCS and its proposed variants by simply changing resistor values, without changing its topology.

The behaviour of the proposed variants in time domain, frequency domain and phase space is examined through simulations in LTspice design environment. Furthermore, the feasibility of the proposed variants is also discussed through presenting an electronic circuit implementation of two of the variants and the results obtained are in good agreement with the LTspice simulations. Monte Carlo (MC) simulations are also included to show the robustness of the proposed circuit against parameter variations.

## 4.2 The Pehlivan Uyaröglu Chaotic System (PUCS)

The governing equations of PUCS are described by (4.1) [15].

$$\dot{x} = y - x \quad (4.1a)$$

$$\dot{y} = ay - xz \quad (4.1b)$$

$$\dot{z} = xy - b \quad (4.1c)$$

where

$x$ ,  $y$  and  $z$  represent the state variables and ‘ $a$ ’ and ‘ $b$ ’ are positive constants whose values for the system to behave chaotically, are 0.5 and 0.5 respectively as reported in [15].



### 4.2.1 Proposed Variants of PUCS

In this subsection, four variants of PUCS are put forward. These variants have same number of terms, non-linearities and parameters. The governing equations of proposed variants are given below:

#### 4.2.1.1 First proposed variant of PUCS (PUCS I)

The first proposed variant of PUCS, as described by governing equations of (4.2) is obtained by multiplying the cross-product term  $xy$  in (4.1c) by the parameter ‘b,’ while keeping other two governing equations same as (4.1a) and (4.1b).

$$\dot{x} = y - x \quad (4.2a)$$

$$\dot{y} = ay - xz \quad (4.2b)$$

$$\dot{z} = bxy - b \quad (4.2c)$$

#### 4.2.1.2 Second proposed variant of PUCS (PUCS II)

In this variant, the cross-product terms  $xz$  and  $xy$ , present in Eq.(4.1b) and Eq. (4.1c), are multiplied by parameters ‘a’ and ‘b’ respectively, as given in Eq.(4.3). The governing equations of PUCS II are given in (4.3).

$$\dot{x} = y - x \quad (4.3a)$$

$$\dot{y} = ay - axz \quad (4.3b)$$

$$\dot{z} = bxy - b \quad (4.3c)$$

#### 4.2.1.3 Third proposed variant of PUCS (PUCS III)

Here, the dynamics of state variables  $x$  and  $z$  are described by (4.4a) and (4.4c) respectively. In the dynamics of state variable  $y$ , the cross-product term  $xz$  is multiplied by parameter ‘a.’ The governing equations of PUCS III are given by (4.4).

$$\dot{x} = y - x \quad (4.4a)$$

$$\dot{y} = ay - axz \quad (4.4b)$$

$$\dot{z} = xy - b \quad (4.4c)$$

#### 4.2.1.4 Fourth proposed variant of PUCS (PUCS IV)

For this variant, the dynamics of state variable  $z$  is kept same as (4.1c). The dynamics of state variables  $x$  and  $y$  of PUCS are modified to (4.5a) and (4.5b) respectively. The governing equations of PUCS IV are given by (4.5).

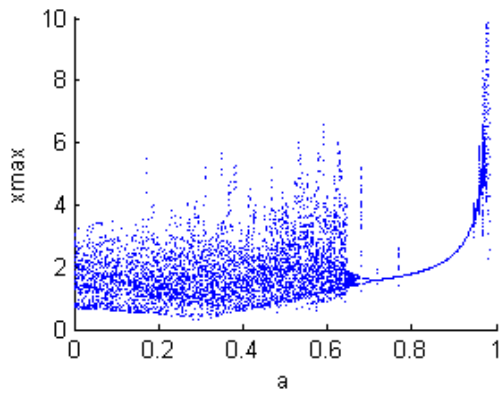
$$\dot{x} = a(y - x) \quad (4.5a)$$

$$\dot{y} = y - xz \quad (4.5b)$$

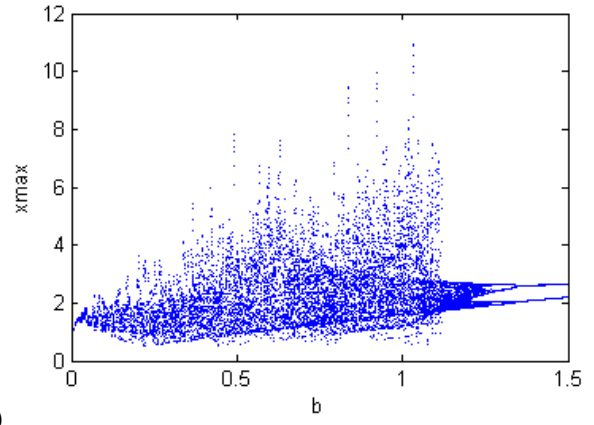
$$\dot{z} = xy - b \quad (4.5c)$$

### 4.3 Estimation of parameters and properties of the PUCS and its proposed variants

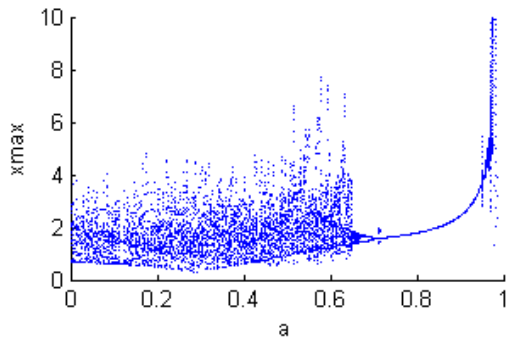
In this section, the bifurcation diagrams for PUCS and its four variants are examined using MATLAB simulations. To obtain the bifurcation diagrams, value of one of the parameters (either 'a' or 'b') is fixed and then the dynamics of the maximum value of one of the state variables ( $x/y/z$ ) is observed for few hundred iterations with the variation in the other parameter [15]. Bifurcation diagrams for maximum value of state variable  $x$  with respect to variations in  $a$  (keeping  $b$  fixed) and  $b$  (keeping  $a$  fixed) respectively are obtained for PUCS and its four proposed variants as depicted in Figs. 4.1(a)- 4.1(e). As evident from Fig. 4.1 (a, b, c and d), the route to chaos with period doubling is from right to left, i.e. with the decreasing values of parameters 'a' and 'b', while for Fig. 4.1 (e), it is from left to right with the variation in parameter 'a' and right to left for parameter 'b'. Thus, Figs. 4.1(a) to (4.1d) display a continuous chaotic region followed by a reverse period-doubling bifurcation to period-1-oscillations, while the case is reverse for Fig. 4.1(e). In other words, it may be inferred that the increasing values of parameters 'a' and 'b' can effectively reduce the complexity in the behaviour of the PUCS, PUCS I, PUCS II and PUCS III, while the increasing value of parameter 'a' increases the chaoticity in PUCS IV. The ranges of parameters 'a' and 'b' for chaotic behaviour of PUCS and its proposed variants are summarized in Table 4.1.



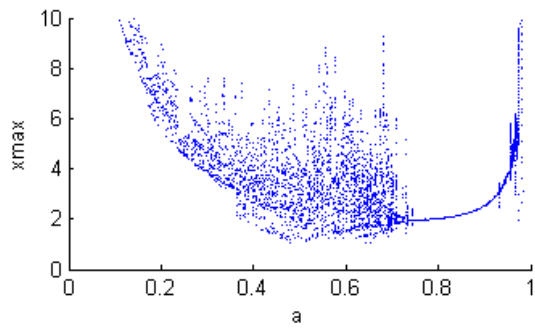
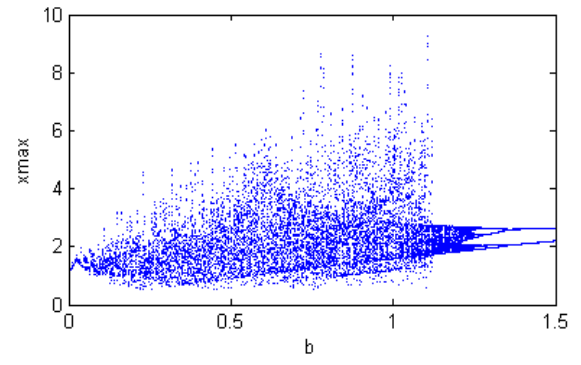
(a)



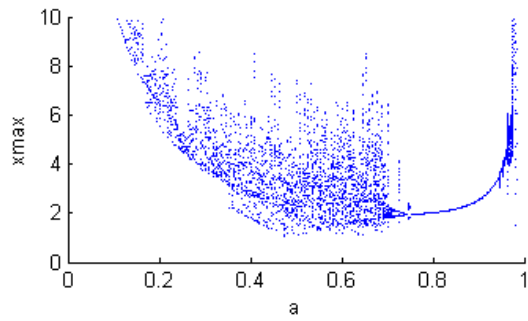
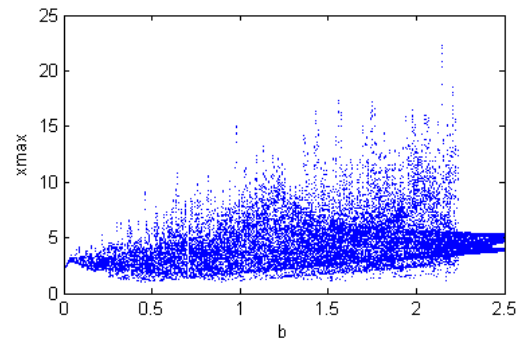
(b)



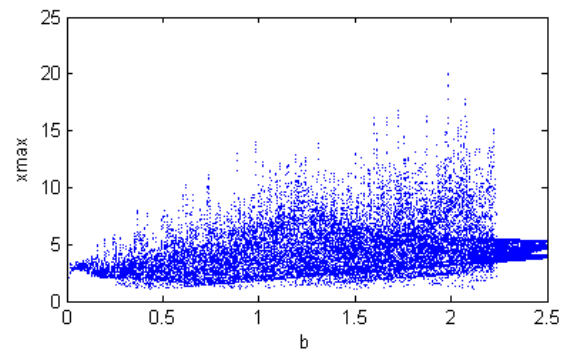
(b)



(c)



(d)



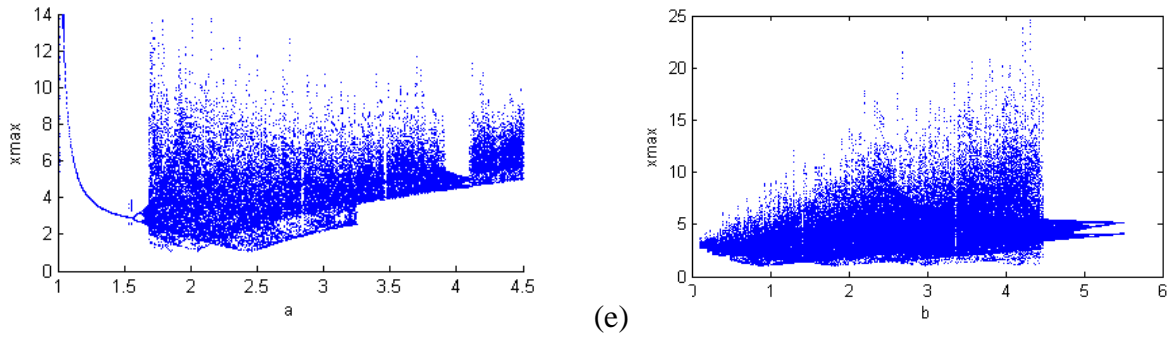


Fig. 4.1 Bifurcation diagrams for (a) PUCS (b) PUCS I (c) PUCS II (d) PUCS III (e) PUCS IV

Table 4.1 Summary of range of parameters ‘a’ and ‘b’ for PUCS and its proposed variants

System	Bifurcation Diagram (BD)	Range of ‘a’ obtained from BD, keeping ‘b’ fixed		Range of ‘b’ obtained from BD, keeping ‘a’ fixed	
		Fixed value of ‘b’	Range of ‘a’	Fixed value of ‘a’	Range of ‘b’
PUCS	Fig. 4.1(a)	0.5	[0,0.665]	0.5	[0.1, 1.25]
PUCS I	Fig. 4.1(b)	0.5	[0, 0.65]	0.5	[0.1, 1.25]
PUCS II	Fig. 4.1(c)	0.5	[0.35, 0.7]	0.5	[0.1, 2.25]
PUCS III	Fig. 4.1(d)	0.5	[0.35, 0.7]	0.5	[0.1, 2.25]
PUCS IV	Fig. 4.1(e)	2	[0.1,4.5]	2	[0.1, 4.5]

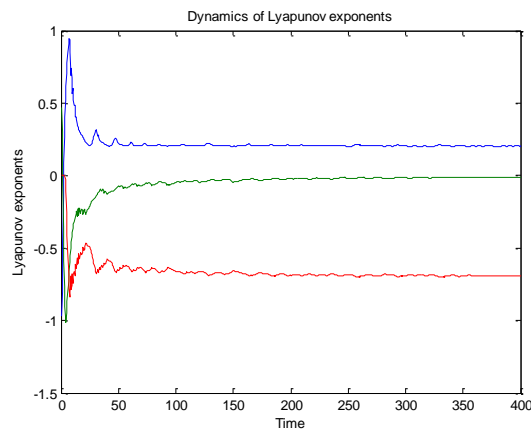
Once the valid ranges of parameters ‘a’ and ‘b’ are determined, the evolution of Lyapunov exponents with time is observed for a particular value of parameters ‘a’ and ‘b’ in order to investigate the system dynamics in more detail. The dynamics of the Lyapunov exponents corresponding to PUCS and its four variants for the values of parameters ‘a’ and ‘b’ taken as 0.5 for PUCS, PUCS I, PUCS II and PUCS III; and 2 for PUCS IV as listed in Table 4.2, and is shown in Fig. 4.2. In all the cases, three Lyapunov exponents are obtained which are negative, zero and positive respectively, therefore all the systems satisfy one more property of chaoticity. The observed values of  $LE_k$  ( $k = 1,2,3$ ) for PUCS and its proposed variants from Fig. 4.2 are summarized in Table 4.2. It may be noted that  $LE_2 = 0$  and  $LE_1 < |LE_3|$  for all PUCSs, so  $D_{KY}$  for PUCS is given by Eq. (4.6).

$$D_{KY} = 2 + \frac{|LE_1|}{|LE_3|} \quad (4.6)$$

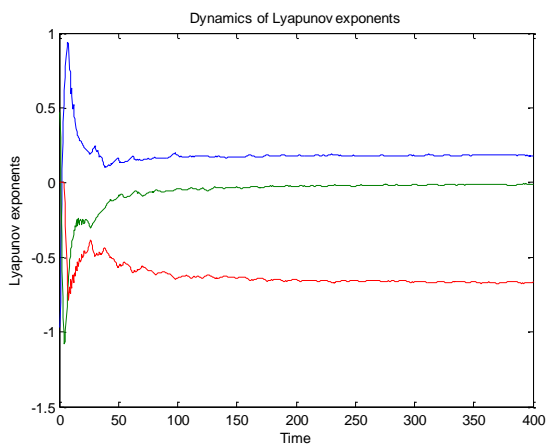
Here, ‘2’ represents the maximum number of Lyapunov exponents whose summation is positive. The value of  $D_{KY}$  is computed for PUCS and its variants using (4.6) and the results are placed in Table 4.2. It may be noted that the order of complexity is (PUCS= PUCS I) > PUCS IV > (PUCS II = PUCS III).

Table 4.2 Summary of Lyapunov Exponents and Kaplan York Dimensions for PUCS

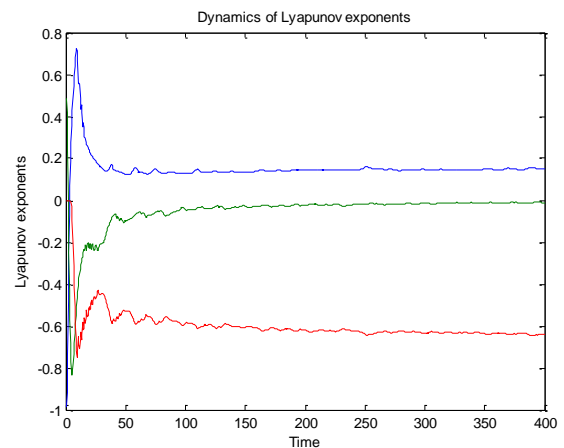
System	Values of Parameter (a, b)	Lyapunov Exponents (LE <sub>1</sub> , LE <sub>2</sub> , LE <sub>3</sub> )	$D_{KY}$
PUCS [17]	(0.5,0.5)	0.3, 0, -0.8	2.38
PUCS I	(0.5,0.5)	0.3, 0, -0.8	2.38
PUCS II	(0.5,0.5)	0.2, 0, -0.7	2.29
PUCS III	(0.5,0.5)	0.2, 0, -0.7	2.29
PUCS IV	(2, 2)	0.5, 0, -1.5	2.33



(a)



(b)



(c)

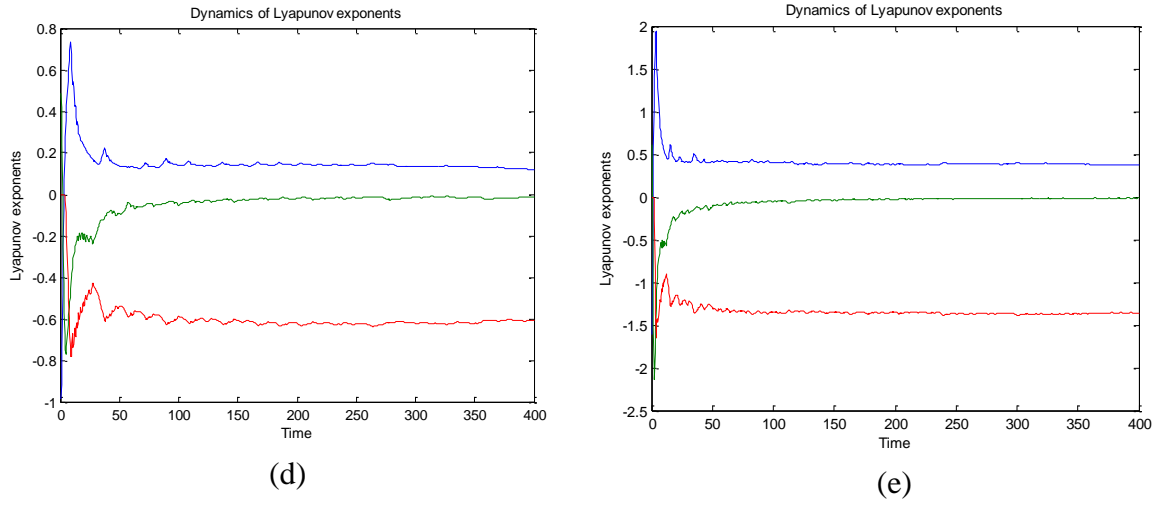


Fig. 4.2 Dynamics of Lyapunov exponents for (a) PUCS, (b) PUCS I, (c) PUCS II, (d) PUCS III, (e) PUCS IV

The divergence, also known as trace, has been calculated for PUCS and its proposed variants. It may be observed that the value is ‘ $a-1$ ’ for PUCS and its first three variants i.e. every volume consisting of these systems’ trajectory approaches zero as  $t \rightarrow \infty$  at an exponential rate of  $(a-1)$ . Thus, PUCS, PUCS I, PUCS II and PUCS III are always dissipative in nature for the range of parameter ‘ $a$ ’ given in Table 4.1, provided  $b = 0.5$  for PUCS, PUCS I, PUCS II and PUCS III. The PUCS IV has trace value of ‘ $-a+1$ ’ so it is conditionally dissipative depending upon the value of ‘ $a$ ’ being more or less than 1 and  $b = 2$ .

#### 4.4 Analysis of fixed points

The stability of PUCS and its proposed variants is examined using Jacobi stability analysis method described in chapter 2, and is detailed below for PUCS I.

(1) The fixed points of PUCS I are found by setting  $\dot{x} = \dot{y} = \dot{z} = 0$  in (4.2).

$$\begin{cases} y - x = 0 \\ ay - xz = 0 \\ bxy - b = 0 \end{cases} \quad (4.7)$$

It may be noted that for  $y = 0$ , fixed points do not exist. Considering  $y \neq 0$  and solving (4.7) gives the following fixed points:

$$p_1 = (1, 1, a) \text{ and } p_2 = (-1, -1, a).$$

(2) The Jacobian matrix for PUCS I consists of three columns. The values in 1<sup>st</sup>, 2<sup>nd</sup> and 3<sup>rd</sup> column are found by differentiating governing equations with respect to x, y and z respectively.

$$J = \begin{bmatrix} -1 & 1 & 0 \\ -z & a & -x \\ by & bx & 0 \end{bmatrix} \quad (4.8)$$

The Jacobian matrices  $J_{p1}$  and  $J_{p2}$  corresponding to fixed points  $p_1$  and  $p_2$  are given by (4.9) and (4.10) respectively.

$$J_{p1} = \begin{bmatrix} -1 & 1 & 0 \\ -a & a & -1 \\ b & b & 0 \end{bmatrix} \quad (4.9)$$

and

$$J_{p2} = \begin{bmatrix} -1 & 1 & 0 \\ -a & a & 1 \\ -b & -b & 0 \end{bmatrix} \quad (4.10)$$

respectively.

(3) The eigenvalues are computed by equating  $|J_{pi} - \lambda I|$  with 0. This results in characteristic equation of (4.11) for both  $p_1$  and  $p_2$ .

$$\lambda^3 + (1 - a)\lambda^2 + b\lambda + 2b = 0 \quad (4.11)$$

Considering  $a = b = 0.5$  in Eq. (4.11) the eigenvalues are computed as

$$\lambda_1 = -1; \lambda_2 = 0.25 + 0.9682i \text{ and } \lambda_3 = 0.25 - 0.9682i.$$

The same process is used to compute the equilibrium points, Jacobian matrices, eigenvalues  $(\lambda_1, \lambda_2, \lambda_3)$  corresponding to equilibrium points for PUCS II and PUCS III by taking parameters  $(a, b)$  as  $(0.5, 0.5)$  while  $(2, 2)$  is considered for PUCS IV. The findings are enlisted in Table 4.3. It may be noted that the eigenvalues corresponding to PUCS and all its proposed variants have negative value of  $\lambda_1$  and positive real part in the complex conjugates for  $\lambda_2$  and  $\lambda_3$ , thus inferring the existence of a stable linear manifold and an unstable spiral manifold, as discussed in Chapter 2. The presence of these manifolds is responsible for the strange attractors of all PUCS systems.

Table 4.3 Parameters of PUCS and its chaotic variants

System	Equilibrium Points; Value of parameter (a, b)	Jacobian Matrix	Eigen Values
PUCS [19]	$(\sqrt{b}, \sqrt{b}, a);$ (0.5.0.5)	$\begin{bmatrix} -1 & 1 & 0 \\ -a & a & -\sqrt{b} \\ \sqrt{b} & \sqrt{b} & 0 \end{bmatrix}$	$\lambda_1=-1; \lambda_{2,3}=$ $0.25\pm 0.9682i$
	$(-\sqrt{b}, -\sqrt{b}, a);$ (0.5.0.5)	$\begin{bmatrix} -1 & 1 & 0 \\ -a & a & -\sqrt{b} \\ -\sqrt{b} & -\sqrt{b} & 0 \end{bmatrix}$	$\lambda_1=-1; \lambda_{2,3}=$ $0.25\pm 0.9682i$
PUCS I	(1, 1, a); (0.5.0.5)	$\begin{bmatrix} -1 & 1 & 0 \\ -a & a & -1 \\ b & b & 0 \end{bmatrix}$	$\lambda_1=-1; \lambda_{2,3}=$ $0.25\pm 0.9682i$
	(-1, -1, a); (0.5.0.5)	$\begin{bmatrix} -1 & 1 & 0 \\ -a & a & 1 \\ -b & -x & 0 \end{bmatrix}$	$\lambda_1=-1; \lambda_{2,3}=$ $0.25\pm 0.9682i$
PUCS II	(1, 1, 1); (0.5.0.5)	$\begin{bmatrix} -1 & 1 & 0 \\ -a & a & -a \\ b & b & 0 \end{bmatrix}$	$\lambda_1=-0.8715; \lambda_{2,3}=$ $0.1857\pm 0.7343i$
	(-1, -1, 1); (0.5.0.5)	$\begin{bmatrix} -1 & 1 & 0 \\ -a & a & a \\ -b & -b & 0 \end{bmatrix}$	$\lambda_1=-1.339; \lambda_{2,3}=$ $0.4195\pm 0.4443i$
PUCS III	$(\sqrt{b}, \sqrt{b}, 1);$ (0.5.0.5)	$\begin{bmatrix} -1 & 1 & 0 \\ -a & a & -a\sqrt{b} \\ \sqrt{b} & \sqrt{b} & 0 \end{bmatrix}$	$\lambda_1=-0.8715; \lambda_{2,3}=$ $0.1857\pm 0.7343i$
	$(-\sqrt{b}, -\sqrt{b}, 1);$ (0.5.0.5)	$\begin{bmatrix} -1 & 1 & 0 \\ -a & a & a\sqrt{b} \\ -\sqrt{b} & -\sqrt{b} & 0 \end{bmatrix}$	$\lambda_1=-0.8715; \lambda_{2,3}=$ $0.1857\pm 0.7343i$
PUCS IV	$(\sqrt{b}, \sqrt{b}, 1);$ (2,2)	$\begin{bmatrix} -a & a & 0 \\ -1 & 1 & -\sqrt{b} \\ \sqrt{b} & \sqrt{b} & 0 \end{bmatrix}$	$\lambda_1=-2; \lambda_{2,3}=$ $0.5\pm 1.9365i$
	$(-\sqrt{b}, -\sqrt{b}, 1);$ (2,2)	$\begin{bmatrix} -a & a & 0 \\ -1 & 1 & \sqrt{b} \\ -\sqrt{b} & -\sqrt{b} & 0 \end{bmatrix}$	$\lambda_1=-2; \lambda_{2,3}=$ $0.5\pm 1.9365i$

#### 4.5 The circuit realization

The dynamics of the governing equations of PUCS and its proposed variants are realized by CFOA and Analog Multipliers (AMs) in this section where the state variables x, y and z are represented by voltages  $V_x$ ,  $V_y$  and  $V_z$  across capacitors  $C_x$ ,  $C_y$  and  $C_z$  respectively. The dynamics of state variables i.e. left-hand side of (4.1) – (4.5) may be obtained by observing current through capacitors as it is proportional to time differentiation of voltage.

The dynamics of state variable x i.e. the right-hand side of (4.1a - 4.5a) requires subtraction of two voltages and passing the resulting current through a capacitor. The desired output may be



obtained by CFOA based arrangement depicted in Fig. 4.3. Here, the current through  $C_x$  may be written as:

$$C_x \frac{dV_x}{dt} = \frac{V_y - V_x}{R_1} \quad (4.12)$$

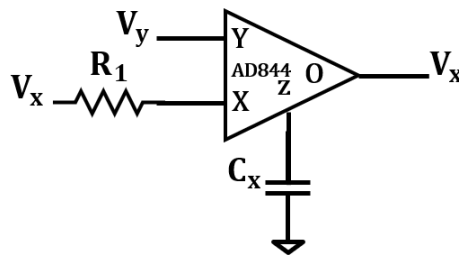


Fig. 4.3 Design for state variable x

Equation (4.12) may be rewritten as

$$\frac{dV_x}{dt} = \frac{V_y - V_x}{R_1 C_x} \quad (4.13)$$

The value of  $R_1 C_x$  for PUCS and its proposed variants may be found by comparison of (4.13) with (4.1a) – (4.5a). It is observed that (4.13) maps to (4.1a, 4.2a, 4.3a, 4.4a) for  $R_1 C_x = 1$  and (4.5a) for  $R_1 C_x = \frac{1}{a}$ .

The implementation of (4.1b) and (4.2b) requires a cross-product term  $V_x V_z$ , scaling of  $V_y$  and subtraction of these two, while implementation of (4.3b), (4.4b) and (4.5b) requires scaling of cross-product term as well. An Analog Multiplier (AM) AD633 and a voltage divider circuit may be used respectively to provide the product term and scaling operation. The subtraction may be obtained by CFOA. The complete arrangement is depicted in Fig. 4.4, the current through  $C_y$  may be written as:

$$C_y \frac{dV_y}{dt} = \frac{V_m - 0.1V_x V_z}{R_4} \quad (4.14)$$

where,

$$V_m = \frac{R_3}{R_2 + R_3} V_y \quad (4.15)$$

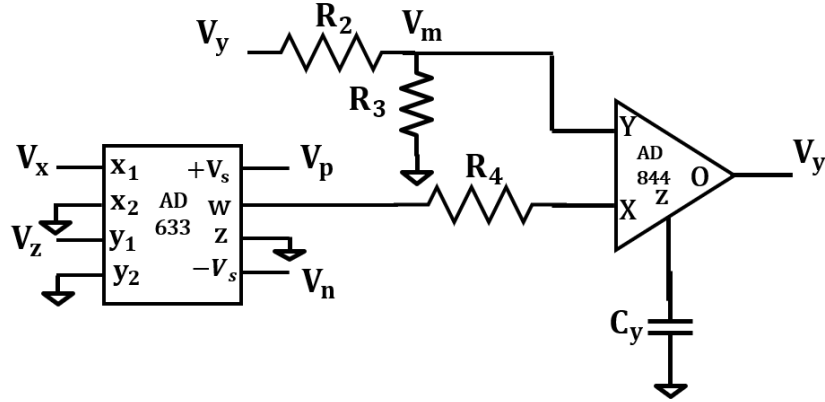


Fig. 4.4 Design for state variable y

Equation (4.14) may be rewritten as

$$\frac{dV_y}{dt} = \frac{V_m - 0.1V_xV_z}{R_4C_y} \quad (4.15)$$

Equation (4.15) maps to (4.1b, 4.2b) for  $R_4C_y = 0.1$  and  $\frac{R_3}{(R_2+R_3)R_4C_y} = a$ , whereas (4.3b, 4.4b) require  $R_4C_y = \frac{1}{10a}$  and  $\frac{R_3}{(R_2+R_3)R_4C_y} = a$  and (4.5b) needs  $R_4C_y = 0.1$  and  $\frac{R_3}{(R_2+R_3)R_4C_y} = 1$ .

Equations (4.1c, 4.4c, 4.5c) have a cross-product term and a constant 'b' being subtracted from it, while equations (4.2c, 4.3c) have a scaling factor 'b' of cross-product term as well. Thus, the realization requires an Analog Multiplier (AM) AD633 and CFOA based subtractor. Fig. 4.5 gives the hardware implementation of (4.1c-4.5c). The current through  $C_z$  may be expressed as

$$C_z \frac{dV_z}{dt} = \frac{0.1V_xV_y - V_b}{R_5} \quad (4.16)$$

Or

$$\frac{dV_z}{dt} = \frac{0.1V_xV_y - V_b}{R_5C_z} \quad (4.17)$$

Equation (4.17) maps to (4.1c, 4.4c, 4.5c) for  $R_5C_z = 0.1$  and  $\frac{V_b}{R_5C_z} = b$  while (4.2c, 4.3c) require  $R_5C_z = \frac{1}{10b}$  and  $\frac{V_b}{R_5C_z} = b$ .

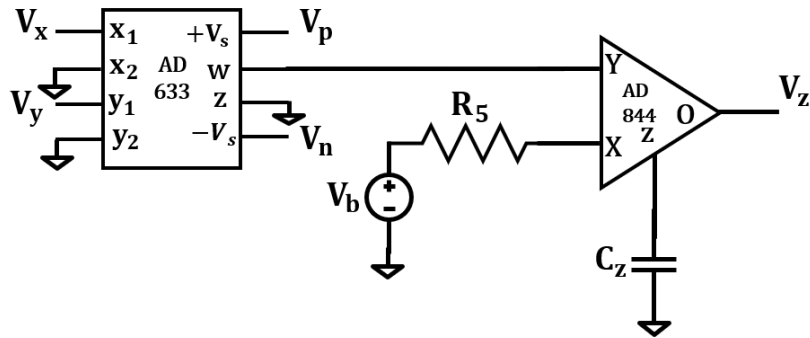


Fig. 4.5 Design for state variable z

The component count of Fig. 4.3, Fig. 4.4 and Fig. 4.5 together are less than that of [15], which uses four voltage mode active building blocks, two AMs and eleven passive components. So, using CFOAs in designing PUCS has assisted us in saving both active blocks and passive components. Also, the same circuit can be used to implement both PUCS and its proposed variants. It may be noted from Table 4.1 that range of parameters ‘a’ and ‘b’ are wider in PUCS IV. Further as the values of ‘a’ and ‘b’ depend on resistor  $R_1$  and voltage source  $V_b$ , so a wide range of  $R_1$  and  $V_b$  is available. The features of the proposed variants are enlisted in Table 4.4. It may be noted that all the variants use same number of hardware components. The difference, however, lies in the chaoticity as evident from Kaplan Yorke Dimension  $D_{KY}$ , tuning range as derived from the range of parameters ‘a’ and ‘b’ and accessibility of dc voltage supply required depending on the value of  $V_b$ .

Table 4.4 Features of the proposed variants

System	Chaoticity	Tuning range	Accessibility of dc voltage supply required
PUCS I	High	Moderate	Easy
PUCS II	Low	Low	Easy
PUCS III	Low	Low	Difficult
PUCS IV	Moderate	Highest	Easy

## 4.6 Simulation Results

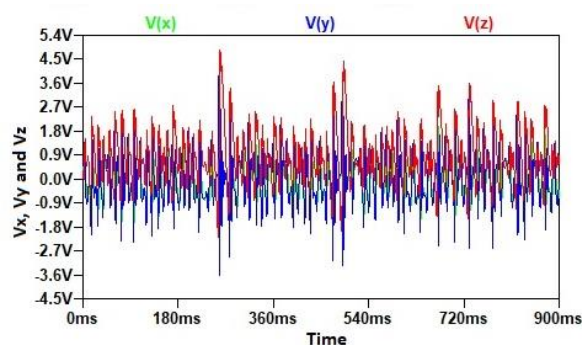
The proposed circuit of PUCS and its variants are simulated in LTspice design environment. The values of parameters ‘a’ and ‘b’ for PUCSs are taken as specified in Table 4.2. Considering scaling factor of 1000, the normalized values of the passive components for the proposed circuit

are listed in Table 4.5. All the capacitors are taken as 100nF. The supply voltages are taken as  $\pm 15V$ .

Table 4.5 Normalized element values of the proposed PUCS circuit

Component	$R_1$	$R_2$	$R_3$	$R_4$	$R_5$	$V_b$
Equation Number	(2a-5a); (6a)	(2b, 3b); (4b,5b,6b)	(2b- 6b)	(2b,3b,6b); (4b,5b)	(2c,5c,6c); (3c,4c)	(2c,5c); (3c,4c); (6c)
Value	10k $\Omega$ ; 5k $\Omega$	19k $\Omega$ ; 9k $\Omega$	1k $\Omega$	1k $\Omega$ ; 2k $\Omega$	1k $\Omega$ ; 2k $\Omega$	0.05V; 0.1V;0.2V

The time domain responses of  $V_x$ ,  $V_y$  and  $V_z$  of PUCS and its variants are shown in Fig. 4.6, which are clearly aperiodic in nature. Figure. 4.7 shows the projections of phase space trajectories of all the systems onto the  $V_x$ - $V_y$ ,  $V_z$ - $V_y$  and  $V_z$ - $V_x$  planes respectively. These attractors, being the visual characteristics of chaotic systems, show the relationship of the variants with the original PUCS system and confirm the correctness of simulation results. The frequency spectrum of PUCS and its variants is also examined to determine the range of frequencies in which these systems can be used. Figure. 4.8 shows the frequency spectrum of  $V_x$ ,  $V_y$  and  $V_z$  for PUCS I. The frequency spectrums for state variables  $V_x$ ,  $V_y$  and  $V_z$  are noise like in frequency range 50Hz to 1.5kHz with no dominant peaks again verifies the chaoticity in the circuit. Also, the frequency spectrum shows that the significant portion of the signals  $x$ ,  $y$  and  $z$  falls in audio frequency range, thus the chaos can be used in audio applications, such as encryption of audio data before transmission in secure communication. Similar results were obtained for other variants also, which have not been included for the sake of brevity.



(a)

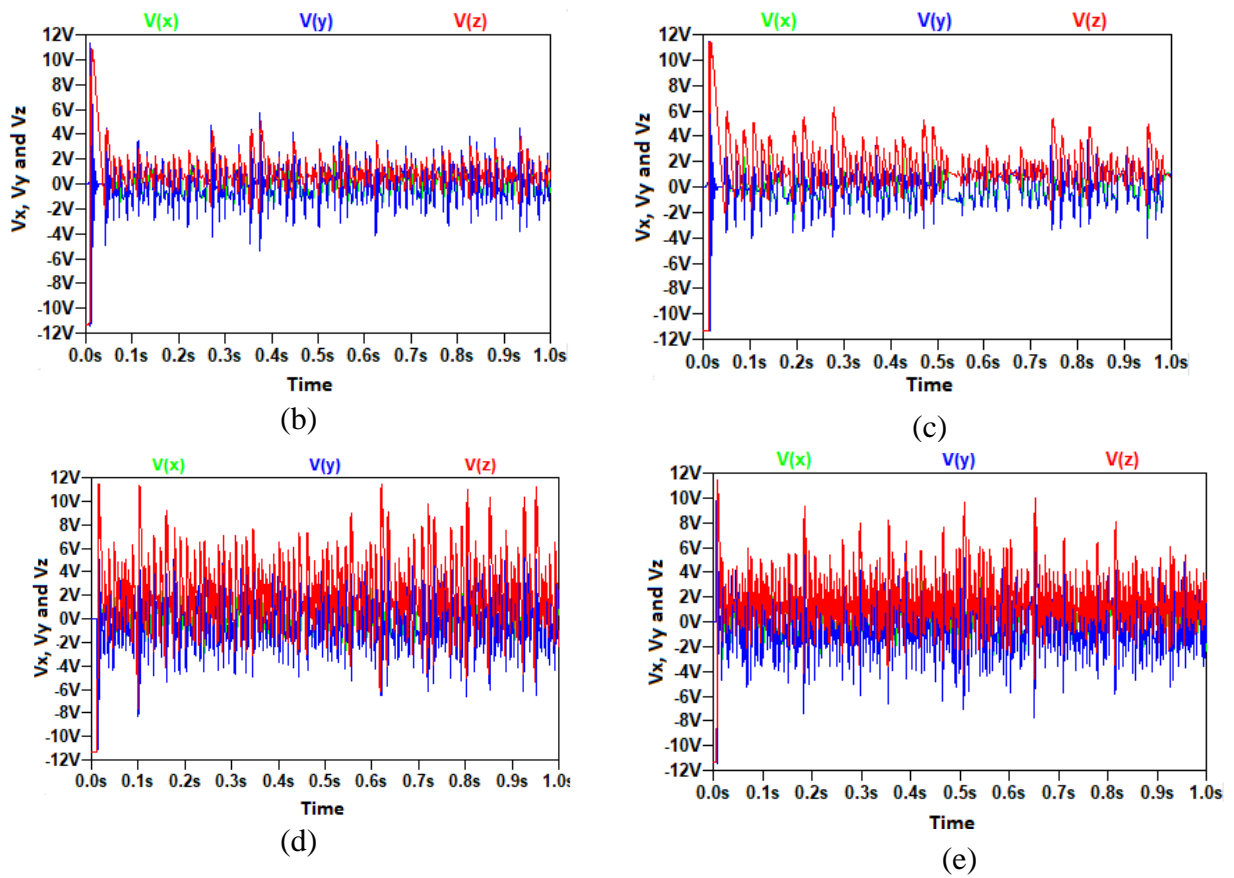
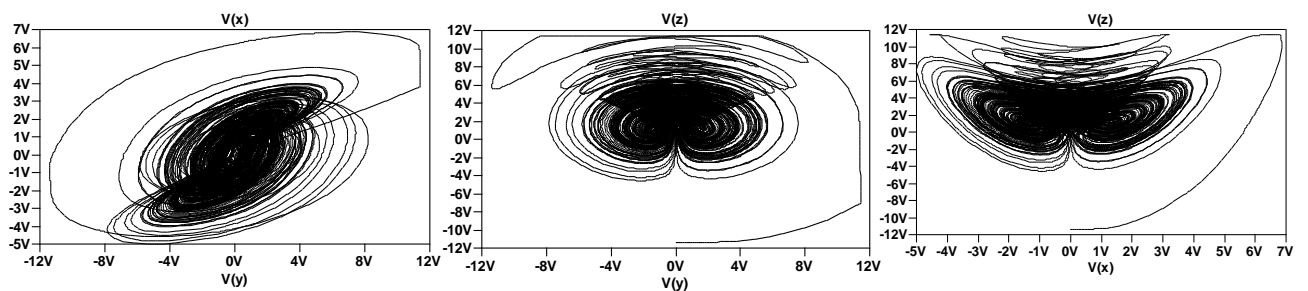
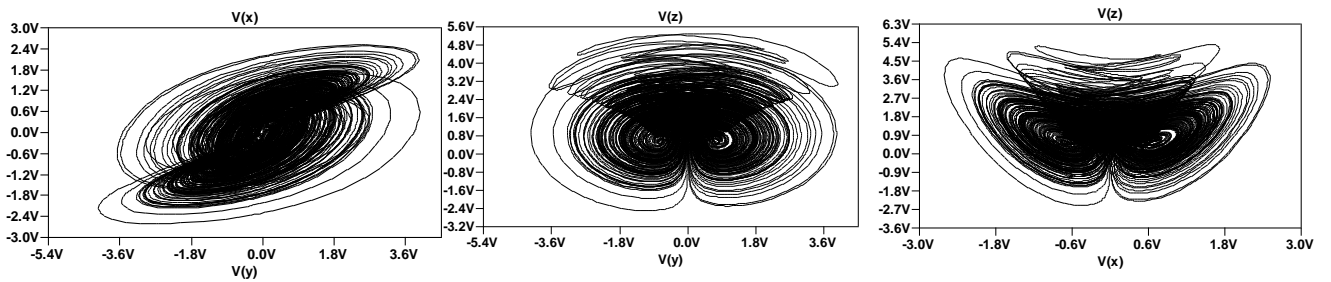


Fig. 4.6 Time domain response of state variables (a) PUCS, (b) PUCS I, (c) PUCS II, (d) PUCS III, (e) PUCS IV



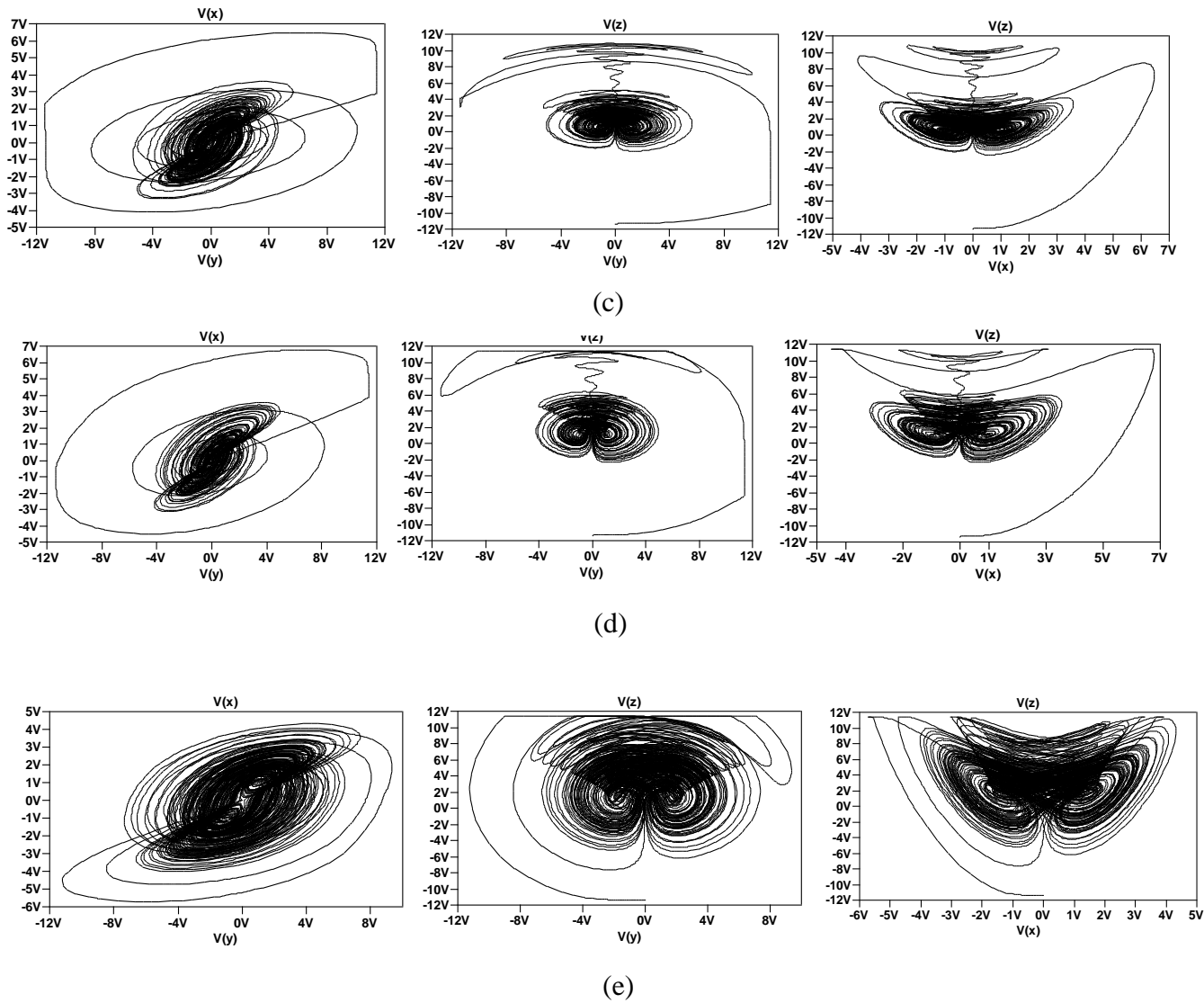


Fig. 4.7 Simulated phase space trajectory  $y_x$ ,  $y_z$  and  $x_z$  for (a) PUCS, (b) PUCS I, (c) PUCS II, (d) PUCS III, (e) PUCS IV

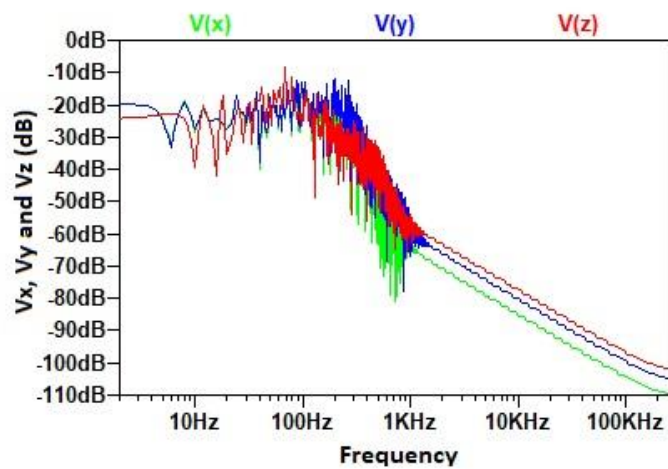


Fig. 4.8 Frequency spectrum plots of state variables (a)  $V_x$ , (b)  $V_y$ , (c)  $V_z$

The chaotic spectrum of the proposed design for PUCS I is examined with Monte Carlo (MC) simulations for all the resistors and capacitors having 10% tolerance in which uniform Gaussian distribution is used. The MC analysis results for PUCS I are shown in Fig. 4.9. It can be stated from MC analysis that the circuit is robust to elements' values with 10% tolerance. Similar results are obtained with MC analysis for other proposed PUCS variants.

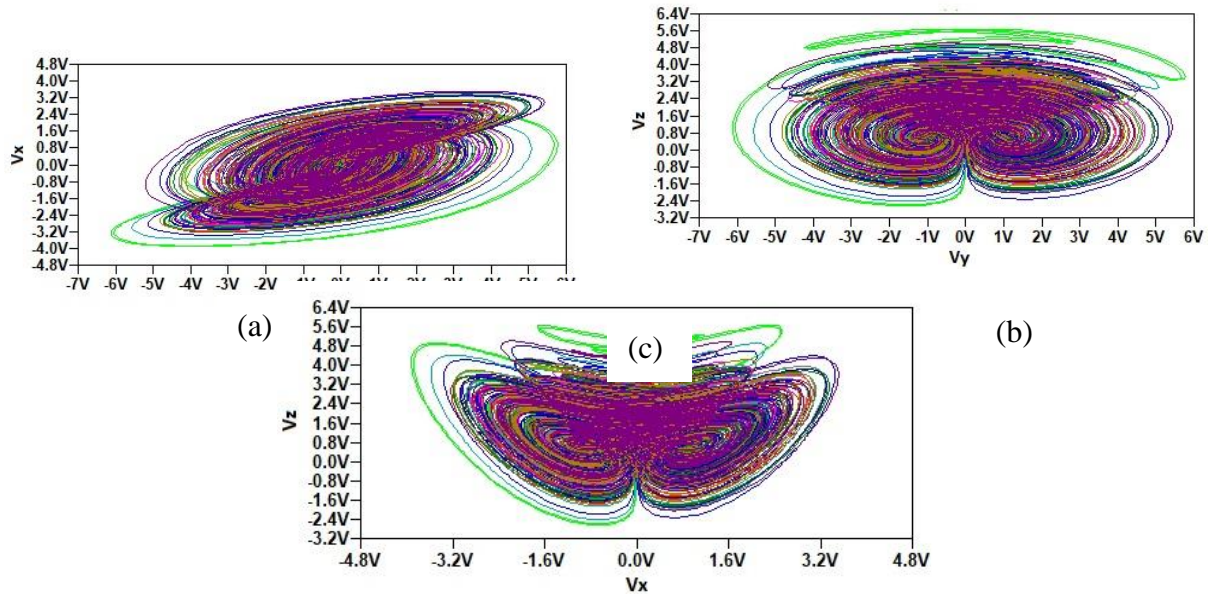


Fig. 4.9 Monte Carlo Analysis of phase trajectories of state variables: (a) x-y, (b) z-y, (c) z-x

## 4.7 Experimental Verification

In this section, the experimental verification of the PUCS I and PUCS IV variants is carried out by bread boarding the complete schematic of Fig. 4.3-4.5 using commercially available ICs AD844 and AD633. The supply voltages and component values are kept same as those used in simulative investigations. The experimental setup and breadboarded circuits for PUCS I and PUCS IV are shown in Fig. 4.10 and Fig. 4.11 respectively. The phase trajectory outputs, on Digital Storage Oscilloscope (DSO) screen, for state variables  $(V_x, V_y)$ ,  $(V_y, V_z)$  and  $(V_x, V_z)$  are shown in Figs. 4.12(a-c) and Figs. 4.12(d-f) for PUCS I and PUCS IV respectively. It may be noted that the experimental results are well inclined with the LTspice simulation results presented in Figs. 4.7(b) and 4.7(e).

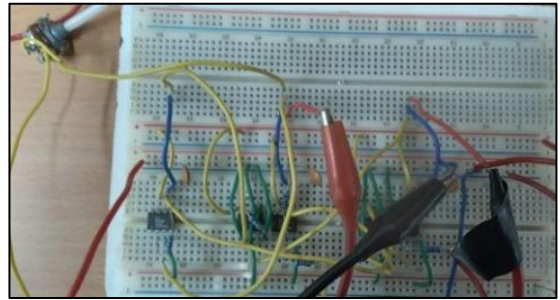


Fig. 4.10 Experimental setup to implement PUCS I

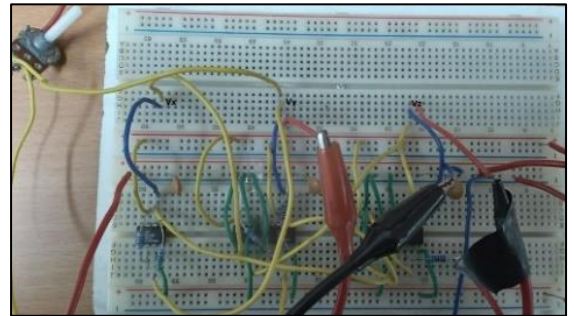
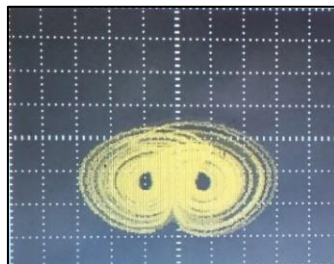


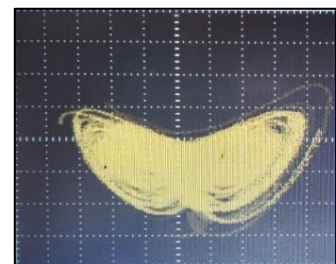
Fig. 4.11 Experimental setup to implement PUCS IV



(a)



(b)



(c)



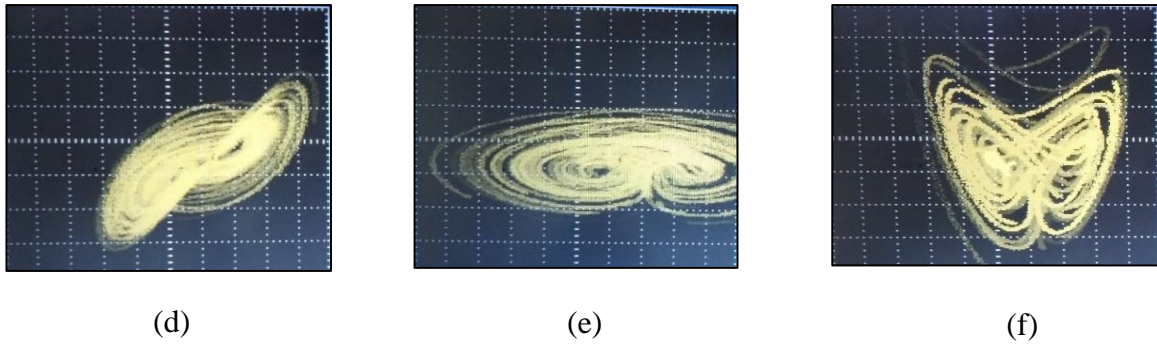


Fig. 4.12 Experimentally obtained phase space trajectories of PUCS I (a)  $yx$ , (b)  $yz$ , (c)  $xz$  and PUCS IV (d)  $yx$ , (e)  $yz$ , (f)  $xz$

## 4.8 Concluding Remarks

In this chapter, the candidate has reported and analysed four new variants of a recent chaotic system introduced by Pehlivan and Uyaröglu PUCS. Non-linear dynamic properties of these systems were investigated and expatiated through bifurcation diagrams, Lyapunov exponents, Kaplan Yorke Dimension, dissipativity, nature of equilibrium points through eigenvalues and chaotic attractors. The simulation results in MATLAB show that the range of parameter ‘a’ and ‘b’ is highest for PUCS IV, i.e., from 0.1 to 4.5, allowing a wide range of resistors. However, the value of  $D_{KY}$  is maximum for PUCS and PUCS I, i.e. 2.38, indicating the maximal chaoticity compared to the other three variants. Finally, an analog circuit design has been presented using current mode active building blocks, which can implement PUCS and all its proposed variants. Simulations are done for time series, frequency responses, phase portraits and Monte Carlo analysis. The frequency spectrums for state variables  $x$ ,  $y$  and  $z$  are noise like in frequency range 50 Hz to 1.5 kHz which falls in the audio signal frequency range of 20 Hz to 20 kHz. Thus, these signals generated from the proposed designs can be used in encryption of audio data before transmission in secure communication. Compared with the existing OpAmp based design of PUCS [15], this design is superior in that it uses lesser number of components. It has used three current mode active building blocks, two Analog Multipliers (AMs) and eight passive elements out of which four are grounded. In [15], four voltage mode active building blocks, two Analog Multipliers (AMs) and eleven passive components were used, all were floating. Moreover, we have reported the experimental verification of two of the proposed variants, PUCS I and PUCS IV, by breadboarding the circuit using off the shelf components, and the oscilloscope results show the feasibility of the proposed design.

# Chapter 5

## Generalized hardware efficient topology of chaotic systems with quadratic non-linearity

---

The content and results of the following paper have been reported in this chapter.

K. Suneja, N. Pandey and R. Pandey, "**Circuit realization of chaotic systems with quadratic nonlinearity using AD633 based generic topology**," *2022 International Conference on Computing, Communication, and Intelligent Systems (ICCCIS)*, Greater Noida, India, 2022, pp. 284-289, doi: 10.1109/ICCCIS56430.2022.10037747.

## 5.1 Introduction

In chapters 3 and 4, the circuit realization of Rössler and PUCS with its proposed variants respectively were presented using CFOAs (AD844) and AMs (AD633). In these circuits, the CFOA count depends upon the number of addition and subtraction operations in governing equations of chaotic system, while the number of quadratic non-linearities decides AM count, thus the overall realization requires two types of analog building blocks.

In this chapter, a generic circuit is presented for implementation of chaotic systems employing quadratic non-linearity. It uses only AD633 as active building block and exploits the inherent features of addition/ subtraction and multiplication of AD633. Therefore, the overall component count reduces significantly. The customization of the proposed topology is elucidated in detail for Rabinovich chaotic system (RCS). Seven other chaotic systems have also been worked upon and findings are comprehended in this chapter.

## 5.2 The generic circuit topology

The AD633 [108] is a versatile active block that has capability of performing addition, subtraction, scaling and generating quadratic nonlinear terms. In chapter 2, it has been presented as voltage mode block. In [82], a minor modification was suggested to convert voltage output to current output as shown in Fig. 5.1(a). Further, various combinations of resistors and capacitors can be placed at the current output to implement the governing equations of a chaotic system with quadratic type non-linearity(ies).

The proposed generic circuit topology is presented in this section and shown in Fig. 5.1(b) that may be customized to realize governing equations of chaotic systems having quadratic nonlinearity(ies).

The complete schematic of the proposed AD633 based topology is shown in Fig. 5.1(c). It can implement differential equations having linear/ non-linear terms and constants. Applying Kirchoff's Voltage Law (KVL) and Kirchoff's Current Law (KCL) in Fig. 5.1(c) gives

$$\dot{V}_{li} = \frac{(V_{x1i}-V_{x2i})(V_{y1i}-V_{y2i})}{10R_{1i}C_{li}} - \frac{V_{li}}{R_{2i}C_{li}} - \frac{V_{li}-V_{mi}}{R_{3i}C_{li}} \quad (5.1)$$

Here subscript  $i = 1,2,3$  and refer to three governing equations of a chaotic system. The values of the input voltages ( $V_{x1i}$ ,  $V_{x2i}$ ,  $V_{y1i}$ ,  $V_{y2i}$ ,  $V_{mi}$ ), resistors ( $R_{1i}$ ,  $R_{2i}$  and  $R_{3i}$ ) and capacitor  $C_{li}$  may be set according to the requirements.

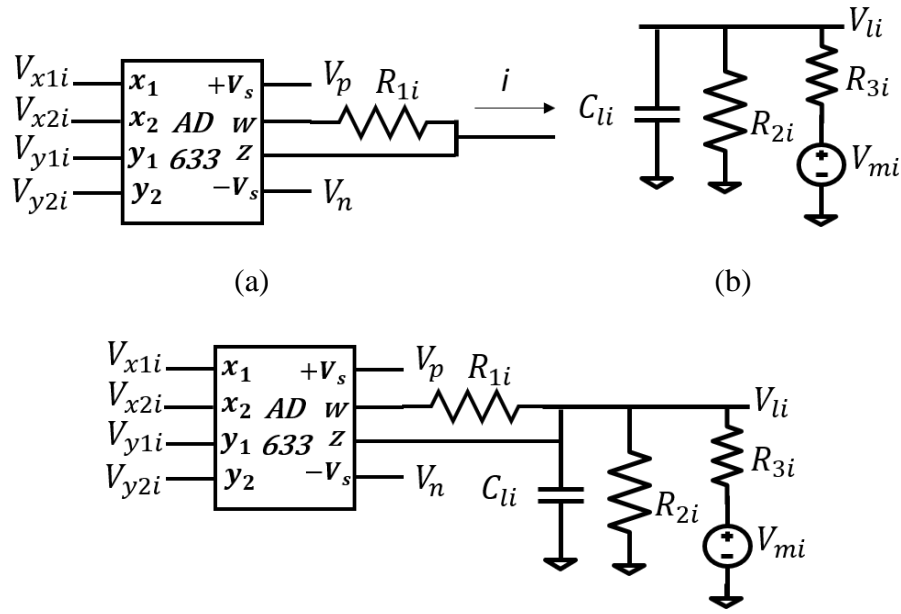


Fig. 5.1 (a) AD633 in current mode; (b) Proposed generalized topology to implement chaotic systems; (c) Complete schematic

The distinctive features of the proposed work are as follows:

1. The total number of AD633s are equal to number of the state variables, i.e. three.
2. It does not require the need of introducing extra terms or any modification in the characteristic equations for the simplification, as reported in [82].

### 5.3 Customization of proposed generic topology for Rabinovich chaotic system (RCS)

The governing equations of Rabinovich chaotic system are given by

$$\dot{x} = hy - ax + yz \quad (5.2a)$$

$$\dot{y} = hx - by - xz \quad (5.2b)$$

$$\dot{z} = -dz + xy \quad (5.2c)$$

where  $x$ ,  $y$  and  $z$  are the three state variables, whose time differentiations are being represented by  $\dot{x}$ ,  $\dot{y}$  and  $\dot{z}$  respectively. As a chaotic system is represented by three state variables, the complete design will require three instances of proposed generic topology.

In circuit representation, the voltage across capacitor is considered as state variable. Let capacitor voltages  $V_{11}$ ,  $V_{12}$  and  $V_{13}$  represent state variables  $x$ ,  $y$  and  $z$  respectively.

Setting  $V_{x2i}$  and  $V_{mi}$  to ground and  $R_{3i}$  to open circuit, (5.1) reduces to

$$C_{l1} \cdot \dot{V}_{l1} = \frac{(V_{x11})(V_{y11}-V_{y21})}{10R_{11}} - \frac{V_{l1}}{R_{21}} \quad (5.3)$$

By setting  $10R_{11}C_{l1} = 1$ ,  $R_{21}C_{l1} = a^{-1}$  and  $V_{y21} = -h$ , (5.3) reduces to

$$\dot{V}_{l1} = (V_{x11})(V_{y11} + V_h) - aV_{l1} \quad (5.4)$$

The correspondence between (5.4) and (5.2a) is established by simply connecting  $V_{x1i}$ ,  $V_{y1i}$  and  $V_{li}$  to  $V_{l2}$ ,  $V_{l3}$  and  $V_{l1}$  respectively. The final equation is given by (5.5).

$$\dot{V}_{l1} = V_{l2}(V_{l3} + V_h) - aV_{l1} \quad (5.5)$$

Again, setting  $V_{x2i}$  and  $V_{mi}$  to ground and  $R_{3i}$  to open circuit, (5.1) reduces to

$$C_{l2} \cdot \dot{V}_{l2} = \frac{(V_{x1})(V_{y1}-V_{y2})}{10R_{12}} - \frac{V_{l2}}{R_{22}} \quad (5.6)$$

Now, by setting  $10R_{12}C_{l2} = 1$ ,  $R_{22}C_{l2} = b^{-1}$  and  $V_{y12} = h$ , and connecting  $V_{x1i}$ ,  $V_{y2i}$  and  $V_{li}$  to  $V_{l1}$ ,  $V_{l3}$  and  $V_{l2}$  respectively, (5.6) reduces to

$$\dot{V}_{l2} = V_{l1}(V_h - V_{l3}) - bV_{l2} \quad (5.7)$$

The same procedure is repeated for (5.2c), where  $V_{x2i}$ ,  $V_{y2i}$  and  $V_{mi}$  were set to ground, making (5.1) look like (5.8).

$$C_{l3} \cdot \dot{V}_{l3} = \frac{(V_{x1})(V_{y1})}{10R_{13}} - \frac{V_{l3}}{R_{23}} \quad (5.8)$$

Putting  $10R_{13}C_{l3} = 1$ ,  $R_{23}C_{l3} = d^{-1}$ , and connecting  $V_{x1i}$ ,  $V_{y1i}$  and  $V_{li}$  to  $V_{l1}$ ,  $V_{l2}$  and  $V_{l3}$  respectively, (5.8) reduces to

$$\dot{V}_{l3} = V_{l1} \cdot V_{l2} - dV_{l3} \quad (5.9)$$

The complete circuit design to implement (5.2) is presented in Fig. 5.2.

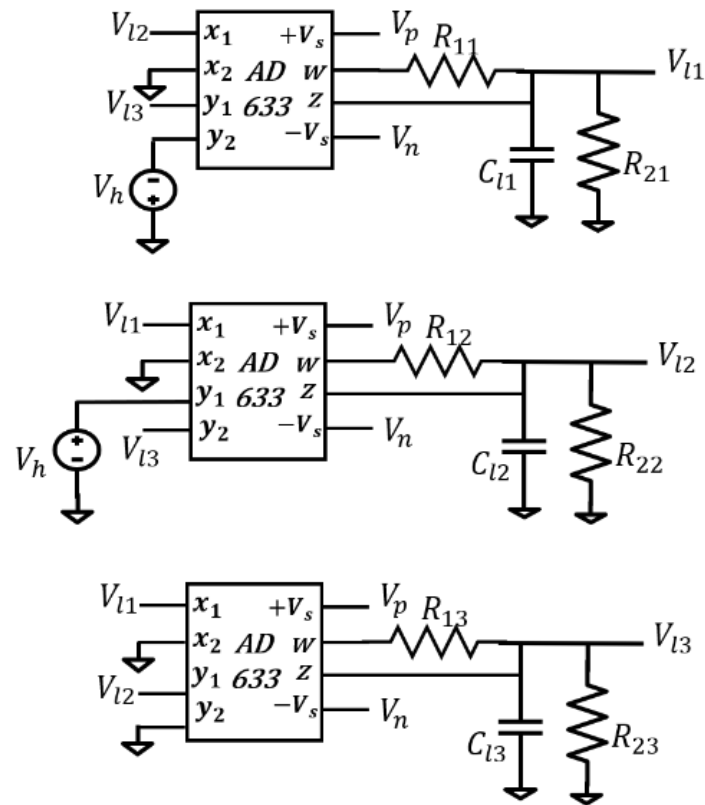


Fig. 5.2 AD633 based complete circuit design of Rabinovich chaotic system

Further, the usefulness of proposed generic topology is examined for seven more chaotic systems. The state variables  $x$ ,  $y$  and  $z$  are represented by  $V_{l1}$ ,  $V_{l2}$  and  $V_{l3}$  for circuit implementation for all chaotic systems and all capacitors are considered as 1 unit and  $R_{1i}$  is taken as 0.1 unit. The input voltages to AD633, the conditions on values of  $R_{2i}$  and  $R_{3i}$  are summarized in Table 5.1.

Table 5.1 Chaotic systems mapped on proposed topology

Ref	Chaotic system and its Governing equations	V <sub>li</sub>	V <sub>x1i</sub>	V <sub>x2i</sub>	V <sub>y1i</sub>	V <sub>y2i</sub>	V <sub>mi</sub>	R <sub>2i</sub>	R <sub>3i</sub>
[1]	$\dot{x} = \sigma(y - x)$ $\dot{y} = \rho x - y - xz$ $\dot{z} = xy - rz$	V <sub>11</sub>	$\sigma$	gnd	V <sub>12</sub>	V <sub>11</sub>	0	$\infty$	$\infty$
		V <sub>12</sub>	V <sub>11</sub>	gnd	$\rho^{****}$ *	V <sub>13</sub>	0	1	$\infty$
		V <sub>13</sub>	V <sub>11</sub>	gnd	V <sub>12</sub>	gnd	0	1/r	$\infty$
[29, 113]	$\dot{x} = a(y - x)$ $\dot{y} = cx - xz$ $\dot{z} = -bz + xy$	V <sub>11</sub>	a	gnd	V <sub>12</sub>	V <sub>11</sub>	0	$\infty$	$\infty$
		V <sub>12</sub>	V <sub>11</sub>	gnd	c	V <sub>13</sub>	0	$\infty$	$\infty$
		V <sub>13</sub>	V <sub>11</sub>	gnd	V <sub>12</sub>	gnd	0	1/b	$\infty$
[27]	$\dot{x} = a(y - x) + yz$ $\dot{y} = cx - y - xz$ $\dot{z} = xy - bz$	V <sub>11</sub>	V <sub>12</sub>	gnd	V <sub>13</sub>	-a	0	1/a	$\infty$
		V <sub>12</sub>	V <sub>11</sub>	gnd	c	V <sub>13</sub>	0	1	$\infty$
		V <sub>13</sub>	V <sub>11</sub>	gnd	V <sub>12</sub>	gnd	0	1/b	$\infty$
[26]	$\dot{x} = -ax + by - yz$ $\dot{y} = x + xz$ $\dot{z} = -cz + y^2$	V <sub>11</sub>	V <sub>12</sub>	gnd	b	V <sub>13</sub>	0	1/a	$\infty$
		V <sub>12</sub>	V <sub>11</sub>	gnd	V <sub>13</sub>	-1V	0	$\infty$	$\infty$
		V <sub>13</sub>	V <sub>12</sub>	gnd	V <sub>12</sub>	gnd	0	1/c	$\infty$
[32]	$\dot{x} = a(y - x)$ $\dot{y} = xz - y$ $\dot{z} = b - xy - cz$	V <sub>11</sub>	a	gnd	V <sub>12</sub>	V <sub>11</sub>	0	$\infty$	$\infty$
		V <sub>12</sub>	V <sub>11</sub>	gnd	V <sub>13</sub>	gnd	0	1	$\infty$
		V <sub>13</sub>	V <sub>11</sub>	gnd	gnd	V <sub>12</sub>	b	1/c	1
[35]	$\dot{x} = a(y - x)$ $\dot{y} = (c - a)x - axz$ $\dot{z} = -bz + xy$	V <sub>11</sub>	a	gnd	V <sub>12</sub>	V <sub>11</sub>	0	$\infty$	$\infty$
		V <sub>12</sub>	V <sub>11</sub>	gnd	k**	$R_4/(R_4+R_2)$ . V <sub>13</sub> *	0	$\infty$	$\infty$
		V <sub>13</sub>	V <sub>11</sub>	gnd	V <sub>12</sub>	gnd	0	$\infty$	$\infty$
[36]	$\dot{x} = -ax - byz$ $\dot{y} = -x + cy$ $\dot{z} = d - y^2 - z$	V <sub>11</sub>	gnd	V <sub>12</sub>	V <sub>13</sub>	gnd	0	1/a	$\infty$
		V <sub>12</sub>	V <sub>12</sub>	V <sub>11</sub>	c'****	gnd	0	1	$\infty$
		V <sub>13</sub>	V <sub>12</sub>	gnd	gnd	V <sub>12</sub>	d	1	1

\* a voltage divider circuit to implement 'az'

\*\* k is a constant voltage equal to (c-a)

\*\*\*  $c' = \left(c + \frac{1}{R_{22}}\right) \cdot (0.1R_{12})$

\*\*\*\*  $\rho' = \frac{\rho \cdot R_{22}}{0.1}$

## 5.4 Simulation Results

This section deals with functional verification of proposed AD633 based chaotic systems realization in LTspice design environment. The simulations have been carried out using Analog Devices macromodel of AD633 [108]. The power supply voltage for all the systems is  $\pm 18V$ . These systems, tabulated in Table 5.1, have been simulated, and three representative examples of chaotic systems RCS, Lorenz chaotic system (LCS) and Yang Chen chaotic system (YCCS) have been shown as follows:

#### 5.4.1 Rabinovich chaotic system (RCS) [37, 38]

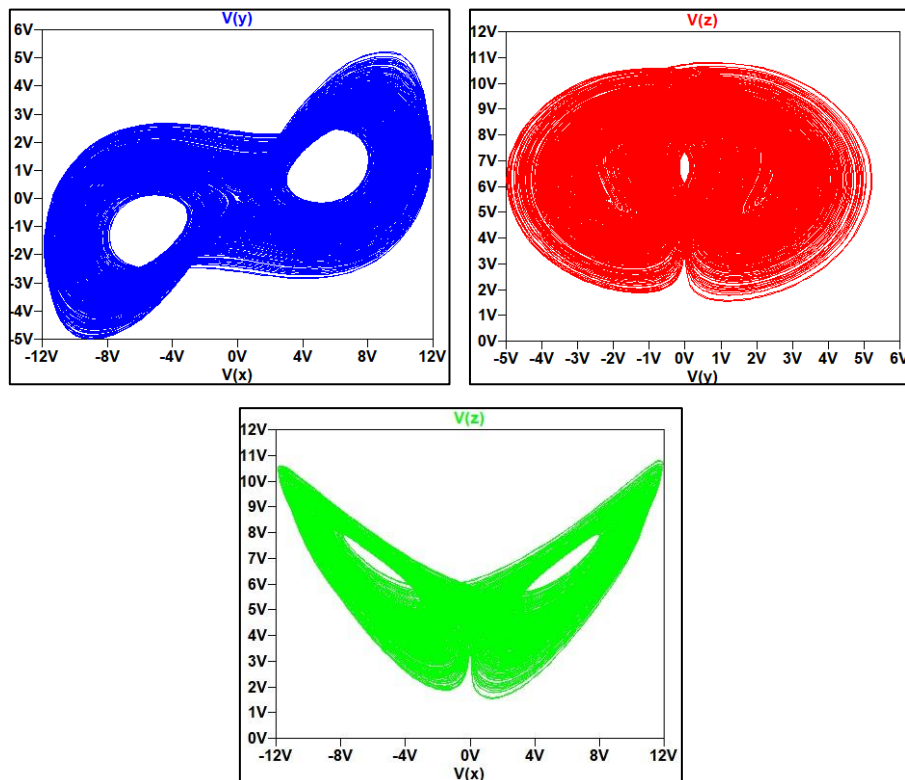
The values of resistors  $R_{1i}$ ,  $R_{2i}$  and  $R_{3i}$  are computed corresponding to parameters  $a = 4$ ,  $b = 1$ ,  $d = 1$  and  $h = 6.75$ . The  $V_{mi}$  is not required for all governing equations and same is true for  $R_{3i}$ . The value of resistors  $R_{1i}$  ( $i=1,2,3$ ) is kept at  $1k\Omega$  while  $R_{21}$ ,  $R_{22}$  and  $R_{23}$  at  $4k\Omega$ ,  $10k\Omega$  and  $10k\Omega$  respectively. Fig. 5.3 (a) shows simulated phase plots in x-y, x-z and y-z planes which confirm to the functionality of RCS.

#### 5.4.2 Lorenz chaotic system (LCS) [1]

Similar to RCS, LCS also does not require  $R_{3i}$  and  $V_{mi}$  ( $i=1,2,3$ ). Using the parameters  $\sigma = 10$ ,  $r = 28$  and  $\rho = 8/3$ , the values of resistors  $R_{11}$ ,  $R_{12}$ ,  $R_{13}$ ,  $R_{22}$ ,  $R_{23}$  are computed as  $1k\Omega$ ,  $100\Omega$ ,  $1k\Omega$ ,  $10k\Omega$  and  $3.75k\Omega$  respectively. It is to be noted that in order to scale the value of  $\rho = 28V$  to  $2.8V$ ,  $R_{12}$  has been reduced to  $100\Omega$ . The phase space plots in x-y, x-z and y-z planes are depicted in Fig. 5.3 (b), where all of them are two scroll in nature.

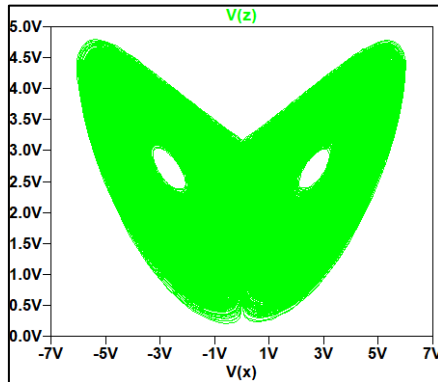
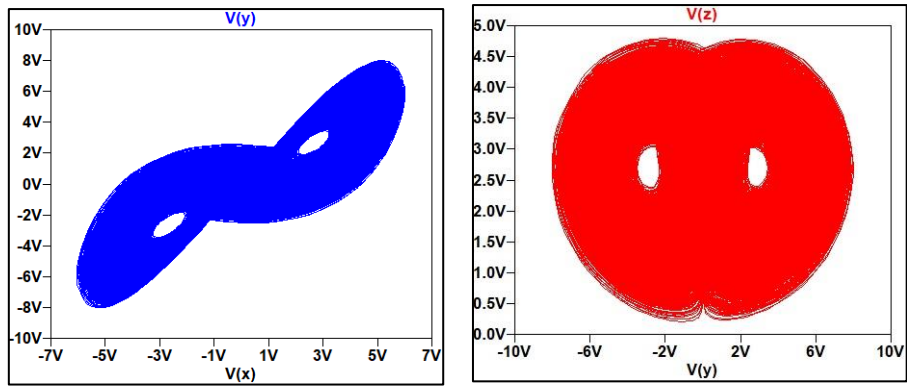
#### 5.4.3 Yang Chen chaotic system (YCCS) [29,113]

For YCCS, using the parameters  $a = 1$ ,  $b = 0.05$  and  $c = 15$ , the values of resistors  $R_{11}$ ,  $R_{12}$ ,  $R_{13}$ ,  $R_{23}$  are computed as  $100\Omega$ ,  $100\Omega$ ,  $100\Omega$  and  $20k\Omega$  respectively. The phase space plots in x-y, x-z and y-z planes are depicted in Fig. 5.3 (c), where all of them are two scroll in nature.

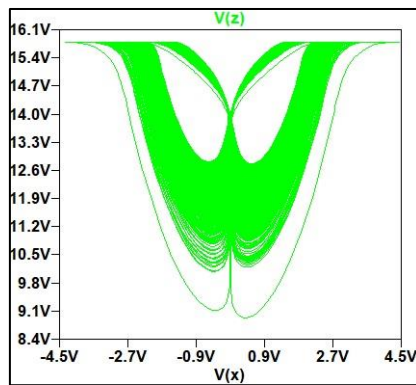
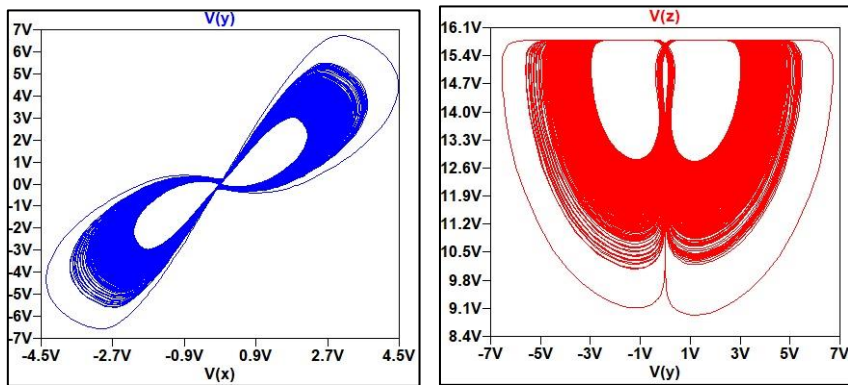


(a)





(b)



(c)

Fig. 5.3 Phase space plots of (a) RCS and (b) LCS and (c) YCCS in x-y, x-z and y-z planes

## **5.5 Concluding Remarks**

An optimized circuit design of chaotic systems with quadratic type non-linearities has been proposed. It utilizes AD633s equal to the dimension of the chaotic system, along with passive linear components, such as resistors and capacitors. This prevents the need for two different types of active building blocks, thus reducing the hardware count significantly. LTspice simulations are in agreement with the numerical simulations existing in literature. Circuit simplification by reducing hardware complexity plays a vital role in the generation of chaotic attractors for various real time applications. This also makes the circuit highly accurate because of the reduced number of components, thus their inherent errors. Thus, it will be beneficial for chaos applications to engineering problems.

# Chapter 6

## New chaotic system with exponential non-linearity

---

The content and results of the following paper have been reported in this chapter.

K. Suneja, N. Pandey and R. Pandey, “**A novel chaotic system with exponential non-linearity and its adaptive self-synchronization: From numerical simulations to circuit implementation,**” Journal of Circuits, Systems and Computers.  
<https://doi.org/10.1142/S0218126623502961>.

## 6.1 Introduction

The chaotic systems based on quadratic non-linearities have been presented in preceding chapters. Besides the number of non-linear terms, the type of non-linearity also affects the behaviour of the chaotic system, both numerically and in circuit design. The chaotic systems may also be realized with inherent exponential non-linearity of diode. There is limited work on such systems [44-47]. In [44], Rössler chaotic system has been modified to incorporate exponential non-linearity instead of quadratic non-linearity, while [45-47] use quadratic exponential type non-linearities.

This work presents a new chaotic system, with exponential non-linearities with a goal to reduce the count of active building blocks used for realization. The fixed points of the proposed system are analysed; and the dynamics of the proposed system is examined through numerical simulations and observing bifurcation diagrams, maximum Lyapunov exponents, Kaplan Yorke dimension and dissipativity. As far as electronic design of chaotic system is concerned, the designs incorporating quadratic non-linearity require AMs, while, in this work, we have proposed a chaotic system which is free of quadratic non-linearity. It employs two diodes to introduce exponential non-linearities in the system, which is an easily available low-cost component. Further, an adaptive controller with parameter update laws based on Lyapunov stability theorem to self-synchronize the proposed chaotic system is also put forward. The numerical simulations are carried out to confirm the feasibility and efficacy of the proposed adaptive controller design. CFOA based realization of the proposed controller is also put forward for illustrating the possibility of hardware design.

## 6.2 Proposed chaotic system and its numerical analysis

The proposed chaotic system uses three state variables ( $x, y, z$ ), two exponential non-linearities and two parameters 'a' and 'b.' The governing equations of the proposed system relate state variables ( $x, y, z$ ) with their time differentiation and are given in (6.1).

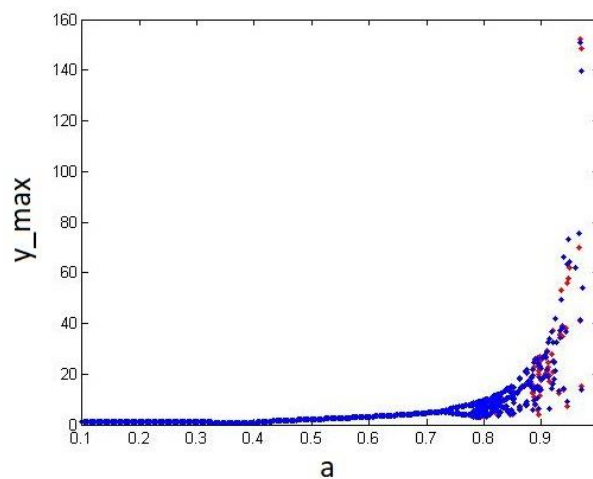
$$\dot{x} = y - x \quad (6.1a)$$

$$\dot{y} = ay - x - z \quad (6.1b)$$

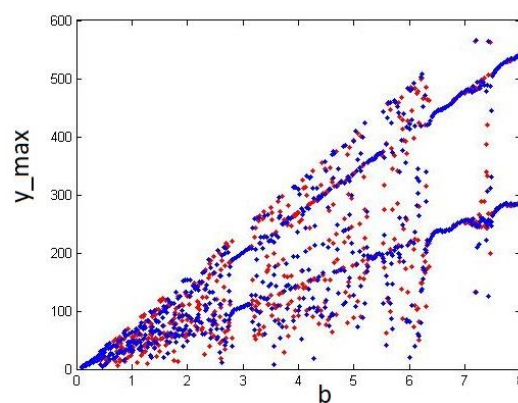
$$\dot{z} = e^x + e^y - b \quad (6.1c)$$

### 6.3 Properties and behaviors of the novel chaotic system

To obtain parameter range in which a system behaves chaotically, bifurcation plots are obtained by varying one parameter while keeping others fixed. Figures 6.1(a) represent two plots (shown in blue and red colour) corresponding to two different initial conditions (1,1,1) and (-1, -1, -1). Figure 6.1(a) shows the bifurcation plot of the proposed system by varying parameter ‘a’ ( $0.1 \leq a \leq 1$ ) while keeping ‘b’ fixed at ‘b’ = 0.5. It may be noted that the proposed system in (6.1) exhibits periodic nature for ‘a’  $\in [0.1: 0.75]$  and chaotic behaviors for ‘a’  $\in [0.8: 0.85]$ ,  $[0.91, 0.94]$ . The bifurcation plot for the proposed system with ‘b’ ( $0 \leq b \leq 8$ ) and keeping ‘a’ = 0.91 is shown in Fig. 6.1(b). The proposed system is found to be chaotic when  $b \in [0.5: 2.7]$ ,  $[3.75: 5.1]$ ,  $[5.75: 6.3]$ .



(a)



(b)

Fig. 6.1 Bifurcation diagrams with change in parameter (a) ‘a,’ (b) ‘b’

The chaotic systems are characterized by some properties, such as Lyapunov exponents, Kaplan Yorke dimension, dissipativity, whose values determine their nature. These properties for the proposed chaotic system have been studied based on numerical simulations in this section.

The chaotic systems have a heavy dependence on initial conditions, this property is quantified by Lyapunov exponents. For the chosen parameter values,  $a=0.91$  and  $b=0.5$ , the Lyapunov exponents are obtained as:

$$L_1 = 0.011475, L_2 = 0.001919, L_3 = -0.103394 \quad (6.2)$$

The plot of Lyapunov exponents with time is shown in Fig. 6.2. Since  $L_1$  is positive,  $L_2$  is very close to zero and  $L_3$  is negative in Fig. 6.2, it follows that (6.1) is chaotic for ‘ $a$ ’=0.91 and ‘ $b$ ’=0.5.

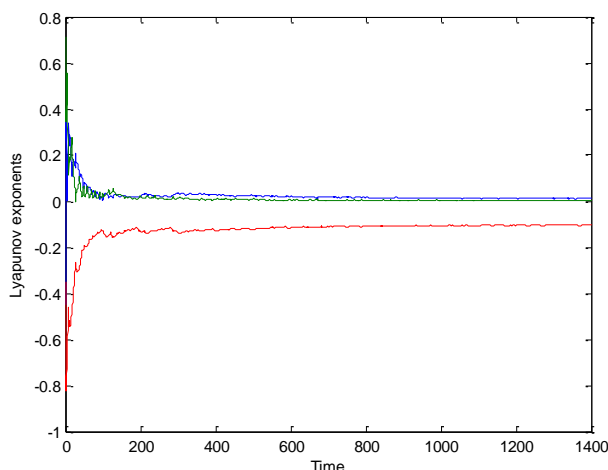


Fig. 6.2 Dynamics of Lyapunov exponents with respect to time

The Kaplan Yorke dimension, an estimate of the dimension of the volume which neither grows nor decays, is calculated as:

$$D_{KY} = 2 + \frac{L_1 + L_2}{|L_3|} = 2.1295 \quad (6.3)$$

This value of  $D_{KY}$  for proposed chaotic system is higher than many existing chaotic systems [17, 20, 22, 24]. This signifies the higher complexity in the proposed system, making it a suitable candidate for applications in encryption and secure communication.

In case of proposed system,  $\nabla \cdot V = -1 + a < 0$ , therefore dissipativity condition holds for this system, which implies that the phase space volume of the attractor of (6.1) at any point of time  $t$  is given by (6.4).

$$V(t) = V_0 e^{(a-1)t} \quad (6.4)$$

Where  $V_0$  is the initial volume at  $t=0$ .

## 6.4 Analysis of fixed points

In this section, the fixed points for the proposed system have been determined, followed by the analysis of the corresponding eigenvalues to study the nature of the attractors being produced by these points.

In mathematics, time differentiation of state variable may be equated to zero to determine fixed points. Applying this to (6.1) gives

$$\begin{aligned} y &= x \\ ay &= x + z \\ e^x + e^y &= b \end{aligned} \quad (6.5a)$$

Solving (6.5a) provides the fixed point values as

$$x = y = \ln\left(\frac{b}{2}\right); z = (a - 1) \ln\left(\frac{b}{2}\right) \quad (6.5b)$$

Hence, the proposed system has only one fixed point 'p' at  $\left(\ln\left(\frac{b}{2}\right), \ln\left(\frac{b}{2}\right), (a - 1) \ln\left(\frac{b}{2}\right)\right)$ .

Further, the eigen values corresponding to fixed points may be found by linearizing (6.1). The resulting Jacobian matrix for proposed chaotic system is computed as:

$$J = \begin{bmatrix} -1 & 1 & 0 \\ -1 & a & -1 \\ e^x & e^y & 0 \end{bmatrix} \quad (6.6)$$

The characteristic equation obtained by  $|J-\lambda I|=0$ , where  $I$  is an identity matrix, is

$$\lambda^3 - \lambda^2(a - 1) - \lambda\left(a - \frac{b}{2} - 1\right) + b = 0 \quad (6.7)$$

Solving (6.7) for  $a=0.91$  and  $b=0.5$  gives three eigenvalues at p:

$$\lambda_1 = -0.677; \lambda_2 = 0.294 + i0.807; \lambda_3 = 0.294 - i0.807$$

Since the three eigen values have non-zero real part, the fixed point is hyperbolic. The proposed chaotic system has one real negative eigenvalue,  $\lambda_1$  and two complex conjugates with non-zero

positive real part,  $\lambda_2$  and  $\lambda_3$ . Negative eigenvalues show the existence of the stable manifolds in a small neighbourhood of a fixed point, while positive ones reveal the unstable manifolds. Thus,  $p$  belongs to the category of index-2 spiral saddle type fixed point. The attractor for this chaotic system will be sinking towards the fixed point in one direction, while expanding spirally in two-dimensions.

## 6.5 Circuit design of the proposed chaotic system

This section presents implementation of proposed chaotic system using CFOA. The exponential non-linearity is realized using diodes which is characterized by  $I = I_0 (e^{\frac{V_d}{\eta V_T}} - 1)$ , where  $I_0$  is the reverse saturation current,  $\eta$  is the emission coefficient, which is 1 for germanium devices and 2 for silicon devices and  $V_T$  is the voltage equivalent of temperature.

Let voltage across capacitors  $C_x$ ,  $C_y$  and  $C_z$  correspond to the state variables  $x$ ,  $y$  and  $z$ . The realization of (6.1) is given in Fig. 6.3 and the governing equations of circuit are given in (6.8). It is to be noted that to obtain ‘ $-V_x$ ’ and ‘ $-V_y$ ’ in Fig. 6.3, two extra CFOAs and four resistors are required.

$$C_x \frac{dV_x}{dt} = \frac{V_y - V_x}{R_1} \quad (6.8a)$$

$$C_y \frac{dV_y}{dt} = \frac{V_m - V_x}{R_4} + \frac{V_m - V_z}{R_5} \quad (6.8b)$$

$$C_z \frac{dV_z}{dt} = \frac{I_0 \left( e^{\frac{V_x}{\eta V_T}} + e^{\frac{V_y}{\eta V_T}} - 2 \right) R_6 - V_b}{R_7} \quad (6.8c)$$

where,

$$V_m = \frac{R_3}{R_2 + R_3} V_y$$



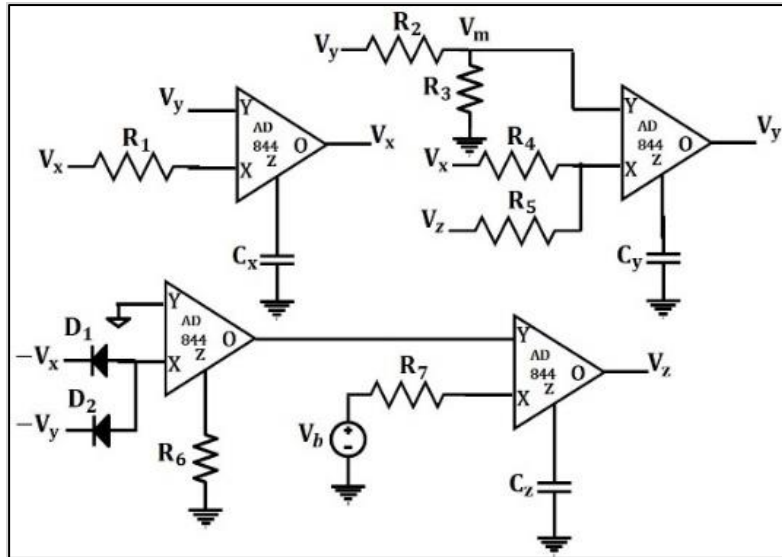


Fig. 6.3 Schematic of CFOA based novel chaotic system

Equating (6.8) with (6.1) will give the desired values of the passive components for the realization of the proposed system. With the following values of parameters,  $a=0.91$  and  $b=0.5$ , for which the theoretical model of (6.1) exhibits chaotic behaviour, the values of circuit components are enlisted in Table 6.1.

Table 6.1 Components' values for the CFOA based design of the proposed system

$R_1$	$R_2$	$R_3$	$R_4$	$R_5$	$R_6$	$R_7$	$C_x$	$C_y$	$C_z$	$V_b$
10k $\Omega$	12k $\Omega$	10k $\Omega$	10k $\Omega$	10k $\Omega$	67k $\Omega$	100k $\Omega$	100nF	100nF	100nF	-0.0015V

The operation of the proposed circuit is verified in LTspice design environment. The macromodel for AD844 is imported from Analog Devices and MUR460 diode's model is taken from LTspice design suite. The supply voltages are chosen as  $\pm 9V$ . The simulated phase space plots for the proposed circuit in  $y-x$ ,  $y-z$  and  $x-z$  planes are shown in Fig. 6.4. It may be observed that the shape of  $V_y-V_x$  phase space plot is oval shaped, whereas  $V_y-V_z$  and  $V_x-V_z$  phase space plots are in the shape of a tent. The occurrence of chaotic attractors in Fig. 6.4 confirms the validity of the proposed circuit.

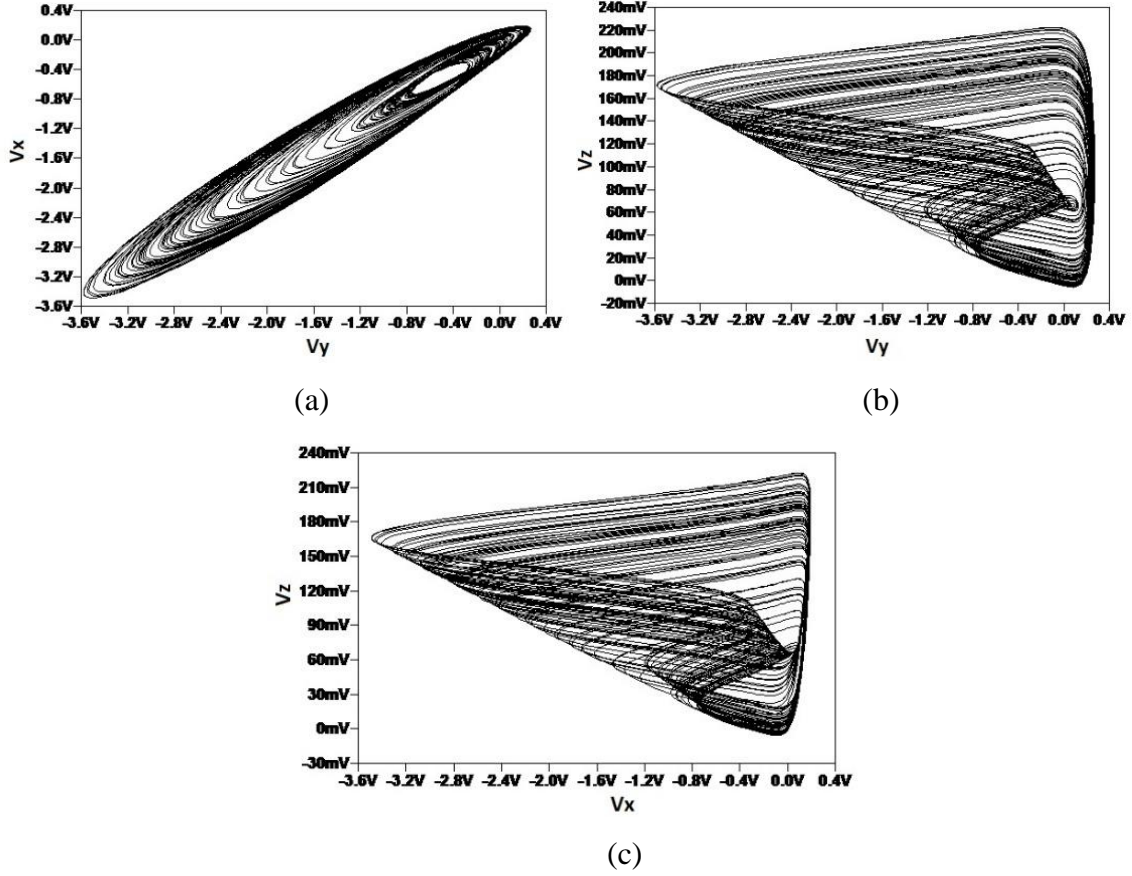


Fig. 6.4 Phase space plots of the designed circuit in (a) y-x plane, (b) y-z plane, (c) x-z plane

## 6.6. Adaptive control synchronization of the proposed chaotic system

Synchronization mechanism plays a critical role for constructing secure communication schemes. Let the master state variables being  $(x_1, y_1, z_1)$  and slave state variables being  $(x_2, y_2, z_2)$ . The step-by-step process of adaptive control synchronization is as follows:

### 6.6.1 Master and slave representation

The drive (master) chaotic system is being represented by (6.9) as

$$\dot{x}_1 = y_1 - x_1 \quad (6.9a)$$

$$\dot{y}_1 = ay_1 - x_1 - z_1 \quad (6.9b)$$

$$\dot{z}_1 = e^{x_1} + e^{y_1} - b \quad (6.9c)$$

The response (slave) chaotic system is expressed as

$$\dot{x}_2 = y_2 - x_2 + u_1 \quad (6.10a)$$

$$\dot{y}_2 = ay_2 - x_2 - z_2 + u_2 \quad (6.10b)$$

$$\dot{z}_2 = e^{x_2} + e^{y_2} - b + u_3 \quad (6.10c)$$

Where,  $u_i$ , ( $i=1$  to  $3$ ) are the non-linear adaptive controllers.

### 6.6.2 Error dynamics

The complete synchronization of the two systems is characterized by the equality of the respective state variables, or the error functions, represented by (6.11), being reduced to zero.

$$e_x = x_2 - x_1; e_y = y_2 - y_1; e_z = z_2 - z_1 \quad (6.11)$$

The corresponding error dynamics is defined by (6.12).

$$\dot{e}_x = \dot{x}_2 - \dot{x}_1; \dot{e}_y = \dot{y}_2 - \dot{y}_1; \dot{e}_z = \dot{z}_2 - \dot{z}_1 \quad (6.12)$$

Using (6.9) and (6.10) and using expressions of (6.11), (6.12) can be rewritten as:

$$\begin{aligned} \dot{e}_x &= e_y - e_x + u_1 \\ \dot{e}_y &= a e_y - e_x - e_z + u_2 \\ \dot{e}_z &= e^{x_2} - e^{x_1} + e^{y_2} - e^{y_1} + u_3 \end{aligned} \quad (6.13)$$

### 6.6.3 Adaptive Controller

The control functions  $u_i$ , ( $i=1,2,3$ ) can be obtained from (6.13) as:

$$\begin{aligned} u_1 &= -k_1 e_x - e_y + e_x \\ u_2 &= -k_2 e_y - \hat{a} e_y + e_x + e_z \\ u_3 &= -k_3 e_z - e^{x_2} - e^{y_2} + e^{x_1} + e^{y_1} \end{aligned} \quad (6.14)$$

Where,  $\hat{a}$  is the estimated value of unknown parameter  $a$ ; and  $k_1$ ,  $k_2$  and  $k_3$  are positive gain constants.

### 6.6.4 Error in parameters' estimation

The parameter estimation error,  $e_a$ , is defined by

$$e_a = a - \hat{a}, \quad (6.15)$$

and its dynamics is given as

$$\dot{e}_a = -\dot{\hat{a}} \quad (6.16)$$

Using (6.14), the dynamics of the slave system and error can be simplified as (6.17) and (6.18) respectively

$$\begin{aligned} \dot{x}_2 &= y_2 - x_2 - k_1 e_x - e_y + e_x \\ \dot{y}_2 &= a y_2 - x_2 - z_2 - k_2 e_y - \hat{a} e_y + e_x + e_z \\ \dot{z}_2 &= e^{x_1} + e^{y_1} - b - k_3 e_z \end{aligned} \quad (6.17)$$

Also, substituting (6.14) in (6.13), we obtain:

$$\dot{e}_x = -k_1 e_x; \dot{e}_y = e_a \cdot e_y - k_2 e_y; \dot{e}_z = -k_3 e_z \quad (6.18)$$

Adaptive control theory is used to derive an update law for  $\hat{a}$ .

### 6.6.5 Lyapunov stability

Consider a candidate Lyapunov function

$$V = \frac{1}{2} (e_x^2 + e_y^2 + e_z^2 + e_a^2) \quad (6.19)$$

Differentiating V provides,

$$\dot{V} = e_x \dot{e}_x + e_y \dot{e}_y + e_z \dot{e}_z + e_a \dot{e}_a \quad (6.20)$$

Putting the values from (6.16) and (6.18) in (6.20) gives:

$$\dot{V} = -k_1 e_x^2 - k_2 e_y^2 + e_a e_y^2 - k_3 e_z^2 - \hat{a} e_a \quad (6.21)$$

For the complete system to be stable,  $\dot{V}$  should be negative. Since all other terms in (6.21) are negative except  $e_a(e_y^2 - \hat{a})$ , so this can be equated to zero.

### 6.6.6 Adaptive Laws

According to Lyapunov stability theory [111], the parameter update law derived from (6.21) is

$$\hat{a} = e_y^2 \quad (6.22)$$

The error dynamics (6.15) under the parameter adaptive rule (6.22) and the adaptive controller (6.14) can be stabilized in finite time asymptotically, i.e., the slave chaotic system (6.10) with different parameters' values will trace the master system asymptotically and the unified chaotic system will be called synchronized.

For the initial values of master system  $(x_{10}, y_{10}, z_{10}) = (1, 1, 1)$  and slave system  $(x_{20}, y_{20}, z_{20}) = (50, 25, 15)$  and  $\hat{a} = 10$  chosen arbitrarily, the synchronization process obtained from numerical simulations is depicted in Fig. 6.5.

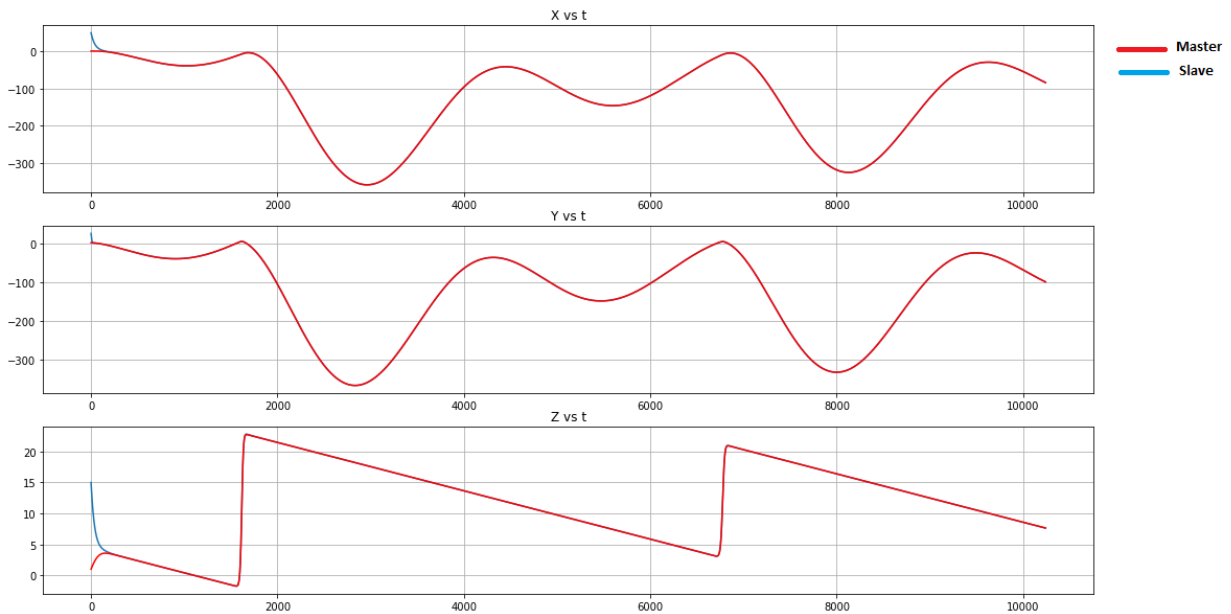


Fig. 6.5 Time variation of state variables  $x$ ,  $y$  and  $z$  with different initial states for master and slave

The proposed adaptive control synchronization process of estimated parameter  $\hat{a}$  of slave system towards the parameter  $a$  of master system is shown in Fig. 6.6, while the error functions  $e_x$ ,  $e_y$  and  $e_z$  are shown in Fig. 6.7. It is evident that response system synchronizes with the drive system in finite time and the error functions reduce to zero. However, the error in variable 'y' takes longer to reduce to zero. This may be due to the dependence of  $y$  on more number of variables ( $x$ ,  $y$  and  $z$ ) in (6.1b).

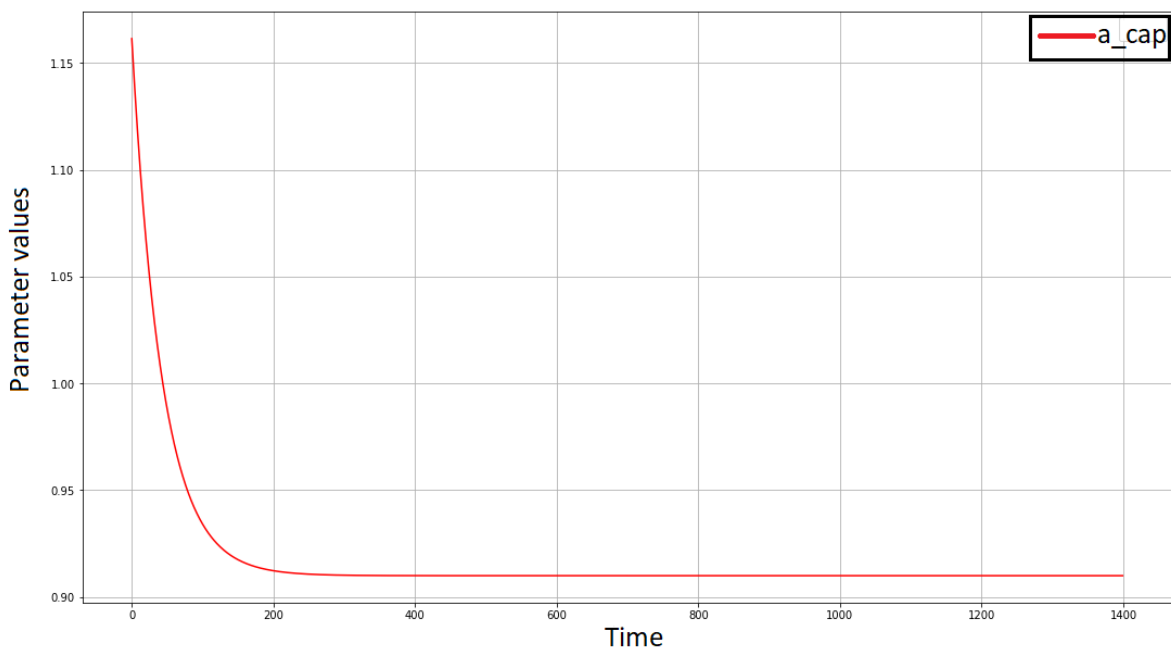


Fig. 6.6 Trace of slave's parameter in synchronization with master system

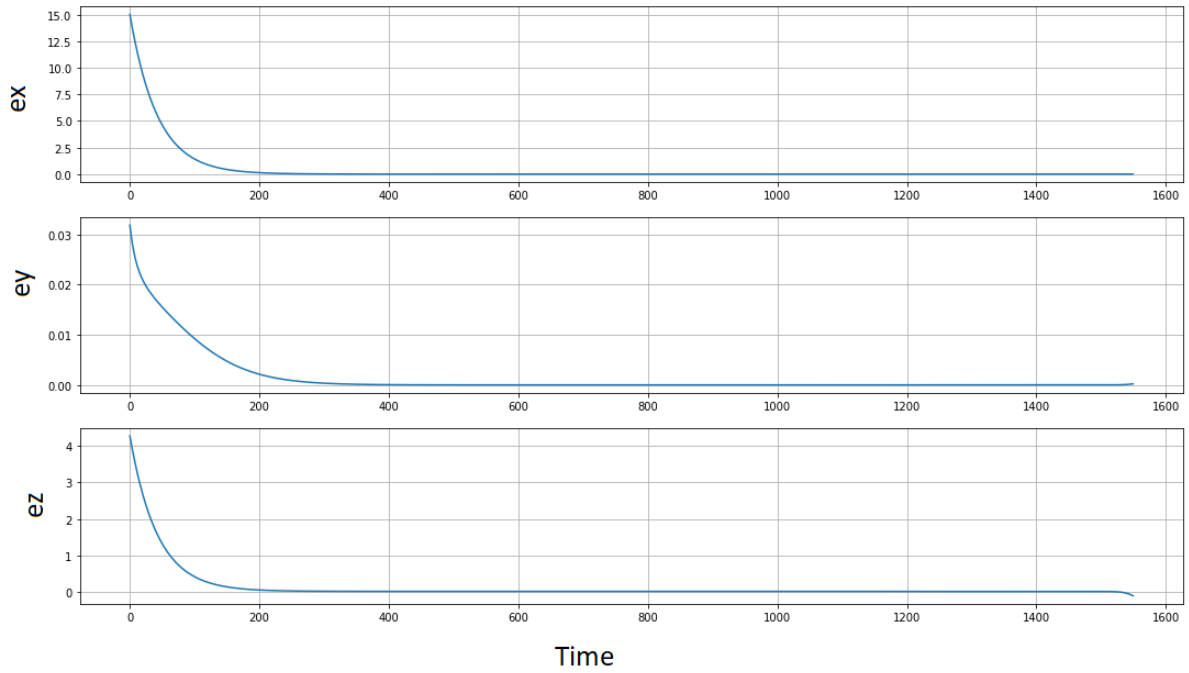
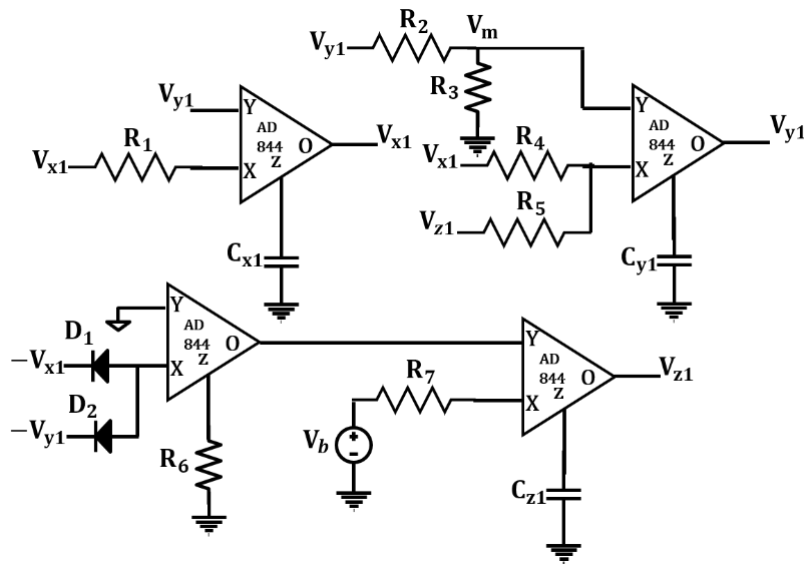
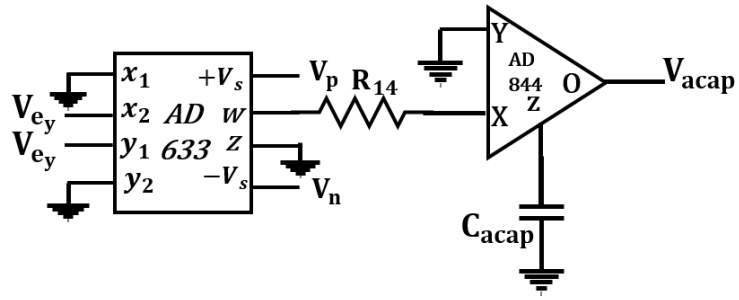


Fig. 6.7 Trajectories of error functions of state variables with time

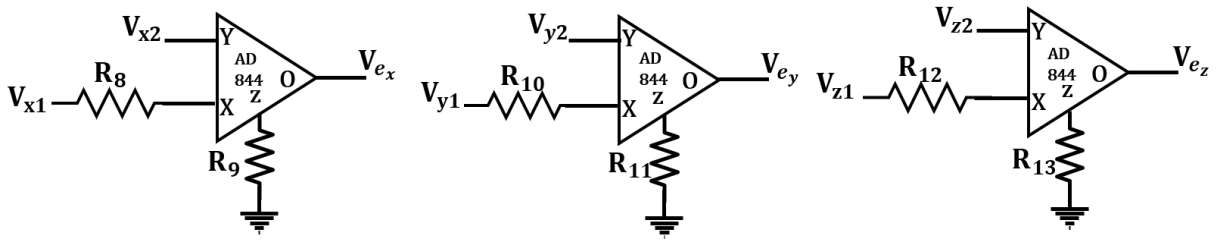
The circuit implementation of the whole scheme of adaptive control synchronization has been proposed in this work as shown in Fig. 6.8. The component values are calculated to satisfy the respective governing equations and tabulated in Table 6.2. The complete circuit is simulated in LTspice design environment. The synchronization of the master and slave circuit is evident from Fig. 6.9, thus proving the reliability and feasibility of the design.



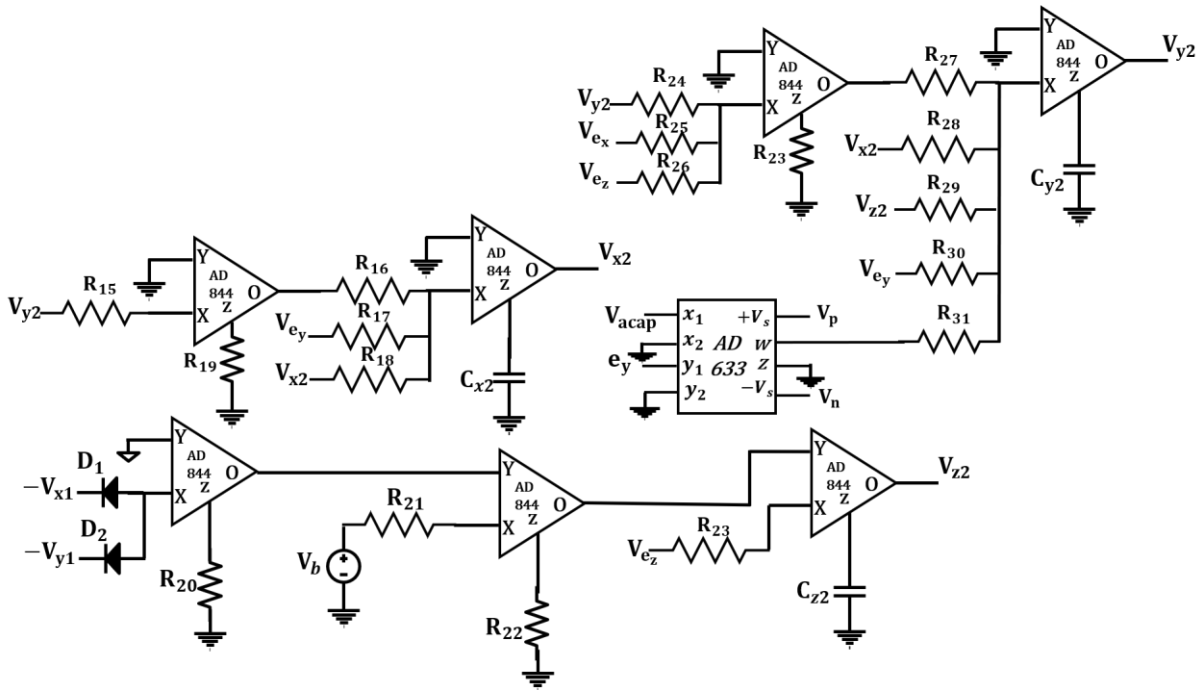
(a)



(b)



(c)



(d)

Fig. 6.8 Circuit design of adaptive synchronization of the proposed system: (a) Master circuit, (b) Error functions, (c) Updation law of slave's parameter, (d) Complete slave circuit

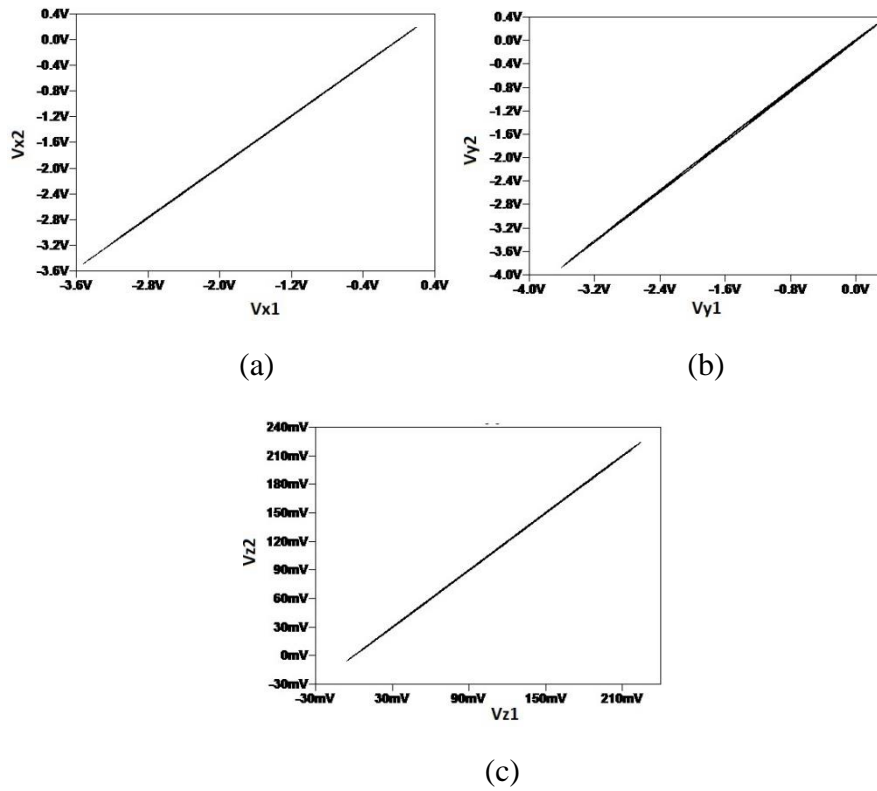


Fig. 6.9 LTspice plot between respective variables of master and slave circuit: (a)  $x_1x_2$ , (b)  $y_1y_2$ , (c)  $z_1z_2$

Table 6.2 Components' values for the CFOA based design of the proposed adaptive synchronization scheme

$R_8$ ( $\Omega$ )	$R_9$ ( $\Omega$ )	$R_{10}$ ( $\Omega$ )	$R_{11}$ ( $\Omega$ )	$R_{12}$ ( $\Omega$ )	$R_{13}$ ( $\Omega$ )	$R_{14}$ ( $\Omega$ )	$R_{15}$ ( $\Omega$ )	$R_{16}$ ( $\Omega$ )	$R_{17}$ ( $\Omega$ )	$R_{18}$ ( $\Omega$ )	$R_{19}$ ( $\Omega$ )
10k	10k	10k	10k	10k	10k	10k	10k	10k	10k	10k	10k
$R_{20}$ ( $\Omega$ )	$R_{21}$ ( $\Omega$ )	$R_{22}$ ( $\Omega$ )	$R_{23}$ ( $\Omega$ )	$R_{24}$ ( $\Omega$ )	$R_{25}$ ( $\Omega$ )	$R_{26}$ ( $\Omega$ )	$R_{27}$ ( $\Omega$ )	$R_{28}$ ( $\Omega$ )	$R_{29}$ ( $\Omega$ )	$R_{30}$ ( $\Omega$ )	$R_{31}$ ( $\Omega$ )
67k	100k	10k	10k	9.1k	10k	10k	10k	10k	10k	10k	1k

## 6.7 Concluding Remarks

In this work, a new chaotic system with two exponential non-linearities has been proposed, analysed for various dynamic properties and designed systematically using CFOAs and diodes. The proposed design uses six CFOAs, two diodes, eleven resistors and three capacitors. This circuit is useful for practical chaos-based applications. Besides, the power supply requirement for the proposed design is  $\pm 9V$ , which is considerably less in comparison to the designs incorporating analog multipliers. This will, in turn, result in lesser power consumption. The feasibility of the proposed design is investigated through simulations in LTspice design



environment with CFOA IC AD844 and diode MUR460. The observed behavior of the circuit confirms the aperiodicity in state variables and strangeness in the phase space trajectories. Besides, the adaptive control synchronization scheme has been designed for the synchronization of two identical proposed chaotic systems, which has been verified both numerically and through circuit implementation in LTspice. This research extends our knowledge of the circuit designs of chaotic systems. However, further studies regarding the role of number of parameters in the complexity of the chaotic system is worthwhile.

# **Chapter 7**

## **Novel hyperchaotic system with two quadratic nonlinearities**

---

## 7.1 Introduction

There has been continuous development of chaotic systems due to the ease with which these explain complex nature of dynamical systems. The work presented so far concerns with the three-dimensional chaotic systems. With the need to enhance the complexity of the system for more secure applications, the dimensions may be increased beyond three. Such systems, if having more than one positive Lyapunov exponents, are known as hyperchaotic systems (HCSs). The literature suggests that there are HCSs existing with quadratic non-linearities [62-67]. To add to the pool of existing HCSs, in this work, a four-dimensional HCS with two quadratic nonlinearities, has been proposed. The dynamical behaviour of the proposed system and its dynamic properties such as Lyapunov exponents, Kaplan Yorke dimension and dissipativity have been examined. To explore the proposed systems' applications in communication world, adaptive control synchronization scheme has also been put forward with its complete circuit design using CFOAs, Analog Multipliers (AMs) and passive components.

## 7.2 Proposed hyperchaotic system (HCS)

The mathematical model of the proposed HCS is presented . The properties such as Lyapunov exponents, Kaplan Yorke dimension and dissipativity are studied to confirm hyperchaotic behaviors and nature of the proposed system. Following this, the eigen values are analyzed to examine the stability of fixed points. A quick comparison with the existing HCSs is also included to show the difference.

The proposed system uses four state variables namely  $x$ ,  $y$ ,  $z$  and  $w$ , the time derivatives of which, are represented by the following mathematical model:

$$\dot{x} = y - x \quad (7.1a)$$

$$\dot{y} = ay - xz + w \quad (7.1b)$$

$$\dot{z} = xw - b \quad (7.1c)$$

$$\dot{w} = cx - w \quad (7.1d)$$

where  $a$ ,  $b$  and  $c$  are the parameters whose values determine the nature of the phase space plots generated by running (7.1) in simulated programs. It is to be noted here that (7.1) has quadratic form of nonlinear terms. Choosing  $a = 0.5$ ,  $b = 2$ ,  $c = 0.8$ , the chaos appears in this system.

### 7.3 Properties of the proposed HCS

The Lyapunov exponents, which determine if the given nonlinear dynamic system is periodic, chaotic or hyperchaotic, have been determined through numerical simulations for the proposed system as follows:

$$L_1 = 0.28116; L_2 = 0.00155; L_3 = -0.60507; L_4 = -0.09398$$

The two positive Lyapunov exponents  $L_1$  and  $L_2$  confirm the hyperchaotic nature of the proposed system. Also, the biggest expansion degree is being indicated by  $L_1$  here, while the degree of contraction by  $L_3$ . Clearly, since  $|L_3| > |L_1|$ , so contraction is the dominating nature of the proposed system.

The Kaplan- Yorke dimension,  $D_{KY}$ , is computed as

$$D_{KY} = 3 + \frac{1}{|-0.60507|} (0.28116 + 0.00155 - 0.09398) \quad (7.2)$$

$$D_{KY} = 3.31 \quad (7.3)$$

The Kaplan Yorke dimension, an indicator of the complexity of a system, is 3.31, which is considerably higher than those of the existing systems [53, 58-60, 62, 64,114].

The divergence of the proposed system is computed as  $(-2+a)$  which is a negative value as 'a' < 1. Thus, the proposed system is dissipative in nature, i.e., the hypervolume  $V(t)$  tends to zero as time  $t$  tends to infinity.

### 7.4 Analysis of fixed points

Solving (7.1) gives the following two fixed points  $p_1$  and  $p_2$ , which are given by:

$$p_1 = \left\{ \sqrt{\frac{b}{c}}, \sqrt{\frac{b}{c}}, a + c, \sqrt{bc} \right\};$$

$$p_2 = \left\{ -\sqrt{\frac{b}{c}}, -\sqrt{\frac{b}{c}}, a + c, -\sqrt{bc} \right\} \quad (7.4)$$

To study the nature of these fixed points, local linearization process has been used and the eigenvalues have been determined from the Jacobian matrix in (7.5).

$$J = \begin{bmatrix} -1 & 1 & 0 & 0 \\ -z & a & -x & 1 \\ w & 0 & 0 & x \\ c & 0 & 0 & -1 \end{bmatrix} \quad (7.5)$$

The eigenvalues of proposed HCS are obtained by solving characteristic equation of (7.6) which obtained by equating  $|J - \lambda I|$  to 0. Here  $I$  is  $4 \times 4$  identity matrix and  $\lambda$  represents the eigenvalues.

$$\lambda^4 + (2 - a)\lambda^3 + (1 - a + c)\lambda^2 + b\lambda + 2b = 0 \quad (7.6)$$

Choosing  $a = 0.5$ ,  $b = 2$ ,  $c = 0.8$ , the chaos appears in system and the eigenvalues corresponding to both  $p_1$  and  $p_2$  are given by  $(0.53 \pm 1.2i)$  and  $(-1.2 \pm 0.8i)$ . The eigenvalues corresponding to both fixed points are complex conjugates with positive and negative real parts respectively. Since the eigenvalues have non-zero real parts, the fixed points are hyperbolic in nature. The presence of positive real part is the indication of the instability, thus the dynamics of the proposed system orbits around two unstable fixed points.

## 7.5 Circuit design of the proposed HCS

This section presents the circuit realization of the proposed HCS represented by (7.1). The circuit realization is shown in Fig. 7.1, wherein the capacitor voltages represent the state variables and current through capacitors represent the time differentiation of state variables. Addition and subtraction operations are implemented through CFOAs, whereas quadratic nonlinearities are introduced through AMs. The governing equations obtained through circuit realization are presented in (7.7).

$$\frac{dV_x}{dt} = \frac{1}{R_1 C_x} (V_y - V_x) \quad (7.7a)$$

$$\frac{dV_y}{dt} = \frac{1}{C_y} \left( \frac{V_m + V_w}{R_5} + \frac{V_m - 0.1V_x V_z}{R_4} \right) \quad (7.7b)$$

$$\frac{dV_z}{dt} = \frac{0.1V_x V_w - 0.2}{R_6 C_z} \quad (7.7c)$$

$$\frac{dV_w}{dt} = \frac{V'_m - V_w}{R_7 C_w} \quad (7.7d)$$

where

$$V_m = \frac{R_2}{R_2 + R_3} \cdot V_y, \quad V'_m = \frac{R_9}{R_9 + R_8} \cdot V_x$$

Equating (7.7) with (7.1) and scaling the product of resistance and capacitance (RC) by 1000 gives the desired values of the circuit components, as tabulated in Table 7.1. The feasibility of electronic realization of Fig. 7.1 is examined through LTspice simulations. The macro models of AD844 and AD633 are taken from Analog Devices [107, 108].

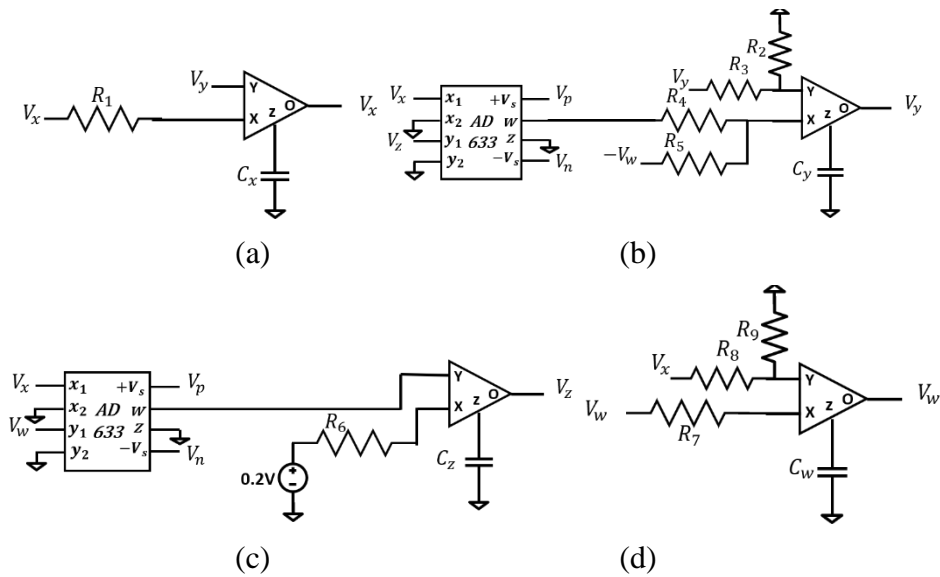
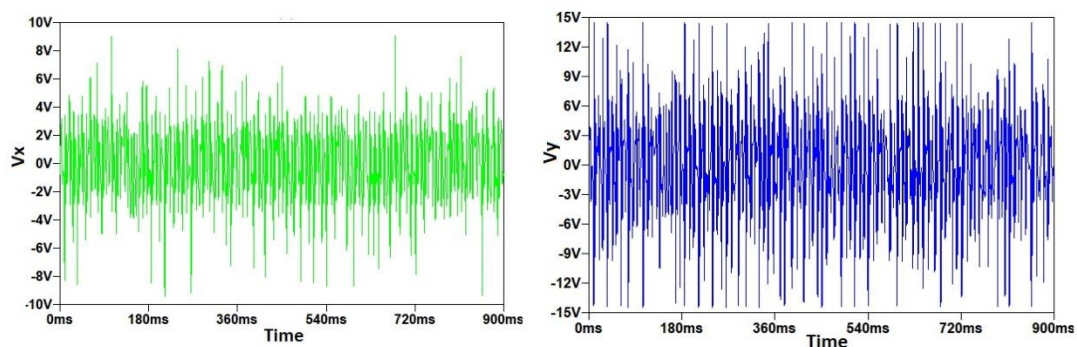


Fig. 7.1 Circuit representation of the proposed HCS

Table 7.1 Component Values of the circuit realization of the proposed systems

Circuit Component	$R_1, R_5, R_7$	$R_2, R_4, R_6, R_8$	$R_3$	$R_9$	$C_x, C_y, C_z, C_w$
Component Value	10k $\Omega$	1k $\Omega$	21k $\Omega$	4k $\Omega$	100nF

Figure 7.2 shows simulated results for state variables  $V_x$ ,  $V_y$ ,  $V_z$  and  $V_w$ . It may be noted that the time series waveforms are aperiodic in nature. The frequency spectrum plots are displayed in Fig. 7.3. The observed spectrums are noise like upto 10kHz for all the four state variables. Figure 7.4 shows simulated results in the form of phase space diagrams which clearly depict existence of two- scroll and four- scroll type hyperchaotic attractors in two dimensions. The attractors in Fig. 7.4, are non-repeating, continuous, confined, regular, abundant and dense in nature, giving an indication of rich chaotic dynamical behavior of the proposed system.



(a)

(b)

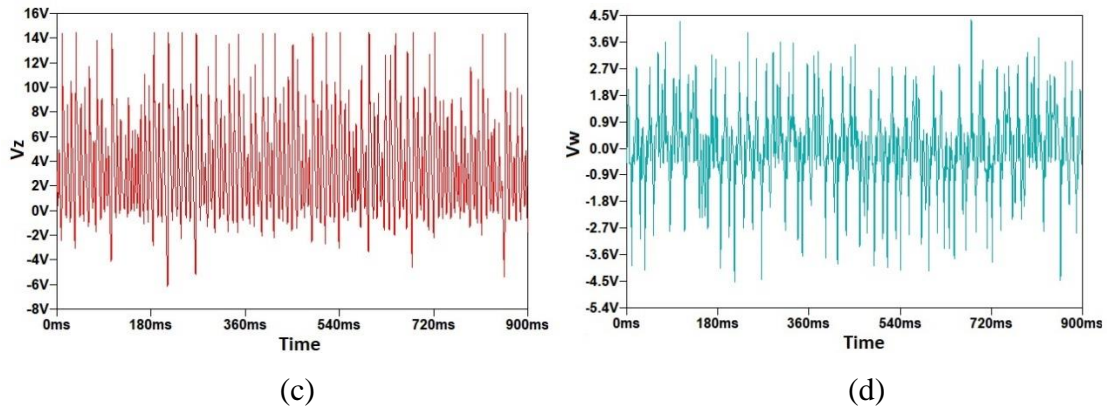


Fig. 7.2 Simulated time series waveforms for (a)  $V_x$ , (b)  $V_y$ , (c)  $V_z$  and (d)  $V_w$

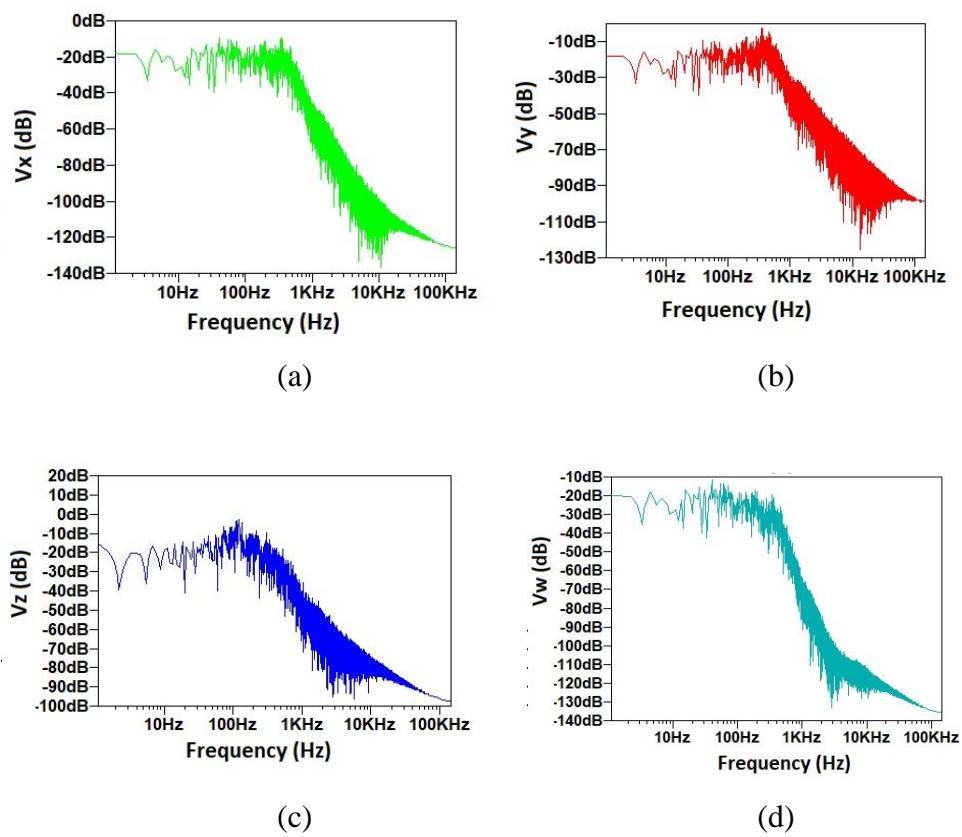
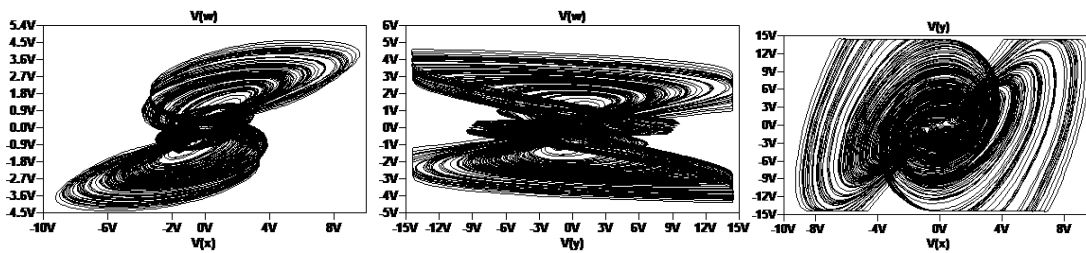


Fig. 7.3 Frequency spectrum plots of state variables (a)  $V_x$ , (b)  $V_y$ , (c)  $V_z$  and (d)  $V_w$



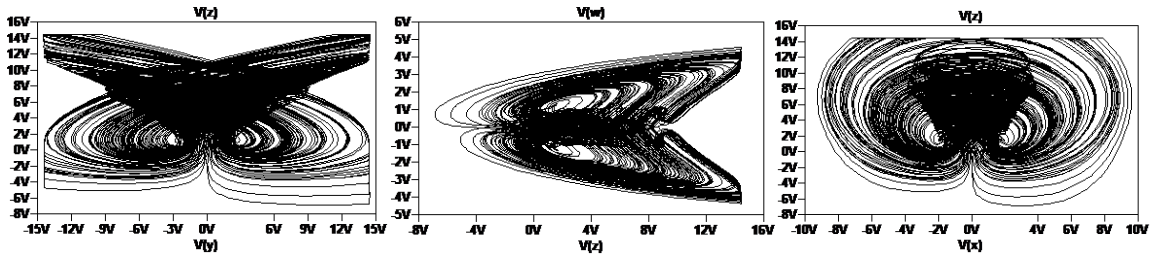


Fig. 7.4 Circuit simulations for the proposed HCS

For the physical realizable systems, the one with lesser hardware requirement for implementation is better. Table 7.2 compares the hardware used for electronic realization of existing and proposed HCS. A close observation of Table 7.2 shows that

- The results have been compared with the existing counterparts in Table 7.2, and the proposed designs clearly outperforms in terms of hardware required from [52, 53, 58-60, 62, 67, 69, 114].
- All HCSs use four energy storing elements. The realizations [68, 115] use inductor, which in turn requires more number of active blocks for implementation, thereby enhancing the active block count.
- OpAmp based realizations [52, 53, 58-60, 62, 67, 114] use extra active blocks in comparison to others.
- Refs. [68, 115] use diodes to provide nonlinear terms whereas others make use of AMs.
- Though the proposed realization makes use of more active blocks than those proposed in [68, 115], it employs all grounded energy storing elements and does not make use of inductor.

Table 7.2 Comparison table of the existing designs with the proposed design

Ref.	Active Blocks used	Number of active blocks	Number of Resistors	Number of Capacitors	Number of Inductors	Number of Diodes
[52]	OpAmp, AM	13	23	4	0	0
[53]	OpAmp, AM	9	15	4	0	0
[58]	OpAmp, AM	9	16	4	0	0



[59]	OpAmp, AM	9	16	4	0	0
[60]	OpAmp, AM	10	18	4	0	0
[62]	OpAmp, AM	10	21	4	0	0
[67]	OpAmp, AM	13	17	4	0	0
[68]	CFOA, inverting buffer	2	1	3	1	2
[69]	CCII+, AM	24	24	4	0	0
[114]	OpAmp, AM	9	13	4	0	0
[115]	OTRA	1	2	3	1	2
Proposed Design	CFOA, AM	6	9	4	0	0

In view of the above, the hardware realization would be compact than available HCSs that employ AMs for nonlinear terms' realization.

## 7.6 Adaptive control synchronization scheme

In this section, the adaptive control laws for synchronizing two identical proposed HCSs are elucidated.

The adaptive control synchronization scheme incorporates a master and a slave system. The governing equations of master and slave systems are given by (7.11) and (7.12) respectively.

### 7.6.1 Master and slave representation

$$\dot{x}_1 = y_1 - x_1 \quad (7.11a)$$

$$\dot{y}_1 = ay_1 - x_1z_1 + w_1 \quad (7.11b)$$

$$\dot{z}_1 = x_1w_1 - b \quad (7.11c)$$

$$\dot{w}_1 = cx_1 - w_1 \quad (7.11d)$$

$$\dot{x}_2 = y_2 - x_2 + u_1 \quad (7.12a)$$

$$\dot{y}_2 = ay_2 - x_2z_2 + w_2 + u_2 \quad (7.12b)$$

$$\dot{z}_2 = x_2w_2 - b + u_3 \quad (7.12c)$$

$$\dot{w}_2 = cx_2 - w_2 + u_4 \quad (7.12d)$$

where  $u_i$  ( $i=1,2,3,4$ ) correspond to adaptive control functions.

### 7.6.2 Error dynamics

The errors  $e_x, e_y, e_z$  and  $e_w$  between the state variables  $x, y, z$  and  $w$  of master and slave are given by (7.13).

$$e_x = x_2 - x_1 \quad (7.13a)$$

$$e_y = y_2 - y_1 \quad (7.13b)$$

$$e_z = z_2 - z_1 \quad (7.13c)$$

$$e_w = w_2 - w_1 \quad (7.13d)$$

The error dynamics is obtained by time differentiation of (7.13). Putting the values of time differentiation of state variables of master and slave systems, the following set of equations for error dynamics are obtained:

$$\dot{e}_x = e_y - e_x + u_1 \quad (7.14a)$$

$$\dot{e}_y = ae_y + x_1z_1 - x_2z_2 + e_w + u_2 \quad (7.14b)$$

$$\dot{e}_z = x_2w_2 - x_1w_1 + u_3 \quad (7.14c)$$

$$\dot{e}_w = ce_x - e_w + u_4 \quad (7.14d)$$

### 7.6.3 Adaptive controller

From (7.14), the adaptive control functions  $u_i$ 's ( $i=1,2,3,4$ ) can be defined as:

$$u_1 = -k_1e_x - e_y + e_x \quad (7.15a)$$

$$u_2 = -k_2e_y - \hat{a}e_y + x_2z_2 - x_1z_1 - e_w \quad (7.15b)$$

$$u_3 = -k_3e_z + x_1w_1 - x_2w_2 \quad (7.15c)$$

$$u_4 = -k_4e_w - \hat{c}e_x + e_w \quad (7.15d)$$

where  $k_1, k_2, k_3$  and  $k_4$  are positive constants.

### 7.6.4 Error in parameters' estimation

The parameter estimation error terms  $e_a, e_b$  and  $e_c$  are defined by

$$e_a = a - \hat{a} \quad (7.16a)$$

$$e_b = b - \hat{b} \quad (7.16b)$$

$$e_c = c - \hat{c} \quad (7.16c)$$

and their dynamics are described by

$$\dot{e}_a = -\hat{a} \quad (7.17a)$$

$$\dot{e}_b = -\hat{b} \quad (7.17b)$$

$$\dot{e}_c = -\hat{c} \quad (7.17c)$$

Using (7.15), the governing equations of slave system and the error dynamics equations may be rewritten as:

$$\dot{x}_2 = y_2 - x_2 - k_1 e_x - e_y + e_x \quad (7.18a)$$

$$\dot{y}_2 = ay_2 + w_2 - k_2 e_y - \hat{a}e_y - x_1 z_1 - e_w \quad (7.18b)$$

$$\dot{z}_2 = x_1 w_1 - b - k_3 e_z \quad (7.18c)$$

$$\dot{w}_2 = cx_2 - w_2 - k_4 e_w - \hat{c}e_x + e_w \quad (7.18d)$$

and

$$\dot{e}_x = -k_1 e_x \quad (7.19a)$$

$$\dot{e}_y = e_a e_y - k_2 e_y \quad (7.19b)$$

$$\dot{e}_z = -k_3 e_z \quad (7.19c)$$

$$\dot{e}_w = e_c e_x - k_4 e_w \quad (7.19d)$$

respectively. Here  $\hat{a}$  and  $\hat{c}$  are the estimated system parameters of slave.

### 7.6.5 Lyapunov stability

Using Lyapunov stability theory, let the Lyapunov function (V) be given by (7.20). If the time differentiation of V is negative, value of V is decreasing along the solutions and the whole system is globally stable.

$$V = \frac{1}{2}(e_x^2 + e_y^2 + e_z^2 + e_w^2 + e_a^2 + e_b^2 + e_c^2) \quad (7.20)$$

Differentiation of (7.20) gives

$$\dot{V} = e_x \dot{e}_x + e_y \dot{e}_y + e_z \dot{e}_z + e_w \dot{e}_w + e_a \dot{e}_a + e_b \dot{e}_b + e_c \dot{e}_c \quad (7.21)$$

Equation (7.21) can be simplified as

$$\dot{V} = -(k_1 e_x^2 + k_2 e_y^2 + k_3 e_z^2 + k_4 e_w^2) + e_a(e_y^2 - \hat{a}) - e_b \hat{b} + e_c(-\hat{c} + e_x e_w) \quad (7.22)$$

### 7.6.6 Adaptive Laws

For the unified system comprising master and slave to be stable,  $\dot{V}$  should be less than zero. This implies:

$$\hat{a} = e_y^2, \hat{b} = 0, \hat{c} = e_x e_w \quad (7.23)$$

The adaptively controlled system has been simulated for different initial conditions:  $(x_0, y_0, z_0, w_0) = (1, 1, 1, 1)$  for master and  $(50, 25, 15, 15)$  for slave respectively and the simulation results have been shown in Fig. 7.5. It may be noted that slave system synchronizes well with master.

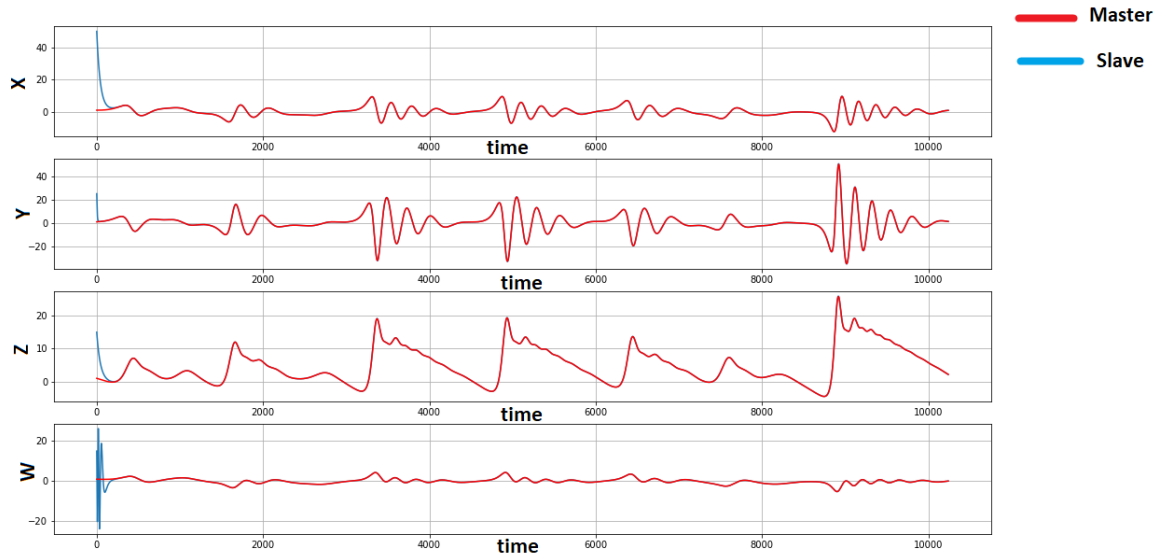


Fig. 7.5 Adaptively synchronized state variables  $x$ ,  $y$ ,  $z$  and  $w$  with different initial conditions for the proposed system

Also, the variation in parameters have been simulated and Fig. 7.6 shows the convergence of the slave parameters  $(a, b, c) = (0.75, 2.1, 0.25)$  towards the original parameters of the system, i.e.  $(0.5, 2, 0.8)$ . The error analysis between the respective state variables of master and slave is depicted in Fig. 7.7 which shows that the proposed HCS gets stabilized eventually. However, the time of stabilization is not same for all state variables. Though  $x$ ,  $z$  and  $w$  get stabilized before 500 time units,  $y$  takes significantly longer time (more than 2000 time units) to get stabilized. This is because of the dependence of  $y$  on more number of variables ( $x$ ,  $y$ ,  $z$  and  $w$ ) as evident from (7.1).

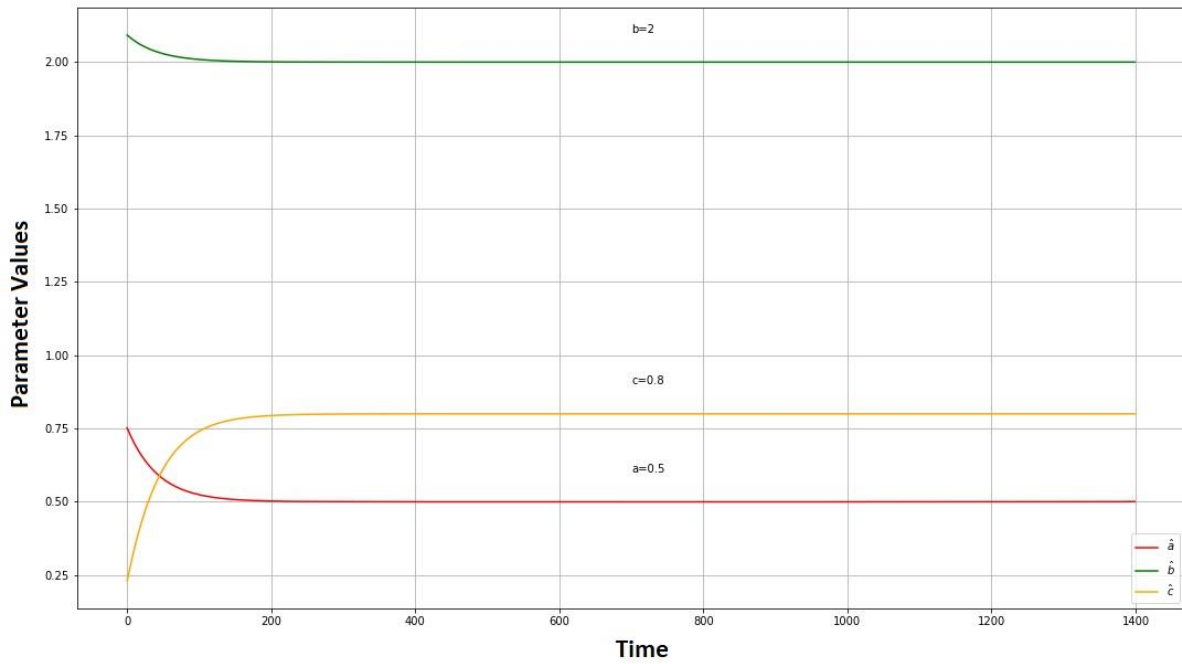
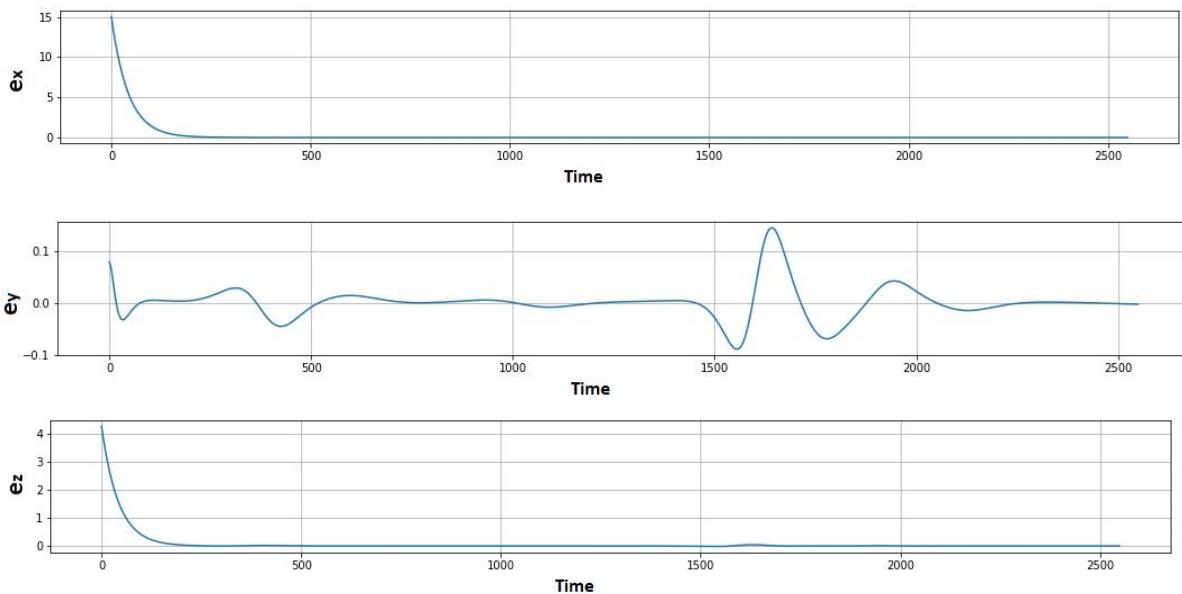


Fig. 7.6 Study of parameter variation in adaptively controlled master-slave system for the proposed system

Circuit implementation of the whole scheme of adaptive control synchronization has also been presented in this work as shown in Fig. 7.8. The component values are calculated to satisfy the respective governing equations.



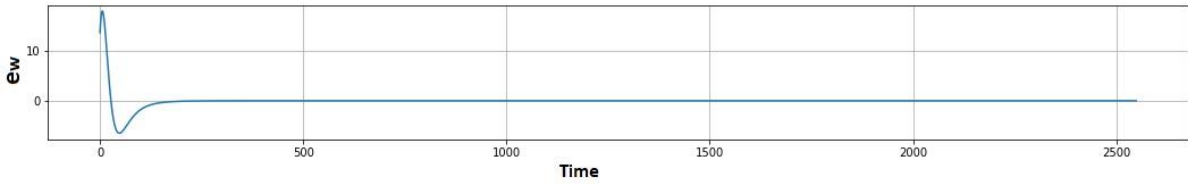
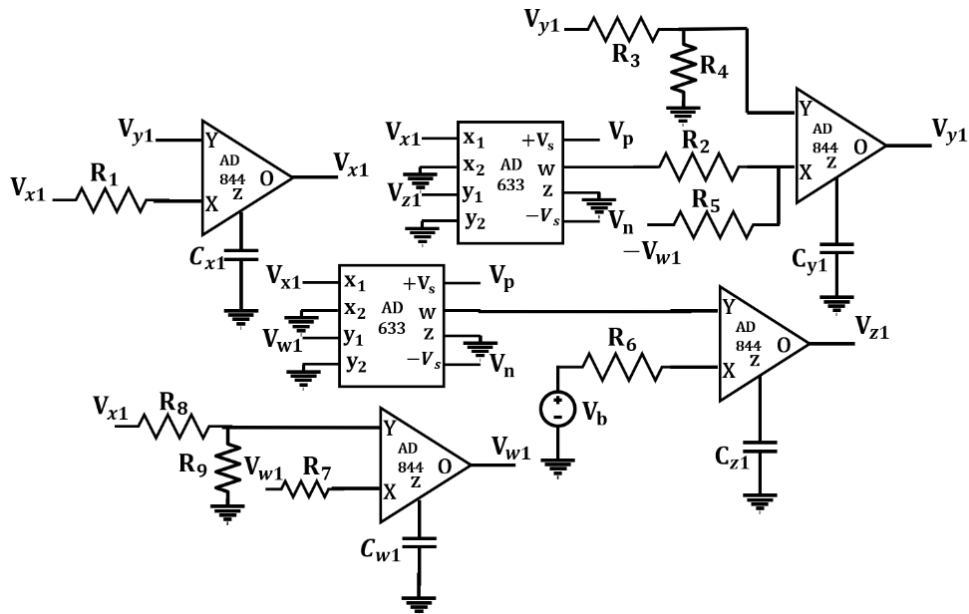
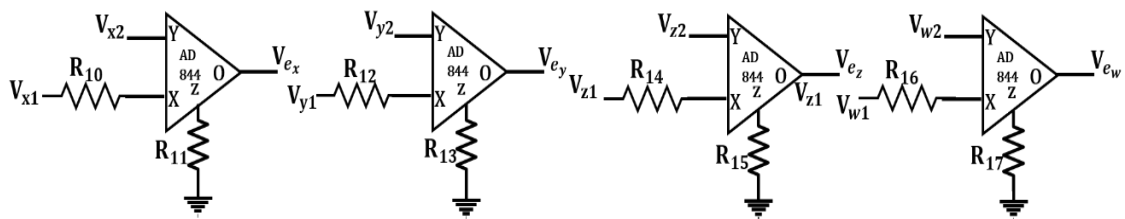


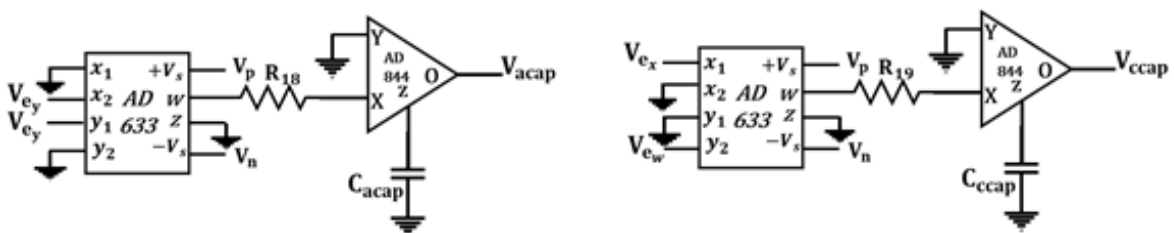
Fig. 7.7 Error analysis of the adaptively controlled master-slave for the proposed system



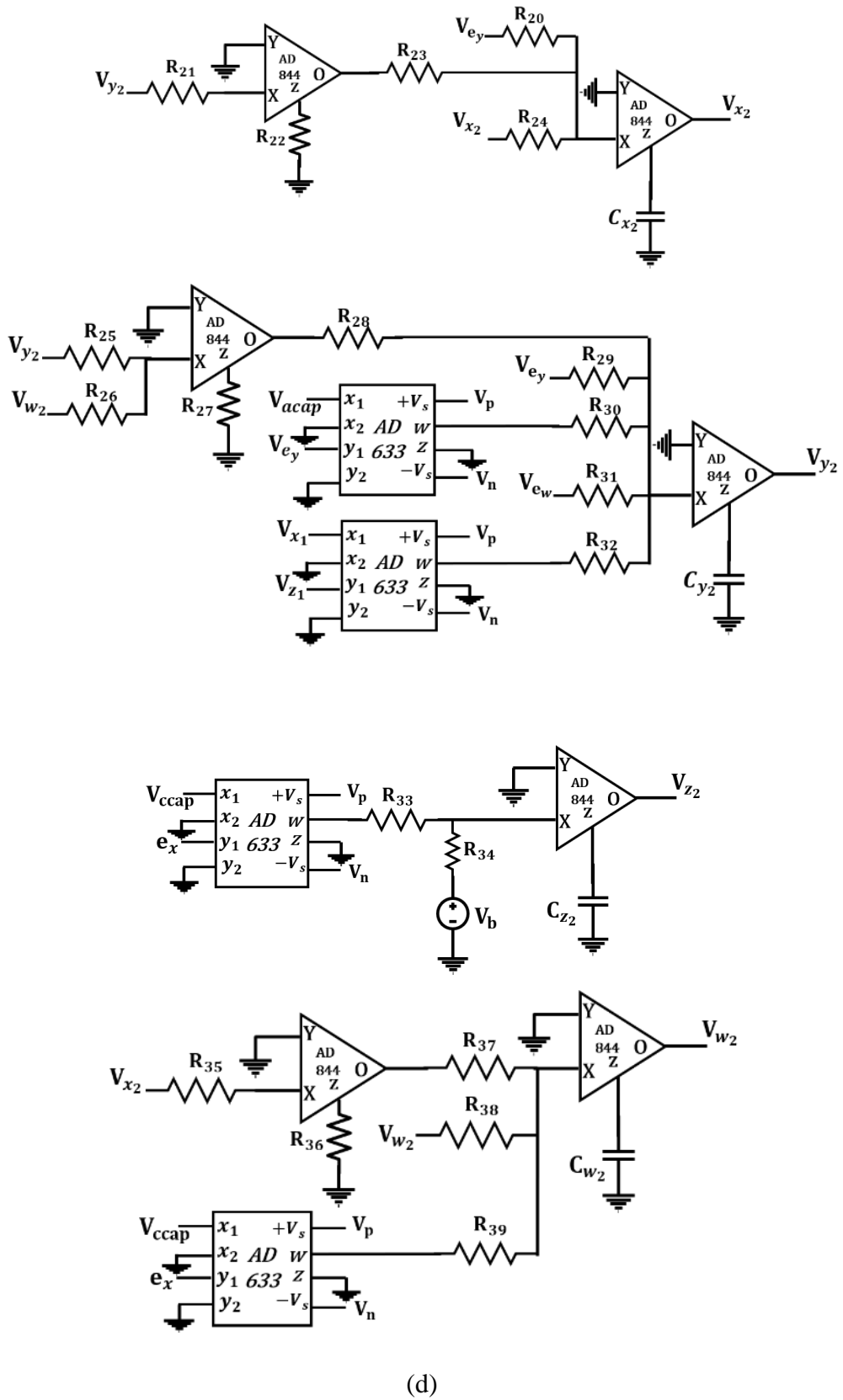
(a)



(b)



(c)



(d)

Fig. 7.8 Circuit design of adaptive control synchronization of the proposed hyperchaotic system: (a) Master circuit, (b) Error functions, (c) Updation law of slave's parameter, (d) Complete slave circuit

The values for components in Fig. 7.8 (a) are imported from Table 7.1. The component values for circuits in Fig. 7.8 (b-d) are computed so that the governing equations are satisfied. A scale of 1000 provides the following values of components  $R_{10} - R_{27} = R_{20} - R_{24} = R_{26} - R_{29} = R_{31} = R_{34} = R_{36} - R_{38} = 10 \text{ k}\Omega$ ;  $R_{18} = R_{19} = R_{30} = R_{32} = R_{33} = R_{39} = 1 \text{ k}\Omega$ ,  $R_{25} = 20 \text{ k}\Omega$ ,  $R_{35} = 8 \text{ k}\Omega$ , and  $C_i$  ( $i=x2, y2, z2, w2, \text{acap}, \text{ccap}$ ) =  $100 \text{ nF}$ . The simulation results have been put forward in the form of graphs between the corresponding state variables of master and slave, as shown in Fig. 7.9.

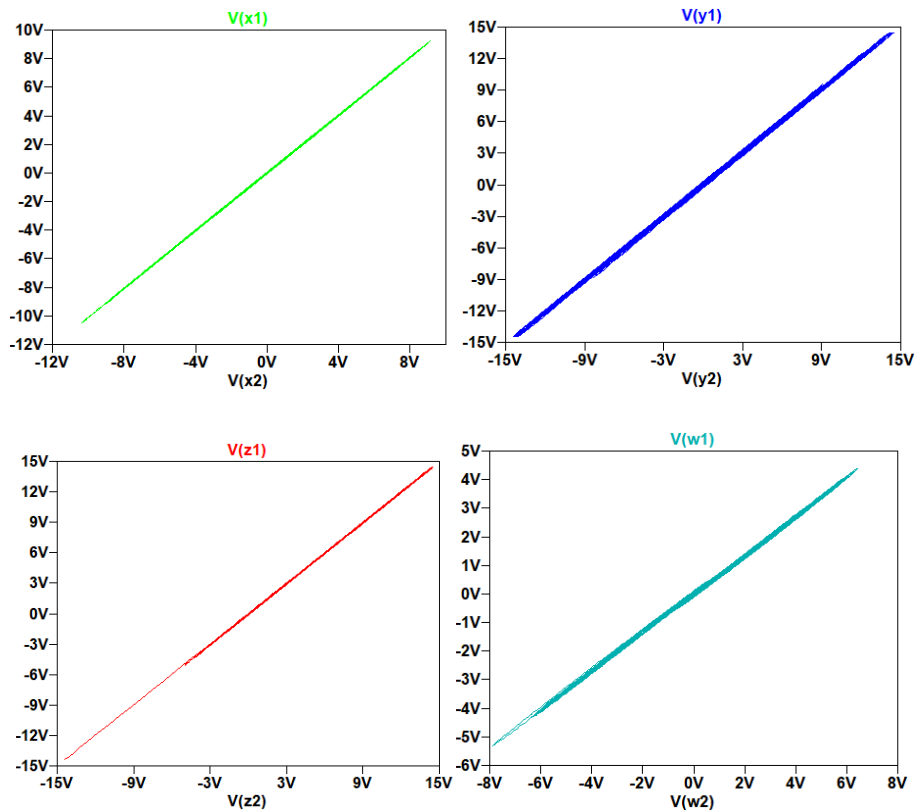


Fig. 7.9 Simulated plots between hyperchaotic signals of master and slave in adaptive control synchronization

The synchronization of the master and slave circuit is evident from Fig. 7.9, thus proving the reliability and feasibility of the design.

## 7.7 Concluding Remarks

A new four-dimensional HCS with quadratic non linearity has been presented, which can generate two and four scroll chaotic attractors with two fixed points. Numerical validation of the dynamical properties of the proposed HCS are presented by means of Lyapunov exponents, Kaplan- Yorke dimension, and dissipativity. The functionality of the proposed HCS is verified through LTspice simulations for which the electronic circuit is designed using CFOAs, Analog



Multipliers (AMs) and passive elements like capacitors and resistors. Also, the effectiveness of the proposed design in terms of hardware requirements has been highlighted based on comparison with the existing ones. Then, adaptive control synchronization scheme is applied to achieve chaos synchronization using master- slave configuration for the proposed system. The results have been presented for different initial conditions, different values of system parameters and the errors between the respective state variables. The circuit design has been simulated, and the simulation results are in good agreement with computer simulations.

# Chapter 8

## Digital design of chaotic systems

---

The content and results of the following paper have been reported in this chapter.

K. Suneja, N. Pandey and R. Pandey, “**FPGA based design of chaotic systems with quadratic non-linearities**,” 4<sup>th</sup> International conference on Data Analytics and Management (ICDAM-2023), London, 2023.

## 8.1 Introduction

In the fast-growing world, digital domain plays an important role besides analog domain. The availability of easily configurable digital resources makes them a favourite choice of circuit designers in the initial phases of design. The work presented so far in this thesis is concerned with analog circuit design of chaotic systems.

In this chapter, a systematic approach to implement chaotic systems with quadratic nonlinearities on digital platform using Runge Kutta 4 (RK4) numerical method has been presented. Owing to their flexibility, reconfigurability and parallelism, the Field Programmable Gate Arrays (FPGAs) have been used for the implementation using Verilog Hardware Description Language (HDL) and the state machine control. The implemented chaotic systems have been evaluated based on hardware utilization and time delay using synthesis results on Xilinx Artix device 7a200tffv1156-1. The simulation results using inbuilt simulator of Vivado design suite have been presented. The simulations results have been validated by python based numerical simulations as well.

## 8.2 Design Methodology

The governing equations of chaotic system are discretized for FPGA implementation. The numerical methods such as Euler method, improved Euler method, fourth order Runge Kutta (RK4) method, etc. [103, 116] may be used for discretization. Here, RK4 method has been chosen because of its higher degree of accuracy in providing solutions [117]. It uses four intermediate points  $K_1$ ,  $K_2$ ,  $K_3$  and  $K_4$  to determine the solution using previous sample. The  $K_1$  corresponds to the beginning,  $K_2$  and  $K_3$  are near middle and  $K_4$  corresponds to the end of the interval. The three chaotic differential equations, corresponding to the state variables  $x$ ,  $y$  and  $z$  are thus discretized using RK4 method and are as represented by (8.1) to (8.6).

$$x(n + 1) = x(n) + \frac{h}{6} [K_{x1} + 2K_{x2} + 2K_{x3} + K_{x4}] \quad (8.1)$$

$$y(n + 1) = y(n) + \frac{h}{6} [K_{y1} + 2K_{y2} + 2K_{y3} + K_{y4}] \quad (8.2)$$

$$z(n + 1) = z(n) + \frac{h}{6} [K_{z1} + 2K_{z2} + 2K_{z3} + K_{z4}] \quad (8.3)$$

Where

$$K_{x1} = f_x[x(n), y(n), z(n)] \quad (8.4a)$$

$$K_{x2} = f_x[x(n) + h \frac{K_{x1}}{2}, y(n) + h \frac{K_{y1}}{2}, z(n) + h \frac{K_{z1}}{2}] \quad (8.4b)$$

$$K_{x3} = f_x[x(n) + h \frac{K_{x2}}{2}, y(n) + h \frac{K_{y2}}{2}, z(n) + h \frac{K_{z2}}{2}] \quad (8.4c)$$

$$K_{x4} = f_x[x(n) + hK_{x3}, y(n) + K_{y3}, z(n) + K_{z3}] \quad (8.4d)$$

$$K_{y1} = f_y[x(n), y(n), z(n)] \quad (8.5a)$$

$$K_{y2} = f_y[x(n) + h \frac{K_{x1}}{2}, y(n) + h \frac{K_{y1}}{2}, z(n) + h \frac{K_{z1}}{2}] \quad (8.5b)$$

$$K_{y3} = f_y[x(n) + h \frac{K_{x2}}{2}, y(n) + h \frac{K_{y2}}{2}, z(n) + h \frac{K_{z2}}{2}] \quad (8.5c)$$

$$K_{y4} = f_y[x(n) + hK_{x3}, y(n) + hK_{y3}, z(n) + hK_{z3}] \quad (8.5d)$$

$$K_{z1} = f_z[x(n), y(n), z(n)] \quad (8.6a)$$

$$K_{z2} = f_z[x(n) + h \frac{K_{x1}}{2}, y(n) + h \frac{K_{y1}}{2}, z(n) + h \frac{K_{z1}}{2}] \quad (8.6b)$$

$$K_{z3} = f_z[x(n) + h \frac{K_{x2}}{2}, y(n) + h \frac{K_{y2}}{2}, z(n) + h \frac{K_{z2}}{2}] \quad (8.6c)$$

$$K_{z4} = f_z[x(n) + hK_{x3}, y(n) + hK_{y3}, z(n) + hK_{z3}] \quad (8.6d)$$

Where  $K_{xi}$ ,  $K_{yi}$  and  $K_{zi}$ ,  $i=1to4$  represent the intermediate slopes of state variables  $x$ ,  $y$  and  $z$  respectively,  $f_x$ ,  $f_y$  and  $f_z$  represent the differential equations corresponding to a given chaotic system and  $h$  is the step size or the interval between consecutive samples.

The set of equations represented by (8.1) to (8.6) are implemented as follows:

The digital design of the chaotic system here has been divided into two parts: the control path to control the flow of the operations and data path implementing all the algebraic operations. The control path consists of one initial state, also known as default state to initialize the state variables and one final state or idle state which waits for the next set of instructions. These two states are represented by  $S_0$  and  $S_6$  respectively. Besides, implementation requires five more states to evaluate (8.1)-(8.6). Thus, the control path requires seven states  $S_0$  to  $S_6$  and the Algorithmic State Machine (ASM) chart of the same is depicted in Fig. 8.1.  $F\_val$  stands for function to evaluate the functions in (8.1) to (8.6). Three state variables are required to represent these states:  $S_0$  (000),  $S_1$  (001),  $S_2$  (010),  $S_3$  (011),  $S_4$  (100),  $S_5$  (101) and  $S_6$  (110).

The function of the seven states in control path  $S_0$  to  $S_6$  [118] are:

S<sub>0</sub>: It is the initial and default state in which the state variables are initialized with the initial conditions' values. The process then passes to the next state S<sub>1</sub> unconditionally.

S<sub>1</sub>: In this state, the  $K_{x1}$ ,  $K_{y1}$  and  $K_{z1}$  increments based on the slopes at the beginning of the interval are calculated using (8.4a), (8.5a) and (8.6a). The process then passes to the next state S<sub>2</sub> unconditionally.

S<sub>2</sub>: The increments based on the slopes near midpoint of the interval,  $K_{x2}$ ,  $K_{y2}$  and  $K_{z2}$  using  $K_{x1}$ ,  $K_{y1}$  and  $K_{z1}$  are calculated in this state using (8.4b), (8.5b) and (8.6b), followed by unconditional transition to the next state S<sub>3</sub>.

S<sub>3</sub>: The increments based on the slopes again near midpoint, but different than that of previous point,  $K_{x3}$ ,  $K_{y3}$  and  $K_{z3}$  using  $K_{x2}$ ,  $K_{y2}$  and  $K_{z2}$  are calculated in this state from (8.4c), (8.5c) and (8.6c), followed by an unconditional transition to next state S<sub>4</sub>.

S<sub>4</sub>: The increments based on the slopes at the end of the interval,  $K_{x4}$ ,  $K_{y4}$  and  $K_{z4}$  using  $K_{x3}$ ,  $K_{y3}$  and  $K_{z3}$  are calculated in this state from (8.4d), (8.5d) and (8.6d), followed by an unconditional transition to next state S<sub>5</sub>.

S<sub>5</sub>: In this state, the next chaotic samples  $x$ ,  $y$  and  $z$  are generated using (8.1) to (8.3). At the next clock cycle, if the counter value  $C_p$  is less than the user defined integer  $N$ , which represents the number of required samples, the process jumps to S<sub>1</sub> for calculating the next solution, else it jumps to S<sub>6</sub> where it stays waiting.

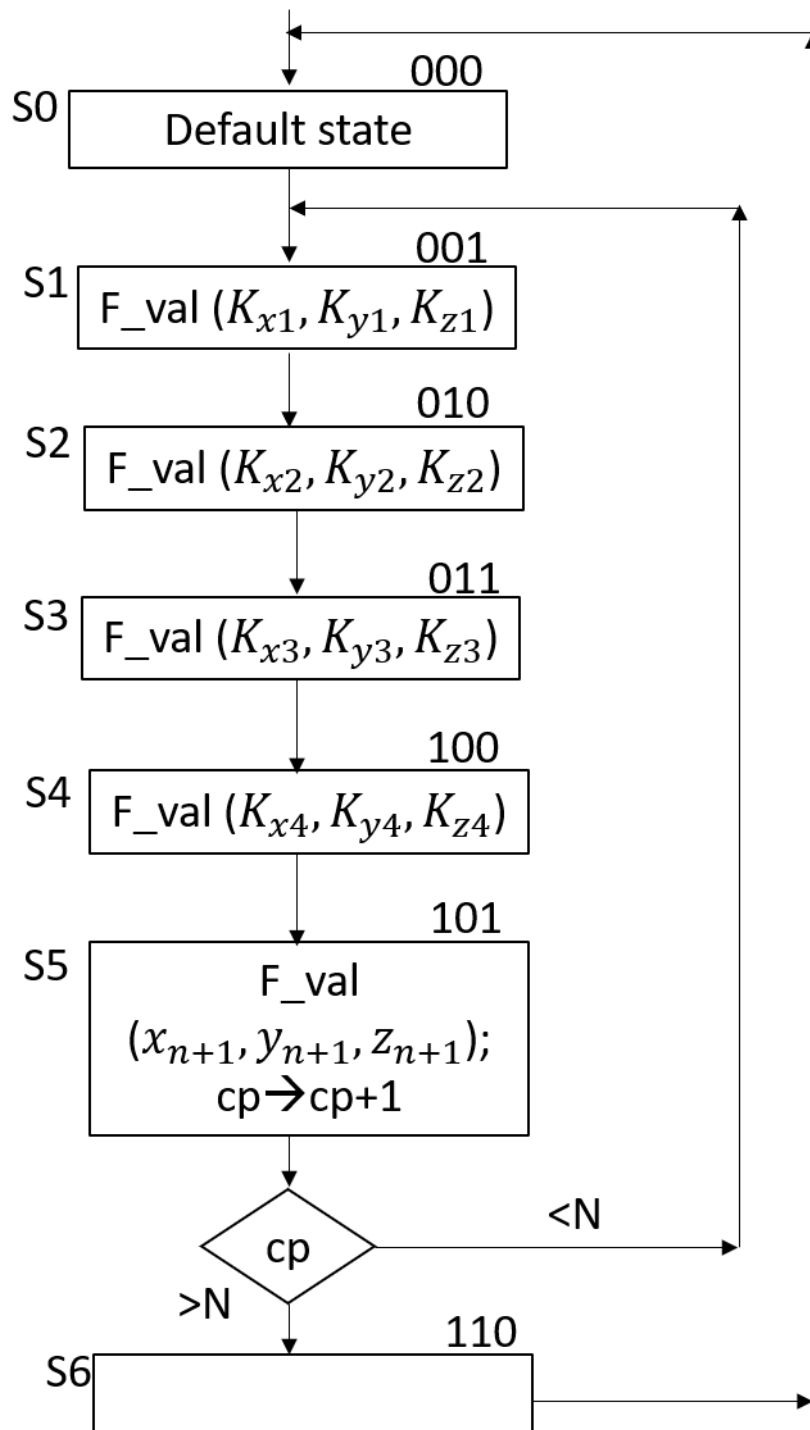


Fig. 8.1 ASM chart of the control path of chaotic system

The data path includes the calculation of algebraic operations in (8.1) to (8.6) within the respective states.

### 8.3 Results

Ten chaotic systems [1,2,15,27,29,32-34,36-38,113], including some popularly known chaotic systems, such as Rössler [2] and Lorenz [1] have been designed using the methodology

described in Section 8.2 on a common FPGA platform for fair comparison and choose the best fit for digital applications. To synthesize these systems, both control and data path codes have been inserted in Xilinx tool using Verilog HDL, the top module for which is shown in Fig. 8.2. It consists of three output signals  $x_n$ ,  $y_n$  and  $z_n$  for chaotic system, each of 32 bits. Clock signal 'clk' and the step size 'h' have been taken as input signals. The value of h has been chosen as '2<sup>-7</sup>'. It is to be noted that it has been taken as a power of two because division and multiplication processes using power of two in binary logic can simply be implemented using right and left shift operations respectively. A counter parameter 'C<sub>p</sub>' has been defined which will increment by '1' every time the samples' values are calculated till it reaches the parameter N = 50,000. The 'N' is variable depending upon the number of samples required in an application. Two tasks were declared: product for multiplication operation in datapath and F\_det to find the values of time derivatives of state variables for certain inputs. All intermediate slopes K<sub>i</sub>s will be evaluated using case statement and product and F\_det tasks will be used in datapath. It is pertinent to mention that the user has to just modify the part of the code defining F\_det task to evaluate time derivatives of state variables in accordance with the governing equations of the different chaotic systems. Rest of the code remains same. Thus, prototyping of a chaotic system on FPGA will be very fast.

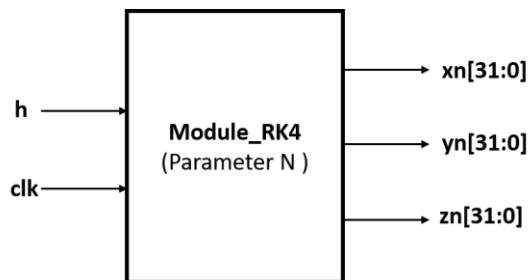


Fig. 8.2 Top module of RK4 method in Verilog

### 8.3.1 Synthesis Results

The methodology suggested above is used to implement ten chaotic systems having quadratic non-linearity(ies). All chaotic systems are implemented on Xilinx's Artix 7 FPGA family's 7a200tffv1156-1, on which 134600 slice LUTs and 740 DSP blocks are available. Table 8.1 enlists the governing equations of the chaotic systems, parameter values, total number of arithmetic operations, percentage utilization of hardware resources and delay. A close

observation of Table 8.1 reveals that hardware requirements increase with the number of operations in governing equations of a chaotic system. Further, it may be noted that number of product terms are minimum in Rössler chaotic system [2], which explains the minimum delay and least use of DSP blocks. Moreover, Pehlivan chaotic system has least number of terms, resulting in lesser requirement of slice LUTs. Overall delay varies from system to system depending upon logical operations and net delay. It may also be observed that all chaotic systems use limited resources from the available ones, therefore hyperchaotic systems may also be implemented as per the user requirements.

Table 8.1 Summary of the hardware and delay requirements for FPGA based implementation of chaotic systems

S. No	Chaotic System [Reference]	Characteristic equations	No. of operations (No. of product terms)	% utilization of resources		Total Delay (nSec)
				Slice LUTs	DSP blocks	
1	Rössler [2]	$\dot{x} = -y - z$ $\dot{y} = x + ay$ $\dot{z} = b + z(x - c)$ a=0.2, b=0.2, c=5.7	7(2)	4.08	8.65	30.745
2	Lorenz [1]	$\dot{x} = a(y - x)$ $\dot{y} = cx - xz - y$ $\dot{z} = xy - bz$ a=10, b=8/3, c=28	9(5)	4.33	12.97	40.117
3	Pehlivan[15]	$\dot{x} = y - x$ $\dot{y} = ay - xz$ $\dot{z} = xy - b$ a=b=0.5	6(3)	3.63	10.81	40.310
4	Li [32]	$\dot{x} = a(y - x)$ $\dot{y} = xz - y$ $\dot{z} = b - xy - cz$ a=5, b=16, c=1	8(4)	4.10	11.89	41.637
5	[27]	$\dot{x} = a(y - x) + yz$	11(6)	4.81	16.22	41.391



		$\dot{y} = cx - y - xz$ $\dot{z} = xy - bz$ $a=35, b=8/3, c=25$				
6	MACM[36]	$\dot{x} = -ax - byz$ $\dot{y} = -x + cy$ $\dot{z} = d - y^2 - z$ $a=2, b=2, c=0.5, d=4$	11(5)	3.78	10.81	47.978
7	[29, 113]	$\dot{x} = a(y - x)$ $\dot{y} = cx - xz$ $\dot{z} = xy - bz$ $a=35, b=3, c=35$	9(5)	4.29	14.05	42.242
8	Rabino- vich[37, 38]	$\dot{x} = hy - ax + yz$ $\dot{y} = hx - by - xz$ $\dot{z} = xy - dz$ $a=4, b=1, d=1, h=6.75$	14(8)	4.61	12.97	45.204
9	Chen[34]	$\dot{x} = a(y - x)$ $\dot{y} = (c - a)x + cy - xz$ $\dot{z} = xy - bz$ $a= 35, b=3, c=28$	11(6)	4.50	15.14	39.717
10	Lü [33]	$\dot{x} = a(y - x)$ $\dot{y} = cy - xz$ $\dot{z} = xy - bz$ $a=36, b=3, c=20$	9(5)	4.29	14.05	40.431

### 8.3.2 Simulation Results

In the flow of FPGA based system design of a chaotic system, the functional verification of the implemented system done using simulation results is a necessary step to validate the design. In order to validate the FPGA based results of the design, all the ten chaotic systems have also been implemented in python using RK4 numerical method, and the simulation results of these

systems have been put with the Xilinx simulation results in Figs. 8.3 to 8.12 for observational confirmation of the correctness of FPGA based results. The simulation results from Xilinx Vivado are in line with the simulation results from python, thus promising the feasibility of implementation of these chaotic systems on FPGA.

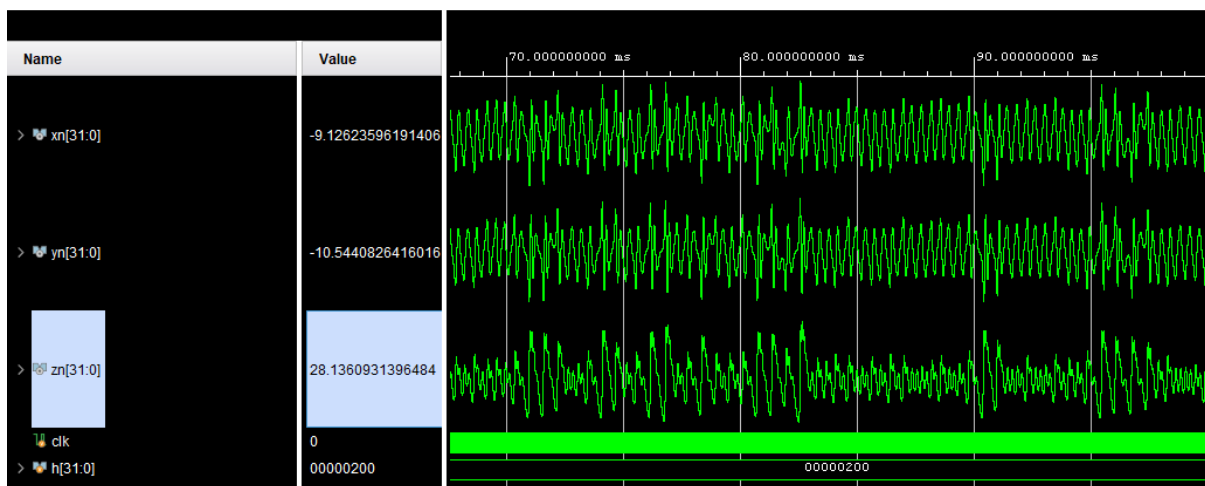
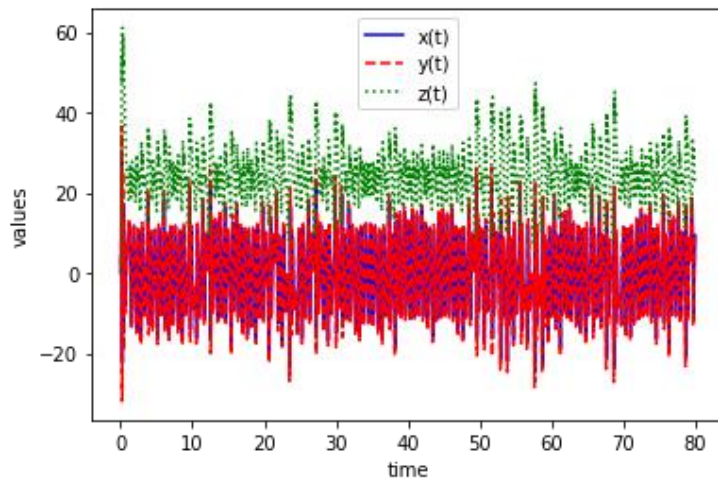


Fig. 8.3 Numerical simulation and Xilinx Vivado simulation results of Chen chaotic system

[34]

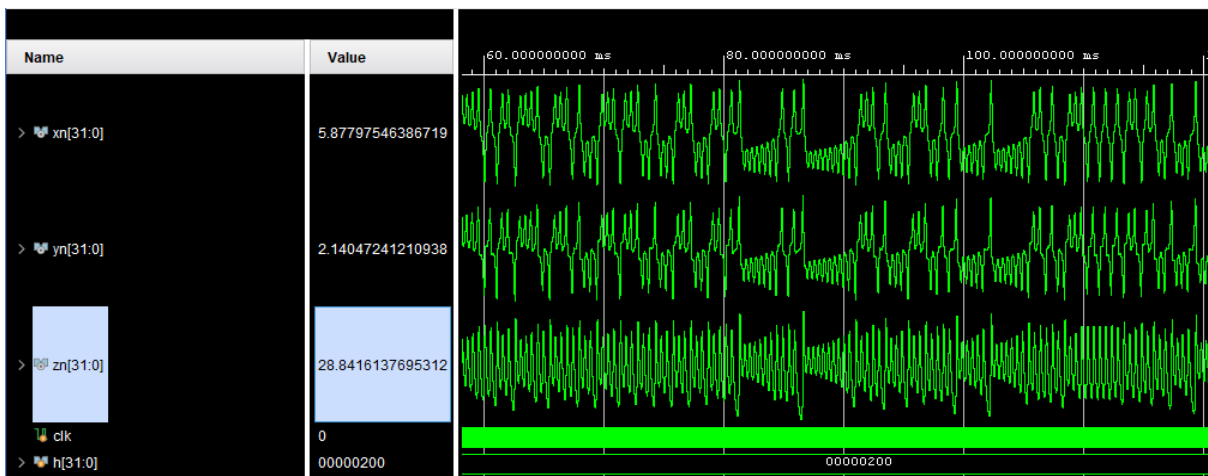
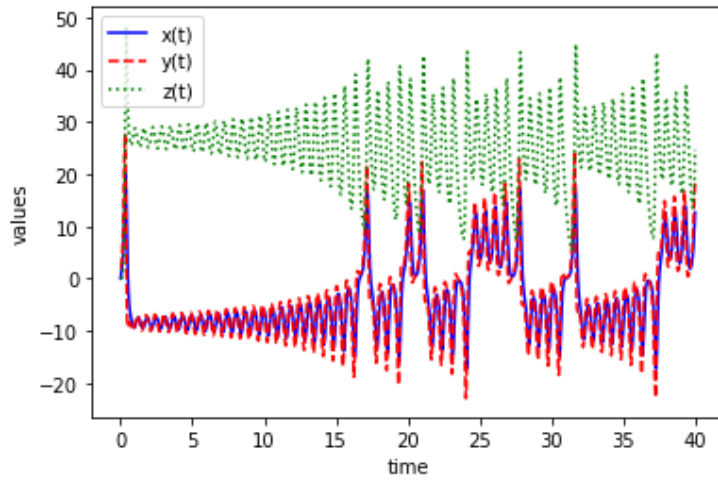
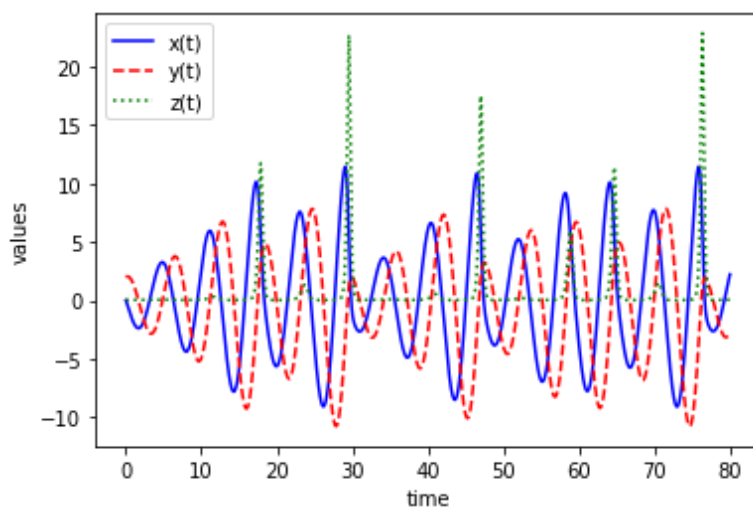


Fig. 8.4 Numerical simulation and Xilinx Vivado simulation results of Lorenz chaotic system [1]



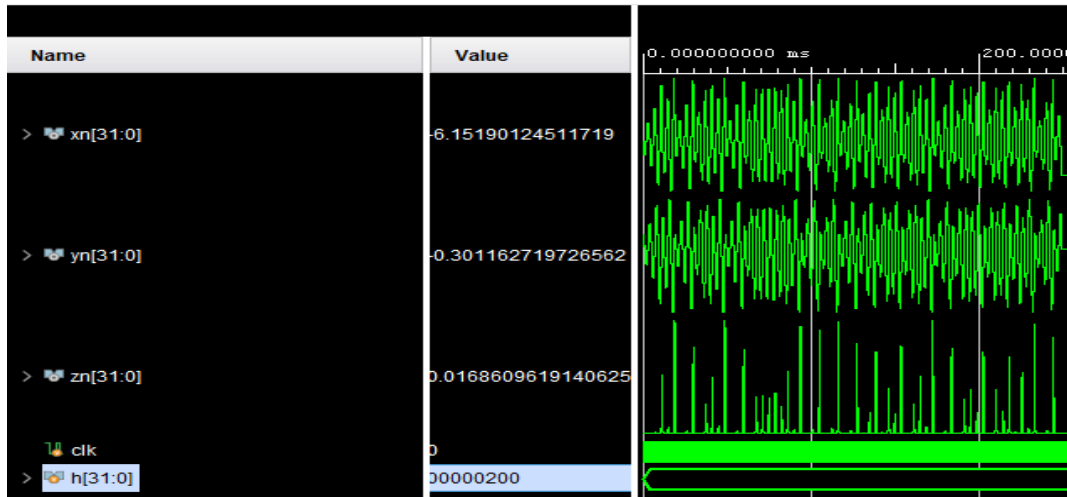
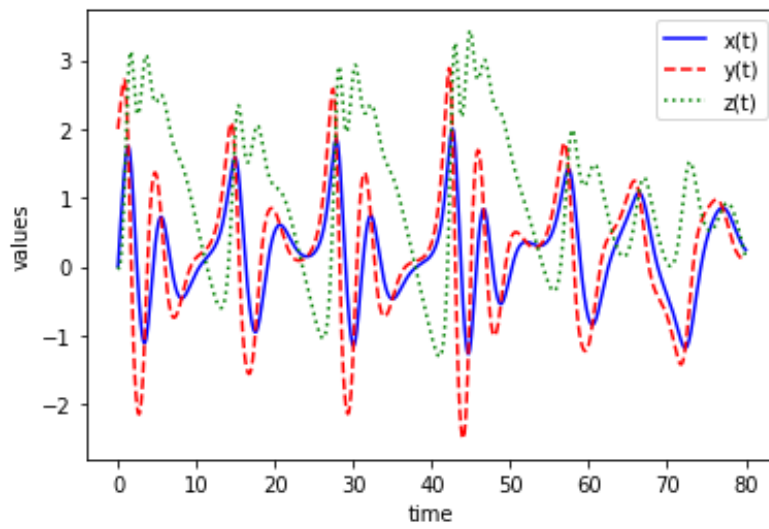


Fig. 8.5 Numerical simulation and Xilinx Vivado simulation results of Rössler chaotic system [2]



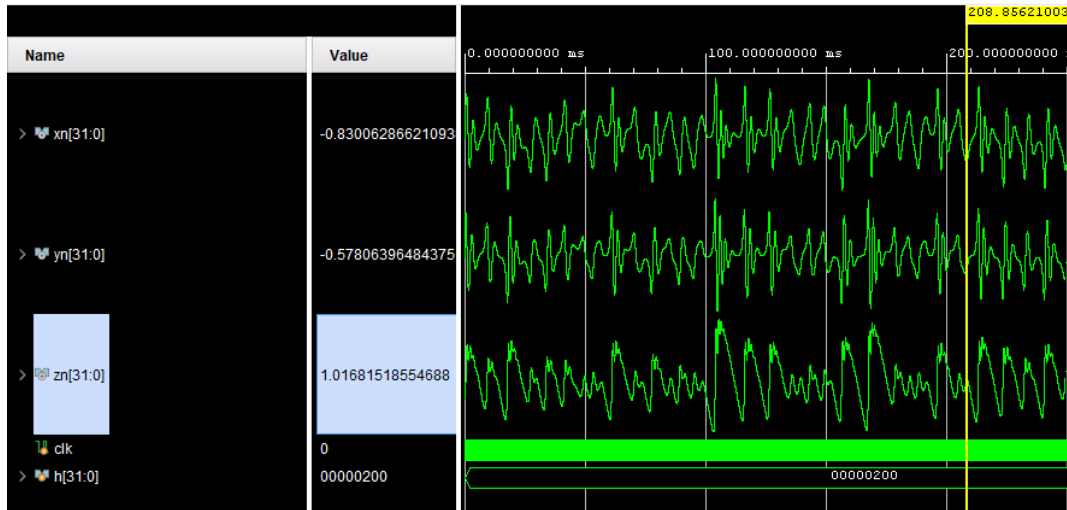


Fig. 8.6 Numerical simulation and Xilinx Vivado simulation results of Pehlivan chaotic system [15]

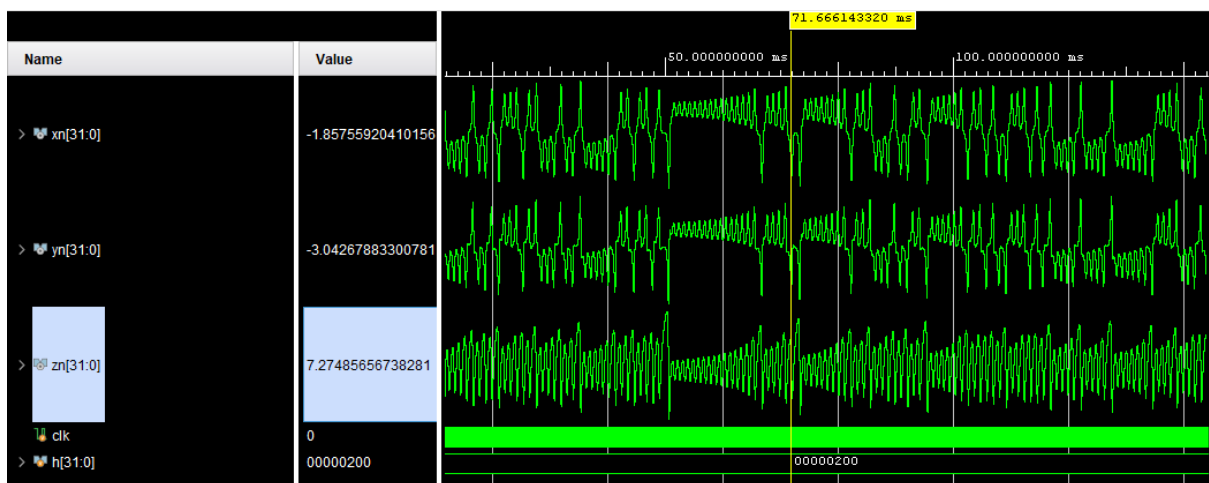
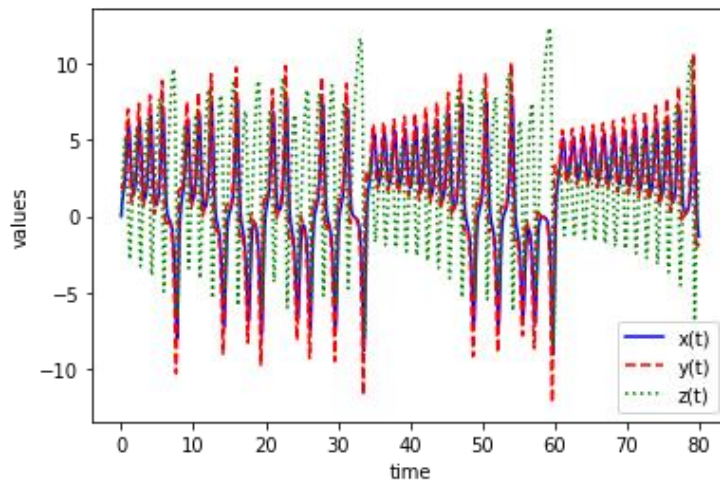


Fig. 8.7 Numerical simulation and Xilinx Vivado simulation results of Li chaotic system [32]

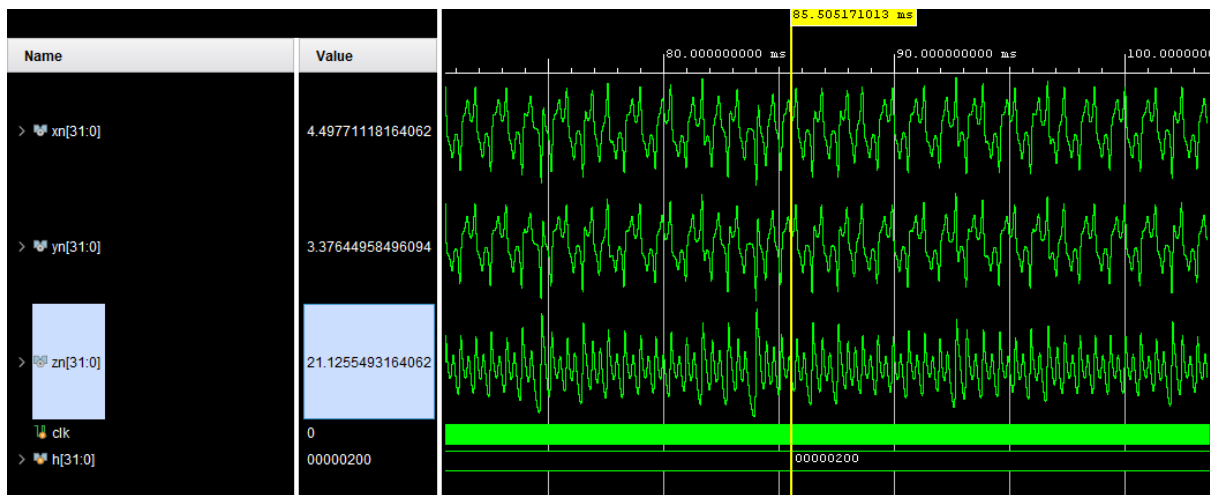
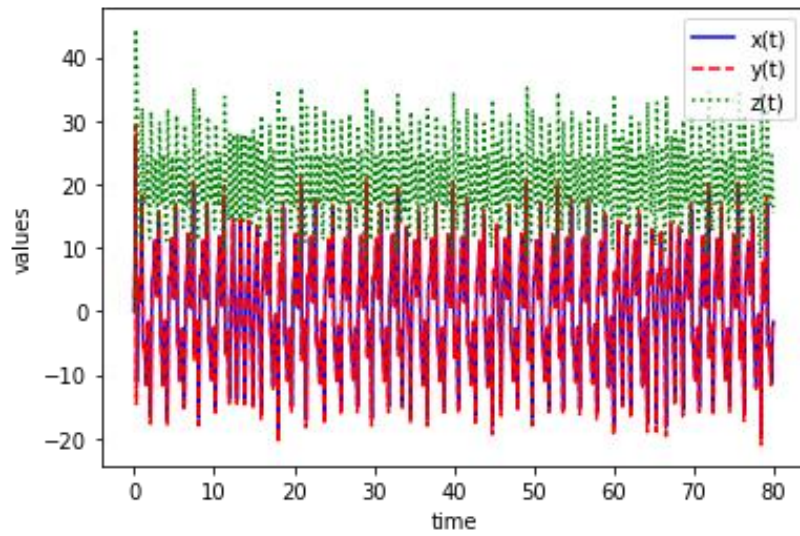


Fig. 8.8 Numerical simulation and Xilinx Vivado simulation results of Lü chaotic system

[33]

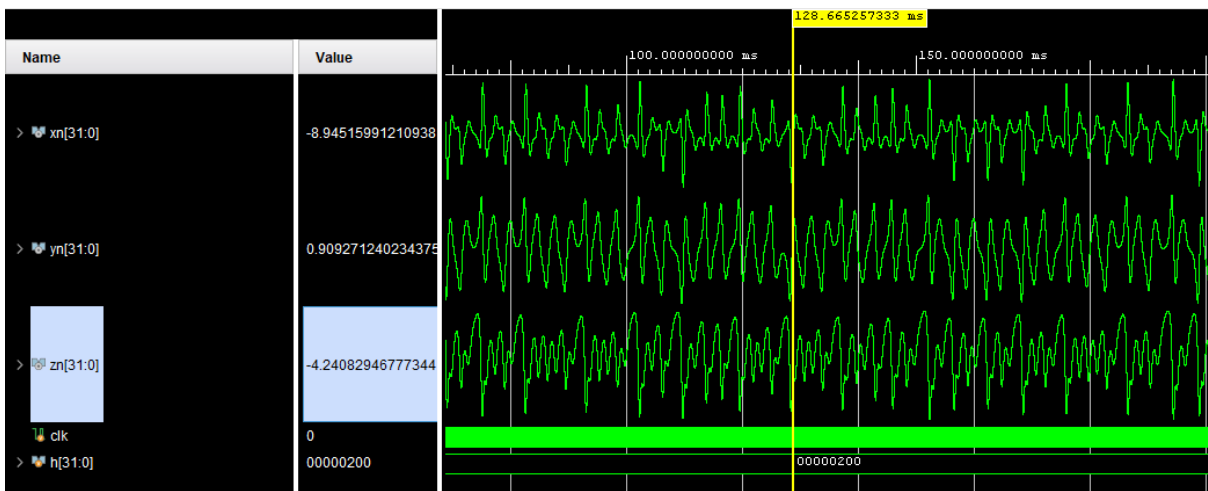
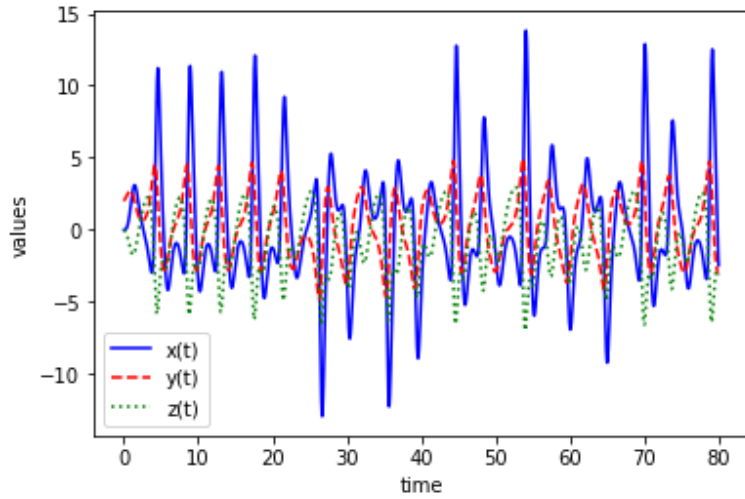
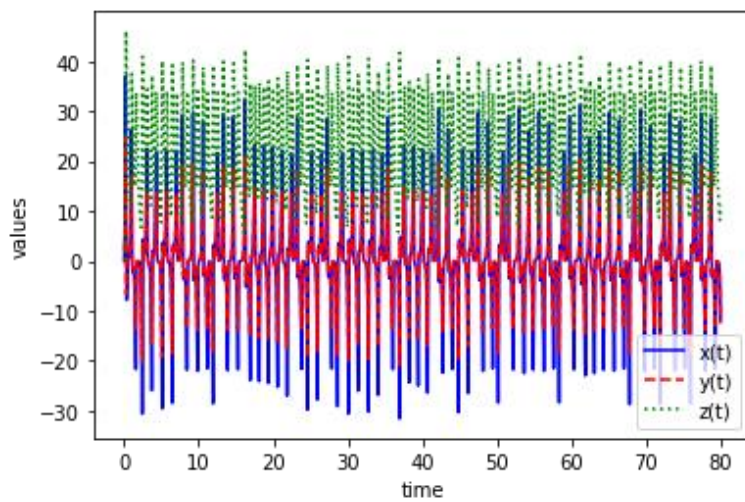


Fig. 8.9 Numerical simulation and Xilinx Vivado simulation results of MACM chaotic system [36]



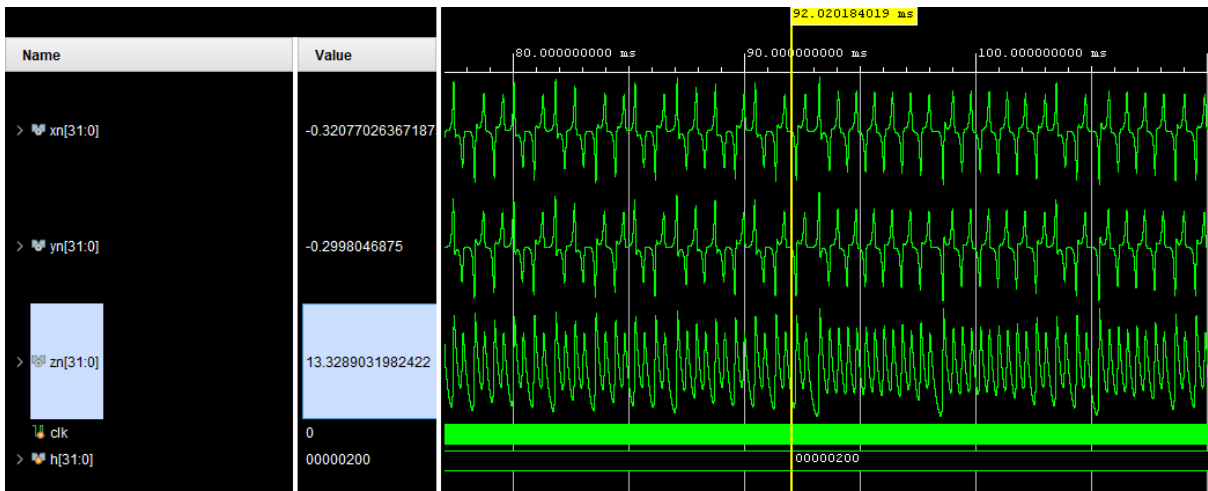


Fig. 8.10 Numerical simulation and Xilinx Vivado simulation results of chaotic system [27]

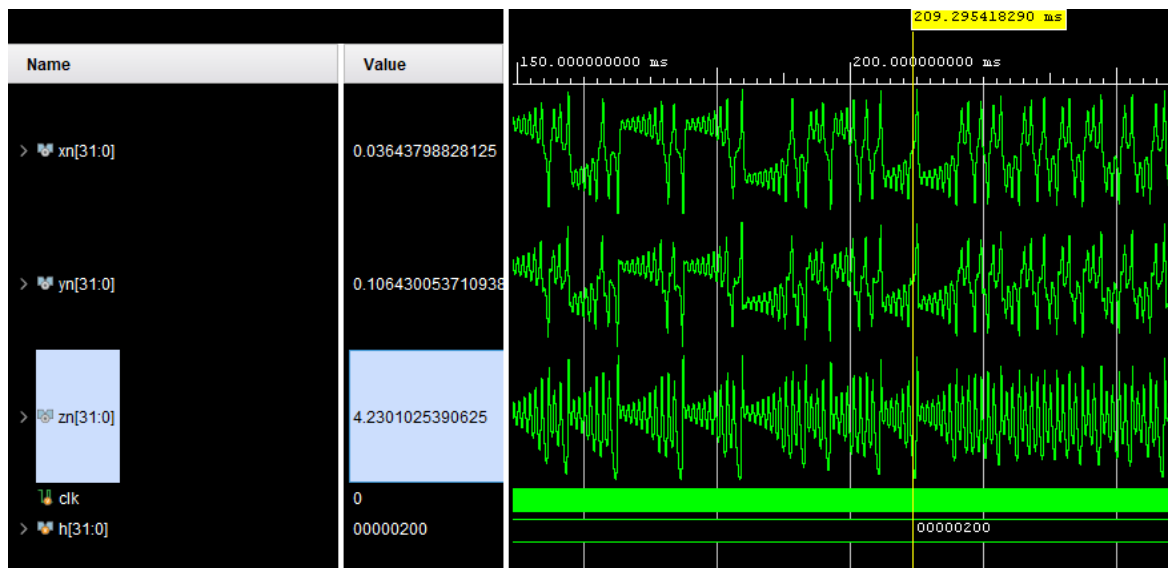
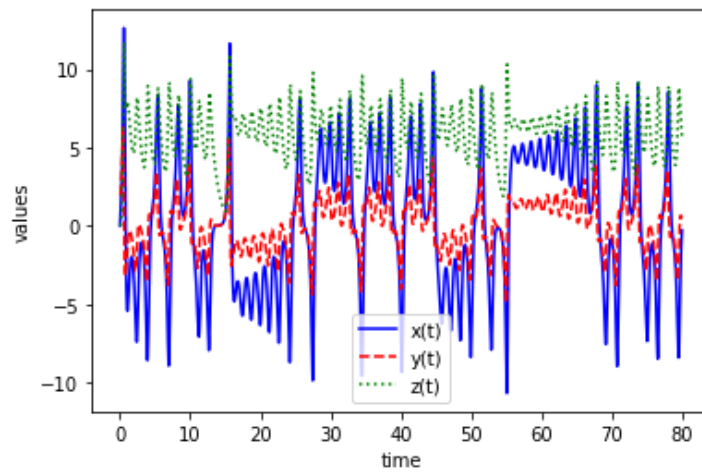


Fig. 8.11 Numerical simulation and Xilinx Vivado simulation results of Rabinovich chaotic system [37,38]



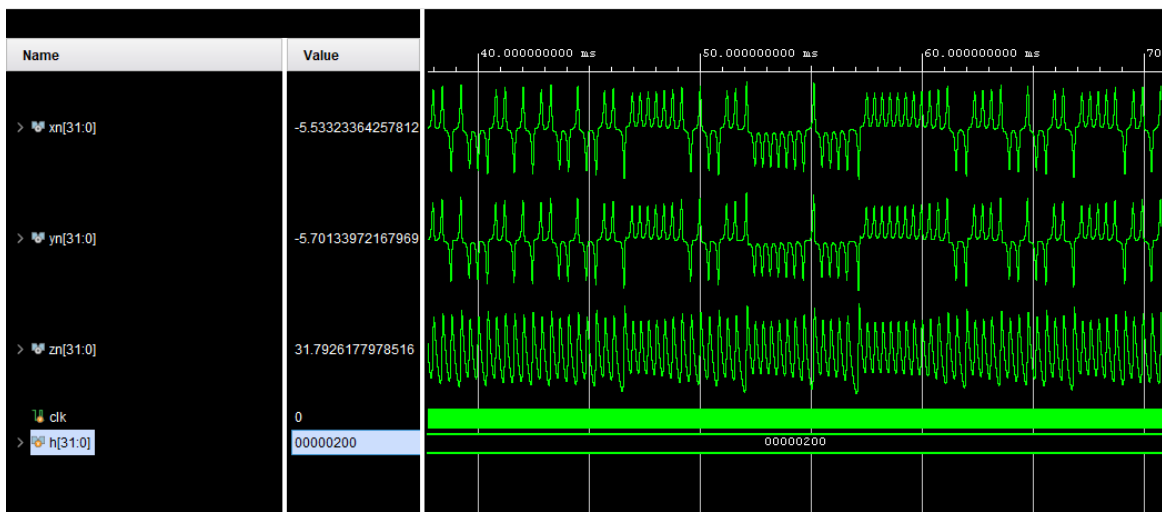
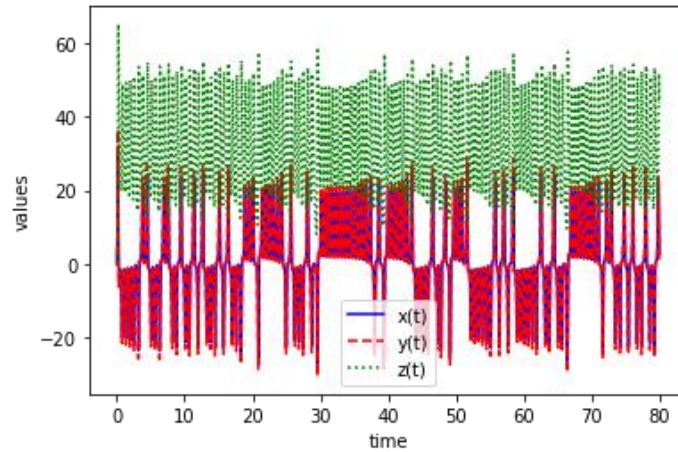


Fig. 8.12 Numerical simulation and Xilinx Vivado simulation results of chaotic system [29, 113]

## 8.4 Concluding Remarks

FPGA based realization of ten chaotic systems using RK4 numerical method in Verilog hardware description language has been presented, and each step of the iterative operation is realized in the designed state machine. The advantage of the proposed methodology is its field programmability and easy implementation of a new chaotic system in comparison to that of their analog counterparts. All considered chaotic systems have been synthesized and compared in terms of percentage utilization of hardware resources on target FPGA device Artix 7 and the total time delay. Rössler chaotic system is best fit for lesser delay and hardware (Slice LUTs and DSP blocks) requirements. The simulations results have also been validated by python based numerical simulations. Based on this design methodology, these chaotic systems can be further used for digital applications.

# **Chapter 9**

## **Conclusion and Future Scope**

---

Chaos is an inherently complex phenomenon, but with an underlying order. The chaotic systems have found many practical applications, especially in secure communication. Mathematically, for a system of non-linear differential equations to behave chaotically, they should have a minimum dimension of three. Extreme sensitivity to initial conditions, a signature property of chaotic systems is quantified as Lyapunov exponents. A three-dimensional chaotic system has one positive Lyapunov exponent. The higher dimensional non-linear differential systems with more than one positive Lyapunov exponents are known as hyperchaotic systems.

This thesis presents study and design of the chaotic systems from their circuit design point of view, both in analog and digital domain. In this work, few new chaotic and hyperchaotic systems have been proposed along with their electronic circuit realizations. Further, hardware optimized circuit design of chaotic systems available in literature have been proposed. An application of these chaotic systems in communication using analog circuitry of adaptive control synchronization has been explored. Lastly, implementation of various existing chaotic systems on FPGA based digital platforms is also presented.

This chapter presents the significant conclusions of the work reported in various chapters of the thesis.

## **9.1 Summary of work presented in this thesis**

The introductory chapter describes evolution of chaotic systems, their applications, and a brief review of various analog and digital domain circuit designs of chaotic systems. A review of earlier work on adaptive control synchronization of chaotic systems has also been presented in this chapter.

Chapter 2 presents the fundamental concepts of the chaotic systems, including Lyapunov exponents, Kaplan Yorke Dimension and dissipativity. Analysis of fixed points in a chaotic system using Jacobi stability analysis is also reported in this chapter. The complete characterization of analog building blocks, namely CFOA and AM, which have been used in this thesis for circuit realization and their basic applications are also put forward in this chapter.

Chapter 3 presents a systematic design of Rössler chaotic system, a chaotic system with single quadratic non-linearity, using CFOAs and AM. The proposed design uses four CFOAs, one analog multiplier, seven resistors, and three capacitors. The passive component count in

proposed circuit is considerably low as compared to existing Rössler chaotic system's design. An application, namely adaptive control synchronization between two Rössler chaotic systems is also put forward to illustrate the usability of the proposed circuit. The workability of the proposed design and its synchronization is examined through LTspice simulations and experimentally using AD844 and AD633 ICs, the commercially available CFOA and AM respectively.

Chapter 4 presents four new variants of an existing chaotic system, namely PUCS with two quadratic non-linearities. The properties of these variants, including Lyapunov exponents, Kaplan Yorke Dimension, nature of equilibrium points through eigenvalues and chaotic attractors, have been evaluated. Finally, an analog circuit design is proposed using current mode active building blocks, which can implement PUCS and all its proposed variants. Simulations are carried out for time series, frequency responses, phase portraits. Monte Carlo analysis is also done to check the robustness of the system. The proposed design is lesser component extensive as compared to the existing OpAmp based electronic design presented in [15]. It uses three current mode active building blocks, two analog multipliers and eight passive elements out of which four are grounded. In [15], four voltage mode active building blocks, two analog multipliers and eleven passive components were used, all were floating. Further, experimental verification of two of the proposed variants, PUCS I and PUCS IV, by breadboarding the circuit using off the shelf components is also done. The experimental results are conforming with the simulation results.

Circuit simplification by reducing hardware complexity plays a vital role in the generation of chaotic attractors for various real time applications. Chaotic systems with quadratic non-linearities are realized with AD633 in chapter 5. The realized chaotic systems have used AD633 blocks equal to the number of governing equations in the respective chaotic systems. This also makes the circuit highly accurate because of the reduced number of components, thus their inherent errors. LTspice simulations are in agreement with the numerical simulations existing in literature.

Chapter 6 presents a new chaotic system with exponential type non-linearity. All the properties of the chaotic systems, including Lyapunov exponents, Kaplan Yorke dimension and dissipativity, mentioned in Chapter 2 are studied for this system with its circuit realization using CFOAs and diodes. Besides, the adaptive control synchronization scheme has been

designed for the synchronization of two identical proposed chaotic systems, which has been verified both numerically and through circuit implementation in LTspice.

Chapter 7 presents a new hyperchaotic system with quadratic type non-linearities. Properties, such as Lyapunov exponents, Kaplan- Yorke dimension, and dissipativity have been studied for the proposed HCS. It's feasibility is validated by designing its analog electronic circuit using CFOA and AM active building blocks in LTspice software. Then, adaptive control synchronization scheme is applied to achieve chaos synchronization for the proposed system. The results have been presented for different initial conditions, different values of system parameters and the errors between the respective state variables. The circuit design has been simulated, and the simulation results are in agreement with numerical simulations.

In chapter 8, various existing quadratic non-linearity based chaotic systems have been implemented in digital domain. The governing equations of the chaotic systems are represented using RK4 numerical method and coded in Verilog HDL. All the systems are synthesized using target FPGA device Artix 7 and compared in terms of percentage utilization of hardware resources and the total time delay. The Verilog simulation results for all realized chaotic systems are found in agreement with numerical simulations.

The advantage of the proposed methodology is its field programmability and ease of implementation. Thus, the chaotic systems designed using this methodology can be used for digital applications.

## **9.2 Author's ending note**

Chaotic systems are an integral part of our daily lives in the form of stock market, weather, pandemics, human body, etc. Exploring these systems and their applications in encryption, secure communication, and modelling may serve the society better.

To make these systems part of portable devices, their circuit models with minimal components is a preferred choice. The existing designs of chaotic systems with one quadratic non-linearity and two quadratic non-linearities have been studied and found that they have been implemented using OpAmps and AMs. This study presents their circuit design using CFOAs and AMs, and a significant reduction in the use of active blocks is evident from the comparison. Besides, this study explored new models of chaotic and hyperchaotic systems, and their applications in adaptive control synchronization. Finally, the digital design of chaotic systems with quadratic

type non-linearities is also presented and a comparison is made based on hardware utilization and delay to choose the best fit for FPGA implementation.

It is expected that this study would serve as a ready reckoner of available information on chaotic circuits designed using minimal number of active blocks.

### **9.3 Future Scope**

The future work in this field includes modelling the observational data of physical chaotic systems, such as weather phenomena, pandemics, human heart activities, etc., mathematically to study their nature, and to control the chaotic behaviour of these systems. Study of the noise induced transitions in chaotic systems can be useful from climate to engineering applications. Another application area of chaotic systems to be explored is where variants of the existing pieces are required, such as music, DNA sequences, art work, etc.

## References

- [1] E.N. Lorenz, "Deterministic non-periodic flows," *J. Atmos. Sci.*, 20, 130-141, 1963.
- [2] O.E. Rössler, "An equation for continuous chaos," *Phys. Lett. A.*, 57(5),397-398, 1976.
- [3] L. O. Chua and G. Lin, "Canonical realization of Chua's circuit family," in *IEEE Transactions on Circuits and Systems*, 37(7), 885-902, July 1990.
- [4] S. Kassim, O. Megherbi, H. Hamiche and M. Bettayeb, "Implementation on microcontroller devices of a secure communication scheme based on fractional-order chaotic systems," 2023 International Conference on Fractional Differentiation and Its Applications (ICFDA), Ajman, United Arab Emirates, pp. 1-6, 2023. doi: 10.1109/ICFDA58234.2023.10153378.
- [5] G. Alvarez, F. Montoya, M. Romera, G. Pastor, "Breaking two secure communication systems based on chaotic masking," *IEEE Trans. Circuits Syst II.*, 51, 505-506, 2004. <https://doi.org/10.1109/TCSII.2004.836047>.
- [6] T. Wang, D. Wang, K. Wu, "Chaotic Adaptive Synchronization Control and Application in Chaotic Secure Communication for Industrial Internet of Things," *IEEE Access*, 6, 8584-8590, 2018. <https://doi.org/10.1109/ACCESS.2018.2797979>.
- [7] L. Zhengguo, L. Kun, W. Changyun, S. Yeng Chai, "A new chaotic secure communication system," *IEEE Trans. Comm.*, 51(8), 1306-1312, 2003. <https://doi.org/10.1109/TCOMM.2003.815058>.
- [8] E. Hato, D. Shihab, "Lorenz and Rossler Chaotic System for Speech Signal Encryption," *Int. J. Computer Applications*, vol. 128, pp. 25-33, 2015.
- [9] M.G. Avasare, V.V. Kelkar, "Image encryption using chaos theory," *Int. Conf. Communication, Information & Computing Technology (ICCICT)*, Mumbai, pp.1-6, 2015.
- [10] A. Paliwal, B. Mohindroo, K. Suneja, "Hardware design of image encryption and decryption using CORDIC based chaotic generator," *Int. Conf. Recent advances and innovations in engineering (ICRAIE)*, Jaipur, pp.1-5, 2020.
- [11] A. Giakoumis, C.K. Volos, J.M. Munoz-Pacheco, L.del.C. Gomez-Pavon, I.N. Stouboulos, I.M. Kyprianidis, "Text encryption device based on a chaotic random bit generator," *IEEE 9th Latin Amer. Symp. Circuits & Systems (LASCAS)*, Puerto Vallarta, pp. 1-5, 2018.
- [12] A. Negi, D. Saxena, K. Suneja, "High level synthesis of chaos based text encryption using modified hill cipher algorithm," *Int. Conf. India Council (INDICON)*, New Delhi, pp.1-5, 2020.
- [13] D.T.F. Shum, R.S.T. Lee, J.N.K. Liu, "Chaotic weatherman: the design and implementation of a chaotic weather prediction system," *IEEE Congr. Evolutionary Computation (IEEE World Congress on Computational Intelligence)*, Hong Kong, pp. 2186-2193, 2008.
- [14] T.A. Fathima, V. Nedumpozhimana, Y.H. Lee, S. Winkler, S. Dev, "A Chaotic Approach on Solar Irradiance Forecasting," *Photonics & Electromagnetics Research Symposium - Fall (PIERS - Fall)*, Xiamen China, pp. 2724-2728, 2019.
- [15] I. Pehlivan, Y. Uyaroglu, "A new chaotic attractor from general Lorenz system family and its electronic experimental implementation," *Turkish Journal of Electrical Engineering and Computer Sciences*, 18 , 171-184, 2020. <https://doi.org/10.3906/elk-0906-67>.
- [16] J.C. Sprott, Some simple chaotic flows. *Phys. Rev.*,50, 647-650, 1994.
- [17] F. Hannachi, "Analysis, dynamics and adaptive control synchronization of a novel chaotic 3-D system," *SN Appl. Sci.*,1, 158, 2019. <https://doi.org/10.1007/s42452-019-0175-3>.

- [18] C. Nwachioma, J.H. Pérez-Cruz, “Analysis of a new chaotic system, electronic realization and use in navigation of differential drive mobile robot,” *Chaos, Solitons & Fractals*, 144,110684, 2021. <https://doi.org/10.1016/j.chaos.2021.110684>.
- [19] S. Moreno, K. Casas-García, J.J. Flores-Godoy, F. Valencia, G. Fernandez-Anaya, “Study of new chaotic flows on a family of 3-dimensional systems with quadratic nonlinearities,” *Journal of Physics: Conference Series.*, 582, 2015. 10.1088/1742-6596/582/1/012016.
- [20] S. Vahedi, Mohd Salmi, Md Noorani, “Analysis of a New Quadratic 3D Chaotic Attractor,” *Abstract and Applied Analysis*, Article ID 540769, 7 pages, 2013. <https://doi.org/10.1155/2013/540769>.
- [21] Z. Faghani, F. Nazarimehr, S. Jafari, J.C. Sprott, “A New Category of Three-Dimensional Chaotic Flows with Identical Eigenvalues,” *International Journal of Bifurcation and Chaos*, 30, 2050026, 2020. 10.1142/S0218127420500261.
- [22] P.P. Singh, B.K. Roy, “A novel chaotic system without equilibria, with parachute and thumb shapes of Poincare map and its projective synchronization,” *Eur. Phys. J. Spec. Top.* 229, 1265–1278, 2020. <https://doi.org/10.1140/epjst/e2020-900259-0>.
- [23] Y. Liao, Y. Zhou, F. Xu, X.B. Shu, “A study on the complexity of a new chaotic financial system,” *Complexity*, Article ID 8821156, 5 pages, 2020. <https://doi.org/10.1155/2020/8821156>.
- [24] X. Wang, V. Pham, S. Jafari, C. Volos, J.M. Munoz-Pacheco, E. Tlelo-Cuautle, “A New Chaotic System With Stable Equilibrium: From Theoretical Model to Circuit Implementation,” *IEEE Access.* 5, 8851-8858, 2017. doi: 10.1109/ACCESS.2017.2693301.
- [25] A. Allahem, “Synchronized Chaos of a Three-Dimensional System with Quadratic Terms,” *Mathematical Problems in Engineering*. Article ID 8813736, 4 pages, 2020. <https://doi.org/10.1155/2020/8813736>.
- [26] X. L, H. Zhu, H. Yao, Analysis of a new three-dimensional chaotic system, *Dynamics.* 67, 2012. 10.1007/s11071-011-9981-x.
- [27] G. Qi, G. z, S. Du, Z. Chen, Z. Yuan, “Analysis of a new chaotic system,” *Physica A: Statistical Mechanics and its Applications.* 352(2–4), 295-308, 2005. <https://doi.org/10.1016/j.physa.2004.12.040>.
- [28] K. Huang, C. Sun, “Dynamics Analysis of a Three-Dimensional Nonlinear System with No or Infinite Equilibria,” *Chinese Control And Decision Conference (CCDC)*,875-879, 2019. doi: 10.1109/CCDC.2019.8832379.
- [29] Y. Liu, Q. Yang, “Dynamics of a new Lorenz-like chaotic system,” *Nonlinear Analysis: Real World Applications*, 11, 2563-2572, 2010. 10.1016/j.nonrwa.2009.09.001.
- [30] G. Cai, Z. Tan, “Chaos synchronization of a new chaotic system via nonlinear control,” *J. Uncertain Systems*, 1, 235-240, 2007.
- [31] M. Wang, J. Li, X. Zhang, H.H.C. Iu, T. Fernando, Z. Li, Y. Zeng, “A Novel Non-Autonomous Chaotic System with Infinite 2-D Lattice of Attractors and Bursting Oscillations,” *IEEE Transactions on Circuits and Systems II: Express Briefs*, 68(3), 1023-1027, 2021. <https://doi.org/10.1109/TCSII.2020.3020816>.
- [32] X.F. Li, K.E. Chlouverakis, D.L. Xu, “Nonlinear dynamics and circuit realization of a new chaotic flow: A variant of Lorenz, Chen and Lü,” *Nonlinear Analysis: Real World Applications*, 10(4), 2357-2368, 2009. <https://doi.org/10.1016/j.nonrwa.2008.04.024>.
- [33] ] J. Lu and G. Chen, “A new chaotic attractor coined,” *Int. J. Bifurcation and Chaos*, 12,1789–1812, 2002.
- [34] G. Chen and T. Ueta, “Yet another chaotic attractor,” *International Journal of Bifurcation and Chaos*, 9(7),1465–1466, 1999.



- [35] G. Tigan and D. Opreș, "Analysis of a 3D chaotic system", *Chaos, Solitons and Fractals*, 36(5), 1315-1319, 2008.
- [36] R. Méndez-Ramírez, C. Cruz-Hernández, A. Arellano-Delgado, R. Martínez-Clark, "A new simple chaotic Lorenz-type system and its digital realization using a TFT touch-screen display embedded system," *Complexity* 2017,6820492.
- [37] A.S. Pikovski, M.I. Rabinovich, V.Y. Trakhtengerts, "Onset of stochasticity in decay confinement of parametric instability," *Soviet Physics JETP*, 47, 715-719, 1978.
- [38] U.E. Kocamaz, Y. Uyaroglu and H. Kizmaz, "Control of Rabinovich chaotic system using sliding mode control," *Int. J. of Adaptive control and Signal Processing*, 28,(12), 1413-1421, 2014.
- [39] J.O. Maaita, Ch. K. Volos, I.M. Kyprianidis, I.N. Stouboulos, "The Dynamics of a Cubic Nonlinear System with No Equilibrium Point," *Journal of Nonlinear Dynamics*, Article ID 257923, 13 pages, 2015. <https://doi.org/10.1155/2015/257923>.
- [40] M. Zhang, Q. Han, "Dynamic analysis of an autonomous chaotic system with cubic nonlinearity," *Optik*, 127(10), 4315-4319, 2016.
- [41] A. Sambas, S. Vaidyanathan, M. Mamat, A. Mohamed Mohamad, W.S. Sanjaya, "A new chaotic system with a pear-shaped equilibrium and its circuit simulation," *International Journal of Electrical and Computer Engineering*, 8, 4951-4958, 2018. 10.11591/ijece.v8i6.pp.4951-4958.
- [42] V.K. Tamba, K. Rajagopal, V.T. Pham, D.V. Hoang, "Chaos in a System with an Absolute Nonlinearity and Chaos Synchronization," *Advances in Mathematical Physics*, Article ID 5985489, 12 pages, 2018. <https://doi.org/10.1155/2018/5985489>.
- [43] J. Liu, Y. Ma, J. Lian, X. Zhang, "Chaotic Systems with Hyperbolic Sine Nonlinearity," *A Collection of Papers on Chaos Theory and Its Applications*, Paul Bracken and Dimo I. Uzunov, IntechOpen. <https://doi.org/10.5772/intechopen.94518>.
- [44] S. Honglad, W.San-Um, "Automatic stand-alone liquid mixer with chaotic PWM control using diode-based Rössler system," *International Electrical Engineering Congress (iEECON)*,1-4, 2014. doi: 10.1109/iEECON.2014.6925910.
- [45] F. Yu, "A Novel Three Dimension Autonomous Chaotic System with a Quadratic Exponential Nonlinear Term," *Engineering, Technology & Applied Science Research*, 2, 209-215, 2012. 10.48084/etasr.86.
- [46] V.T. Pham, S. Vaidyanathan, C.K. Volos, S. Jafari, "Hidden attractors in a chaotic system with an exponential nonlinear term," *The European Physical Journal Special Topics*, 224, 1507-1517, 2015. 10.1140/epjst/e2015-02476-9.
- [47] S. Vaidyanathan, "Complete chaos synchronization of six-term Sundarapandian chaotic systems with exponential nonlinearity via active and adaptive control," *International Conference on Green Computing, Communication and Conservation of Energy (ICGCE)*, 608-613, 2013. doi: 10.1109/ICGCE.2013.6823508.
- [48] X. Wang, G. Chen, "A chaotic system with only one stable equilibrium," *Communications in Nonlinear Science and Numerical Simulation*,17(3), 1264-1272, 2012.
- [49] M.D., Vijayakumar, A. Karthikeyan, J. Zivcak, O. Krejcar, and H. Namazi, "Dynamical Behavior of a New Chaotic System with One Stable Equilibrium," *Mathematics* 9(24): 3217, 2021.
- [50] V.T.Pham, S. Jafari, T. Kapitaniak, C. Volos, S.T. Kingni, "Generating a chaotic system with one stable equilibrium," *Int J Bifurcation Chaos*, 27 (4), Article 1750053, 2017.

- [51] W.B. Liu, G. Chen, "A new chaotic system and its generation," *Int. J. Bifurcation and Chaos*, 12, 261-267, 2003.
- [52] S. Pang, Y. Liu, "A new hyperchaotic system from the Lü system and its control," *Journal of Computational and Applied Mathematics*, 235(8), 2775-2789, 2011. <https://doi.org/10.1016/j.cam.2010.11.029>.
- [53] S. Emiroglu, A. Akgul, Y. Adiyaman, T. Gümüő, Y. Uyaroglu, M.A. Yalcin, "A new hyperchaotic system from T chaotic system: Dynamical analysis, circuit implementation, control and synchronization," *Circuit World*. 48(2), 265-277, 2021. <https://doi.org/10.1108/CW-09-2020-0223>.
- [54] J. Li-Xin, D. Hao, H. Meng, "A new four-dimensional hyperchaotic Chen system and its generalized synchronization," *Chinese Physics B*, 19(10), 2010.
- [55] H. Jia, Z. Guo, S. Wang, R. Wang, "Analysis and circuit implementation for a novel fractional-order hyperchaotic system based on chen system," in 9th International Conference on Modelling, Identification and Control (ICMIC), pp. 641-646, 2017.10.1109/ICMIC.2017.8321534.
- [56] G. Zhang, F. Zhang, X. Liao, D. Lin, P. Zhou, "On the dynamics of new 4D Lorenz-type chaos systems," *Adv Differ Eqn*. **217**, 2017. <https://doi.org/10.1186/s13662-017-1280-5>.
- [57] X.Y. Wang, M.J. Wang, "A hyper-chaos generated from Lorenz system," *Physica A Statistical Mechanics and its Applications*, Elsevier. **387**(14), 3751-3758, 2008.
- [58] X. Tong, Y. Liu, M. Zhang, H. Xu, Z. Wang, "An Image Encryption Scheme Based on Hyperchaotic Rabinovich and Exponential Chaos Maps," *Entropy*. **17**(1), 181-196, 2015. <https://doi.org/10.3390/e17010181>.
- [59] R.D. Méndez-Ramírez, A. Arellano-Delgado, M. Murillo-Escobar, C. Cruz-Hernández, "A New 4D Hyperchaotic System and Its Analog and Digital Implementation," *Electronics*. **10**, 2021. [10.3390/electronics10151793](https://doi.org/10.3390/electronics10151793).
- [60] Y. Gao, C. Liang, "A New 4D Hyperchaotic System and Its Generalized Function Projective Synchronization," *Mathematical Problems in Engineering*. **2013**, 701756, 2013. <https://doi.org/10.1155/2013/701756>.
- [61] L. Xu, G. Cai, S. Zheng, "A Novel Hyperchaotic System and Its Control," *Journal of Uncertain Systems*. **3**(2),137-144, 2009.
- [62] B. Bocheng, L. Zhong, X. Jianping, "New chaotic system and its hyperchaos generation," *Journal of Systems Engineering and Electronics*, 20(6),1179-1187, 2009.
- [63] D. Chen, L. Shi, Chen Hai-Tao, Ma Xiao-Yi, "Analysis and control of a hyperchaotic system with only one nonlinear term," *Nonlinear Dynamics*, 67, 1745–1752, 2012. [10.1007/s11071-011-0102-7](https://doi.org/10.1007/s11071-011-0102-7).
- [64] G. Qi, M. Wyk, B. Van Wyk, G. Chen, "On a new hyperchaotic system," *Physics Letters A*, 372, 124–136, 2008. [10.1016/j.physleta.2007.10.082](https://doi.org/10.1016/j.physleta.2007.10.082).
- [65] M. Rahim, H. Kadhim, N. Fataf, S. Banerjee, "Dynamics of a new hyperchaotic system and multistability," *The European Physical Journal Plus*, 134, 2019. [10.1140/epjp/i2019-13005-5](https://doi.org/10.1140/epjp/i2019-13005-5).
- [66] B. Hani, A. Mjily, A. AL-Aaragee, "A novel 4 dimensional hyperchaotic system with its control, Synchronization and Implementation," *International Journal of Electrical and Computer Engineering (IJECE)*, 11, 2021. [10.11591/ijece.v11i4.pp2974-2985](https://doi.org/10.11591/ijece.v11i4.pp2974-2985).
- [67] Z. Wang, S. Cang, E. Ochola, Y. Sun, "A hyperchaotic system without equilibrium," *Nonlinear Dynamics*, 69, 2011. [10.1007/s11071-011-0284-z](https://doi.org/10.1007/s11071-011-0284-z).

- [68] M. Joshi, A. Ranjan, "New simple chaotic and hyperchaotic system with an unstable node," *AEU - International Journal of Electronics and Communications*, 108, 1-9, 2019. <https://doi.org/10.1016/j.aeue.2019.05.042>.
- [69] A. Karthikeyan, S. Cicek, K. Rajagopal, P. Duraisamy, A. Srinivasan, "New hyperchaotic system with single nonlinearity, its electronic circuit and encryption design based on current conveyor," *Turk J Elec Eng & Comp Sci*, 29, 1692 – 1705, 2021. doi:10.3906/elk-2005-86.
- [70] C. Wu, Y. Zhang, N. Yang, "Analysis of a novel four-wing hyperchaotic system from pseudo to real and circuit experimental research," in *2014 International Conference on Information Science, Electronics and Electrical Engineering*, pp. 1138-1142, 2014. doi: 10.1109/InfoSEEE.2014.6947848.
- [71] B. Bao, N. Wang, M. Chen et al, "Inductor-free simplified Chua's circuit only using two-op-amp-based realization", *Nonlinear Dynamics*, vol.84, pp. 511–525, 2016.
- [72] K. Gopakumar, B. Premlet & K.G. Gopchandran, "Implementation of Chua's circuit using simulated inductance," *International Journal of Electronics*, vol. 98, no. 5, pp. 667-677, 2011.
- [73] R. Senani and S.S. Gupta, "Implementation of Chua's chaotic circuit using current feedback op-amps," *Electronics Letters*, vol. 34, pp. 829 – 830, 1998.
- [74] A.K. Kushwaha and S. K. Paul, "Chua's oscillator using operational transresistance amplifier", *Revue Roumaine des Sciences Techniques- Serie Electrotechnique et Energetique*, vol. 61, pp. 299-303, 2016.
- [75] K. Suneja, N. Pandey and R. Pandey, "Realization of Chua's circuit using VDBA based nonlinear resistor and inductor simulator," *2022 International Mobile and Embedded Technology Conference (MECON)*, Noida, India, 2022, pp. 367-371, doi: 10.1109/MECON53876.2022.9751973.
- [76] R. Trejo-Guerra, E. Tlelo-Cuautle, C.Cruz-Hernández, and C.Sanchez-Lopez, "Chaotic communication system using Chua's oscillators realized with CCII+s," *International Journal of Bifurcation and Chaos*, vol. 19, no.12, pp. 4217-4226, 2009.
- [77] C. K. Choubey, S. K. Paul, "Implementation of chaotic oscillator by designing a simple Chua's diode using a single VDTA," *AEU - International Journal of Electronics and Communications*, vol. 124, 2020.
- [78] A.K. Kushwaha, S.K. Paul, "Inductorless realization of Chua's oscillator using DVCCTA," *Analog Integr Circ Sig Process* 88, 137–150, 2016. <https://doi.org/10.1007/s10470-016-0746-9>.
- [79] K. M. Cuomo, A. V. Oppenheim and S. H. Strogatz, "Synchronization of Lorenz-based chaotic circuits with applications to communications," in *IEEE Transactions on Circuits and Systems II: Analog and Digital Signal Processing*, vol. 40, no. 10, pp. 626-633, Oct. 1993, doi: 10.1109/82.246163.
- [80] K.M. Ibrahim, R.K. Jamal, F.H. Ali, "Chaotic behaviour of the Rossler model and its analysis by using bifurcations of limit cycles and chaotic attractors," *J. Phys. Conf. Ser*, 1003 012099, 2018. <https://doi.org/10.1088/1742-6596/1003/1/012099>.
- [81] Gunay, Alci and Yildirim, "High Frequency Chaotic Oscillator Design via CFOA Based Cellular Neural Network," *2006 IEEE 14th Signal Processing and Communications Applications*, 2006, pp. 1-4, doi: 10.1109/SIU.2006.1659810.
- [82] J. Wu, C. Li, X. Ma, T. Lei and G. Chen, "Simplification of Chaotic Circuits With Quadratic Nonlinearity," in *IEEE Transactions on Circuits and Systems II: Express Briefs*, vol. 69, no. 3, pp. 1837-1841, March 2022, doi: 10.1109/TCSII.2021.3125680.
- [83] L. M. Pecora and T. L. Carroll, "Synchronization in chaotic systems," *Phys. Rev. Lett.* 64, 821, 1990.

- [84] M. Haeri, B. Khademian, "Comparison between different synchronization methods of identical chaotic systems," *Chaos, Solitons & Fractals*, 29(4), 1002-1022, 2006.
- [85] T.L. Liao, S.H. Lin, "Adaptive control and synchronization of Lorenz systems," *Journal of the Franklin Institute*, 336 (6), 925- 937, 1999.
- [86] S. Vaidyanathan, I. Pehlivan, "Analysis, control, synchronization, and circuit design of a novel chaotic system," *Mathematical and Computer Modelling*, 55, (7–8), 1904-1915, 2012.
- [87] S. Vaidyanathan , " Adaptive Control and Synchronization of Rössler Prototype-4 System" (August 22, 2019). Available at SSRN: <https://ssrn.com/abstract=3441103> or <http://dx.doi.org/10.2139/ssrn.3441103>.
- [88] A.S. Hegazi, H.N. Agiza and M.M. EL-Dessoky, "Adaptive Synchronization For Rössler And Chua's Circuit Systems," *International Journal of Bifurcation and Chaos*, 12(07), 1579-1597, 2002. <https://doi.org/10.1142/S0218127402005388>.
- [89] S.Vaidyanathan, A.T. Azar, "Adaptive Control and Synchronization of Halvorsen Circulant Chaotic Systems," In: Azar, A., Vaidyanathan, S. (eds) *Advances in Chaos Theory and Intelligent Control. Studies in Fuzziness and Soft Computing*, vol 337. Springer, Cham, 2016. [https://doi.org/10.1007/978-3-319-30340-6\\_10](https://doi.org/10.1007/978-3-319-30340-6_10).
- [90] R. R. Babu and R. Karthikeyan, "Adaptive synchronization of novel chaotic system and its FPGA implementation," 2015 International Conference on Smart Technologies and Management for Computing, Communication, Controls, Energy and Materials (ICSTM), Avadi, India, pp. 449-454, 2015. doi: 10.1109/ICSTM.2015.7225459.
- [91] S.Vaidyanathan, K. Rajagopal, C. Volos, I. Kyprianidis, I. Stouboulos, "Analysis, Adaptive Control and Synchronization of a Seven-Term Novel 3-D Chaotic System with Three Quadratic Nonlinearities and its Digital Implementation in LabVIEW," *Journal of Engineering Science and Technology Review*, 8, 130-141, 2015.
- [92] E.M. Elabbasy, H.N. Agiza, M.M. El-Dessoky, "Adaptive Synchronization of a Hyperchaotic System With Uncertain Parameter," *Chaos, Solitons & Fractals*, 30, 1133–42, 2006. doi:10.1016/j.chaos.2005.09.047.
- [93] J. Qiang, "Adaptive Control and Synchronization of a New Hyperchaotic System With Unknown Parameters," *Phys Lett A*, 362, 424–9, 2007. doi:10.1016/j.physleta.2006.10.044.
- [94] G. Cai, S. Zheng, L. Tian L, "Adaptive Control and Synchronization of an Uncertain New Hyperchaotic Lorenz System," *Chin Phys B*, 17, 2412–9, 2008. doi:10.1088/1674-1056/17/7/014.
- [95] S. Li, Y. Wu, G. Zheng, "Adaptive synchronization for hyperchaotic Liu system," *Front. Phys., Sec. Statistical and Computational Physics*, 9, 2021. <https://doi.org/10.3389/fphy.2021.812048>
- [96] M. Tuna, M. Alçın, I. Koyuncu, C.B. Fidan, I. Pehlivan, "High speed FPGA-based chaotic oscillator design," *Microprocessors and Microsystems*, 66, 72-80, 2019.
- [97] M.Tuna, C.B. Fidan, "Electronic circuit design, implementation and FPGA-based realization of a new 3D chaotic system with single equilibrium point," *Optik*, 127(24), 11786-11799, 2016.
- [98] S. Chen, S. Yu, J. Lü, G. Chen, J. He, "Design and FPGA-Based Realization of a Chaotic Secure Video Communication System," In *IEEE Transactions on Circuits and Systems for Video Technology*, 28(9), 2359-2371, 2018. doi: 10.1109/TCSVT.2017.2703946.
- [99] J.C. Nuñez-Perez, V.A. Adeyemi, Y. Sandoval-Ibarra, F.J. Pérez-Pinal, E. Tlelo-Cuautle, "FPGA Realization of Spherical Chaotic System with Application in Image

- Transmission,” *Mathematical Problems in Engineering*, Article ID 5532106, 16 pages, 2021.
- [100] J. Schmitz, L. Zhang, “Rössler-based chaotic communication system implemented on FPGA,” In: 2017 IEEE 30th Canadian Conference on Electrical and Computer Engineering (CCECE), pp. 1-4, 2017. doi: 10.1109/CCECE.2017.7946729.
- [101] M.F. Tolba, A.S. Elwakil, H. Orabi, M. Elnawawy, F. Aloul, A. Sagahyroon, A.G. Radwan, “FPGA implementation of a chaotic oscillator with odd/even symmetry and its application,” *Integration*, 72, 163-170, 2020.
- [102] Q.Y. Shi, X. Huang, F. Yuan, Y.X. Li, “Design and FPGA implementation of multi-wing chaotic switched systems based on a quadratic transformation,” *Chinese Phys.*30(2), 020507-1- 020507-10, 2021.
- [103] I. Koyuncu, A.T. Ozcerit and I. Pehlivan, “Implementation of FPGA-based real time novel chaotic oscillator,” *Nonlinear Dyn* 77, 49–59, 2014. <https://doi.org/10.1007/s11071-014-1272-x>.
- [104] J.L. Kaplan, J.A. Yorke, “Chaotic behavior of multidimensional difference equations,” In: Peitgen, HO., Walther, HO. (eds) *Functional Differential Equations and Approximation of Fixed Points*. Lecture Notes in Mathematics, vol 730. Springer, Berlin, Heidelberg, 1979. <https://doi.org/10.1007/BFb0064319>.
- [105] E. Köse, A. Akcayoglu, Examination of the eigenvalues Lorenz chaotic system, *European Scientific Journal*, ESJ. 10(10), 114-121, 2014. <https://doi.org/10.19044/esj.2014.v10n10p%25p>.
- [106] J.C. Sprott, “Strange attractors with various equilibrium types,” *European Physical Journal: Special Topics*. 224, 1409-1419, 2015. 10.1140/epjst/e2015-02469-8.
- [107] <https://www.analog.com/en/products/ad844.html>
- [108] <https://www.analog.com/en/products/ad633.html#product-overview>.
- [109] Y. Itoh, M. Adachi, “Reconstruction of bifurcation diagrams using time-series data generated by electronic circuits of the Rössler equations,” In: *International Symposium on Nonlinear Theory and Its Applications (NOLTA) (IEICE)*.pp. 439-442, 2017.
- [110] S. Larptwee, W. San-Um W, “Implementation of Rössler chaotic system through inherent exponential nonlinearity of a diode with two-channel chaotic synchronization applications,” In: *Fourth International Conference on Intelligent Control and Information Processing (ICICIP)*. Beijing, China. pp. 787–791, 2013. <https://doi.org/10.1109/ICICIP.2013.6568179>.
- [111] H.K. Khalil, “Lyapunov’s Stability Theory,” Baillieul J., Samad T. (eds) *Encyclopedia of Systems and Control*. Springer, London, 2015. doi.org/10.1007/978-1-4471-5058-9\_77.
- [112] Z. Gosar, “Chaotic dynamics - Rössler system. Datoteka: seminar\_kaoticka\_dinamika\_Rossler\_koncna, Zadnja sprememba: 17.09.13. 10.13140/RG.2.2.27897.62564.
- [113] Q. Yang, G. Chen, “A chaotic system with one saddle and two stable node-foci,” *Internat. J. Bifur. Chaos*, vol.18, pp. 1393-1414, 2008.
- [114] Y. Feng, Z. Wei, U.E. Kocamaz, A. Akgül, I. Moroz, “Synchronization and Electronic Circuit Application of Hidden Hyperchaos in a Four-Dimensional Self-Exciting

Homopolar Disc Dynamo without Equilibria,” Complexity. Article ID 7101927, 11 pages, 2017. <https://doi.org/10.1155/2017/7101927>.

- [115] M. Joshi, A. Ranjan, “An autonomous chaotic and hyperchaotic oscillator using OTRA,” *Analog Integrated Circuits and Signal Processing*, 1-13, 2019. 10.1007/s10470-019-01395-0.
- [116] A. Garg, B. Yadav, K. Sahu, K. Suneja, K., “An FPGA based Real time Implementation of Nosé Hoover Chaotic System using different numerical Techniques,” In: *2021 7th International Conference on Advanced Computing and Communication Systems (ICACCS)*, Coimbatore, India, pp. 108-113, 2021. doi: 10.1109/ICACCS51430.2021.9441923.
- [117] J.H.E Cartwright, O. Piro, “The Dynamics of Runge-Kutta Methods,” *Int. J. Bifurcation and Chaos*, 2, 427-449, 1992.
- [118] S. Sadoudi, C. Tanougast, M.S. Azzaz, et al. ,”Design and FPGA implementation of a wireless hyperchaotic communication system for secure real-time image transmission,” *J Image Video Proc* 2013, 43, 2013. <https://doi.org/10.1186/1687-5281-2013-43>.

## LIST OF PUBLICATIONS

### International Journals:

1. K. Suneja, N. Pandey and R. Pandey, “ Systematic Realization of CFOA Based Rössler Chaotic System and Its Applications,” *Arabian Journal for Science and Engineering*, 10.1007/s13369-021-06379-9.
2. K. Suneja, N. Pandey and R. Pandey, “Novel Pehlivan–Uyaröglu Chaotic System Variants and their CFOA Based Realization,” *Journal of Circuits, Systems and Computers*. 10.1142/S0218126622501717.
3. K. Suneja, N. Pandey and R. Pandey, “A novel chaotic system with exponential non-linearity and its adaptive self-synchronization: From numerical simulations to circuit implementation,” *Journal of Circuits, Systems and Computers*. <https://doi.org/10.1142/S0218126623502961>.

### International Conferences:

1. K. Suneja, N. Pandey and R. Pandey, "Circuit realization of chaotic systems with quadratic nonlinearity using AD633 based generic topology," *2022 International Conference on Computing, Communication, and Intelligent Systems (ICCCIS)*, Greater Noida, India, 2022, pp. 284-289, doi: 10.1109/ICCCIS56430.2022.10037747.
2. K. Suneja, N. Pandey and R. Pandey, “FPGA based design of chaotic systems with quadratic non-linearities,” 4<sup>th</sup> International conference on Data Analytics and Management (ICDAM-2023), London, 2023.